SCUOLA DI DOTTORATO
UNIVERSITÀ DEGLI STUDI DI MILANO-BICOCCA

Dipartimento di / Department of

Scienza dei Materiali

Dottorato di Ricerca in / PhD program Scienza e Nanotecnologia dei Materiali Ciclo / Cycle XXXI

Materials and devices for solar generation of electricity and fuels

Cognome / Surname Boldrini Nome / Name Chiara Liliana

Matricola / Registration number 063524

Tutore / Tutor: prof. A. Abbotto

Coordinatore / Coordinator: prof. M. Bernasconi

ANNO ACCADEMICO / ACADEMIC YEAR 2017-2018

Università degli Studi di Milano-Bicocca

Scuola di dottorato in Scienza e Nanotecnologia dei Materiali

XXXI Cycle

Materials and devices for solar generation of electricity and fuels

Ph.D. thesis of

Chiara Liliana Boldrini

Tutor: prof. Alessandro Abbotto

Coordinator: prof. Marco Bernasconi

A.A. 2017/2018

TABLE OF CONTENTS

Abstract

This PhD thesis has been focused on two main themes related to solar energy exploitation for solar fuels and electricity production. Essentially, this thesis has been devoted to the study of two different kinds of photoelectrochemical cells (PEC).

In fact, there are two basic categories of PEC cells: photo-electrosynthetic cells, which include PEC water splitting, and regenerative PEC cells. The latter include the well-known dye-sensitized solar cells (DSSCs), in which redox couples such as I^-/I_3^- collect the photogenerated charge carriers at the surface of semiconductors and perform the opposite redox reaction at a counter electrode to generate electricity.[1]

The first type, that was the main focus of this work, has been extensively studied broaching several issues, aiming to a so called "artificial leaf", a prototype where artificial photosynthesis can take place generating fuels (hydrogen) starting from water and sunlight. As it is widely known, in the near future we will have to limit exploitation of fossil fuels for transport and energy production, both because of their shortage and their dramatic effects on pollution, so research has to focus on clean and cheap renewable energy sources. The main limitation related to current renewable technologies is that they usually generate electricity, and stocking electric energy is a difficult task. A further limitation of photovoltaic panels is the intermittent production of energy, obviously connected to day and night cycles and to weather conditions. The development of a system capable of producing solar fuels using sunlight is thus demanding. Solar fuels are molecules that can be synthesised through a photo-activated process and that can be easily stocked and released when needed. Such a system is called an "artificial leaf", since its working principles are the same of natural photosynthesis, that enables oxygen and carbohydrates production from water and CO_2. In particular, the aim of the device that has been studied during this

thesis was to carry out the water oxidation process, that means producing oxygen and protons from water and light thanks to a photosensitized photoanode. Protons are then reduced to hydrogen by a passive cathode.

In parallel, an established technology of PEC has been employed for the production of solar electricity, namely Dye Sensitized Solar Cells (DSSC). In particular, the attention has been focused on the electrolyte composition, substituting the commonly used electrolyte solvent, based on volatile organic compounds, with eco-friendly and innovative solvents.

In fact, one part of this PhD project has been devoted to the study of dye-sensitized solar cells containing eco-friendly solvents in the electrolyte solution, namely Deep Eutectic Solvents (DES). Traditional organic solvents used for this scope (usually nitriles mixtures) have many drawbacks, such as volatility and often toxicity. This can be a problem if the cell is not perfectly sealed, because it would involve toxic vapours in the environment and also a fast deterioration of the performance of the cell, that cannot work without the liquid electrolyte. DES instead are not volatile and can be produced from many different components, generally safe and cheap, that confer to the resulting solvent different properties, that can be widely tuned according to the specific need.

Two different DES have been studied, a hydrophilic and a hydrophobic one (respectively, a mixture of choline chloride, also known as Vitamin B_4, and urea, diluted with water, and a mixture of DL-menthol and acetic acid, diluted with ethanol) with proper dyes absorbed onto TiO_2. Many variables have been considered, such as different TiO_2 precursors and layer thickness, different iodides (both inorganic and ionic liquids, IL), different ions concentration, presence of additives and of disaggregating agents.

The efficiency of the optimized cell was 1.9% at 0.5 sun for the hydrophilic system and 2.5% at 1 sun for the hydrophobic solvent, compatible with traditional organic-solvent-based cells.

Concerning the production of hydrogen from the artificial photosynthesis process, metal-free organic sensitizers with di-branched configuration, bearing different heteroaromatic donor moieties, have been used in a systematic study upon the effect of the sensitizers at the photoanode in the photoelectrochemical hydrogen production. Namely, phenothiazine, phenoxazine and carbazole based dyes have been tested in presence of a sacrificial electron donor (SED) to evaluate charge transfer phenomena and the external quantum efficiency (EQE) of the system. Moreover, the three sensitizers have been tested in presence of a common water oxidation catalyst (WOC) to preliminary evaluate the stability in photoelectrochemical water splitting and hydrogen and oxygen evolution. According to experimental data, the phenothiazine based derivative **PTZ-Th** has been recognized as the best performing sensitizer, considering its superior light harvesting capability and more efficient electron injection into the semiconductor, in photoelectrochemical water splitting.

1 Chapter 1: Introduction

1.1 Energy: an issue for the near future

Contrary to what is commonly believed, our current lifestyle is the result of the cheap price we pay for energy, as it will be showed later in this chapter. But energy is also one of the biggest issues that has to be broached in the near future. In fact, nowadays energy is mainly derived from oil and other not renewables sources, but these sources are going to be depleted and, most importantly, are responsible of the global warming that is destroying so many ecosystems. Burning any carbon-based fuel unavoidably produces carbon dioxide, that is known for being responsible of the greenhouse effect. Nonetheless, it is possible to have a global "zero carbon footprint" combustion: for example, if wood is burnt, CO_2 is released, but it is the same CO_2 that the plant has stored during its life. In this case, the net CO_2 contribution to the atmosphere is zero. The problem arises when fossil fuels are burnt. Fossil fuels are the result of the fossilization of wood and other natural organisms living over 100 million years ago, so that the CO_2 they contained has been fixed as a solid, liquid or gas (coal, oil and natural gas). When these materials are used as a fuel, the CO_2 is released in the atmosphere and, considering also the deforestation ongoing all around the world, our planet is not able to process and store it anymore. This correlation between the use of fossil fuels and global warming is clear if we look at plots showing the mean temperature and the CO_2 concentration in the atmosphere: they show the very same trend (**Figure 1.1**). Even if fossil fuels were inexhaustible sources, it is compulsory to find alternative ways to produce the energy we need to maintain our lifestyle, otherwise we are going to destroy our planet, and finding another one to live in would be even more difficult.

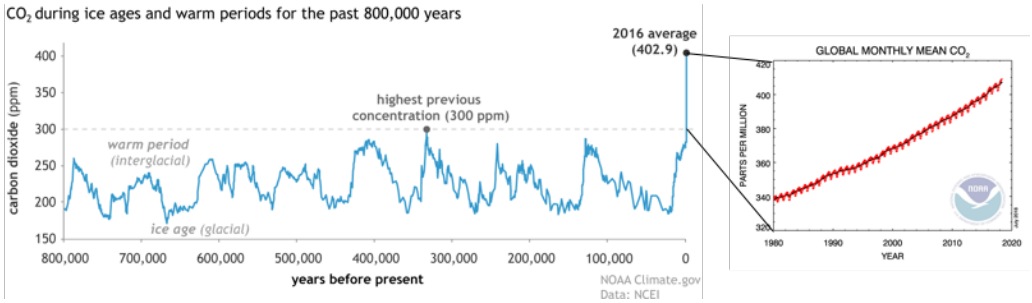

***Figure 1.1**. Left: atmospheric carbon dioxide concentrations in parts per million (ppm) for the past 800 000 years, based on EPICA (ice core) data. The peaks and valleys in carbon dioxide levels track the coming and going of ice ages (low carbon dioxide) and warmer interglacials (higher levels). Throughout these cycles, atmospheric carbon dioxide was never higher than 300 ppm; in 2016, it reached 402.9 ppm (black dot). NOAA Climate.gov, based on EPICA Dome C data (Lüthi, D., et al., 2008) provided by NOAA NCEI Paleoclimatology Program. Right: global monthly mean CO_2 since 1980 from NOAA.*

1.1.1 Energy: how much of it is really necessary?

Along history, humankind has experienced very different energy consumptions, so that energy can be considered strictly linked to social development.

In fact, at the very beginning a man could consume only the energy from food to survive, that is around 2000 kcal per person per day. Then, when primitive men became hunters and gatherers, they required around 5000 kcal per person per day considering food and heat to cook it, and when they started using animals for agriculture and hard works their requirement doubled (primitive agriculture) until reaching 20 000 kcal per person per day in advanced agriculture societies, due to improvements in agriculture and to growth of crafts, commerce and cities. Then industrial revolution started, so at first 60 000 kcal per person per day were spent, and in modern industry this value has doubled, thanks to mechanized farming, energy-intensive industries, and affluent lifestyles. In some nations this consumption is even higher, that is to say 250 000 kcal pro capita in the USA and Canada.[2]

Is such a high energy demand really indispensable to have a good lifestyle? There is a very wide spread in the energy consumed in the different countries of the world, so the question to understand where the need finishes and the waste starts naturally arises.

There are many parameters that can work as an indicator of the quality of life; among them it is possible to choose as an example the infant mortality. An high value means little food, little water and a poor health service, and if hospitals and food are not enough and people cannot be properly cured the quality of life is bad, so the lower this value the better the expected lifestyle. In **Figure 1.2** the infant mortality is reported versus the annual energy consumption per capita expressed in toe (ton of oil equivalent), that is a unit of energy defined as the amount of energy released by burning one ton of crude oil. It is approximately 42 GJ, 10 Gcal or 11.63 GWh. As expected, developing countries usually show a very high infant mortality, while developed ones have a near-zero value. The interesting data in this graph arises when looking at the x-axe: over a certain value of consumption, around 3 toes per year, the mortality does not grow anymore, and instead it can even increase in some cases. An optimal consumption value can thus be defined as 2.8 toe per year, about 77 000 kcal per person per day.[3] As suggested by these data, an higher consumption does not mean a better quality of life, it is just an unmotivated waste of our precious energy, often allowed by its extremely low price in some countries (USA, Saudi Arabia, Qatar). Finally, the last obvious consideration that can be made is that there are enormous differences in energy availability around the world, often reflecting the socio-economic conditions of different countries. Such a big inequality can be a destabilizing factor in international equilibria, since it is intuitive that anybody living with very little energy will try all his best to improve his living conditions, through migrations as it is already happening or even through wars. Solving the energy issue is thus not only a challenge to be broached for science sake, but also for a future of peace and equality.

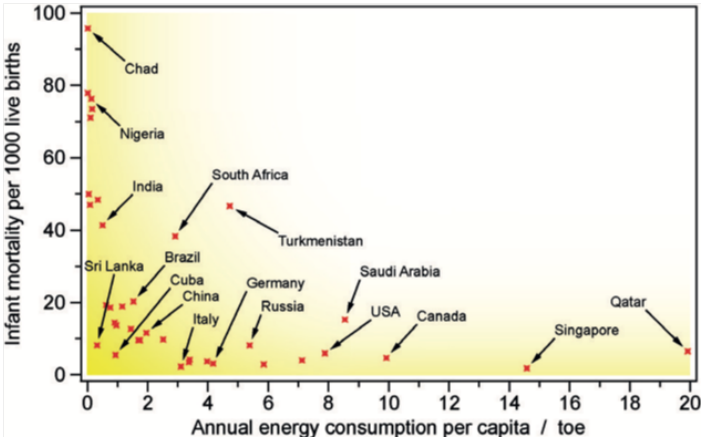

***Figure 1.2**. Infant mortality versus per capita annual energy consumption of selected nations. Reproduced from Ref. 3 with permission from Wiley.*

An example of unmotivated energy waste is linked to food waste, another consequence of consumerism and loss of care for our planet, that also implies a waste of cultivated land, irrigation water and pesticides, and a useless evolution of methane in landfills. In fact, 10% of U.S. energy is used to make food available, such as for packaging, refrigeration, agriculture, transport and sale,[4] and the US Department of Agriculture estimates that between 30 and 40% of food is thrown away from the farmer to the consumer: this means that 3-4% of US energy is wasted too.

1.1.2 Energy producing other energy (EROI)

It is intuitive that energy is needed to produce any device, and this is also true when speaking about energy producing devices. So, to produce new energy some energy is needed. There is a parameter indicating how much the process is efficient, and it is called Energy Return On Investment (EROI).[5] EROI is a unitless ratio, defined as the ratio of the gross energy output over the operating lifetime for an energy supply system, and the sum of the energy for manufacture, construction, operation and maintenance, decommissioning and disposal/recycling during the system's project life-cycle. A related concept to

EROI is that of net energy, defined as the difference between the energy acquired from a given source (gross energy, E_{out}) and the energy used to obtain and deliver that energy (E_{in}), measured over a full life cycle:

$$EROI = \frac{E_{out}}{E_{in}}$$

$$net\ energy = E_{out} - E_{in} = E_{out}(1 - \frac{1}{EROI})$$

An high EROI value means that just a small amount of energy has to be used to produce a very big amount of new energy, and this usually means that energy price is low. Considering 0.38 €/L the present crude oil price, it is cheaper than many natural water or soft drink bottle, and even considering 1.60 €/L the price for petrol (taxed over 65%), it is still less expensive than the price of some expensive famous brand water bottles (for example, Perrier water price is over 3 €/L). It is thus clear that a high demanding lifestyle like the one we are used to is possible only with high EROI energy sources and the low price we pay for them.[3]

In **Figure 1.3** EROI and net delivered energy are reported for different energy sources.

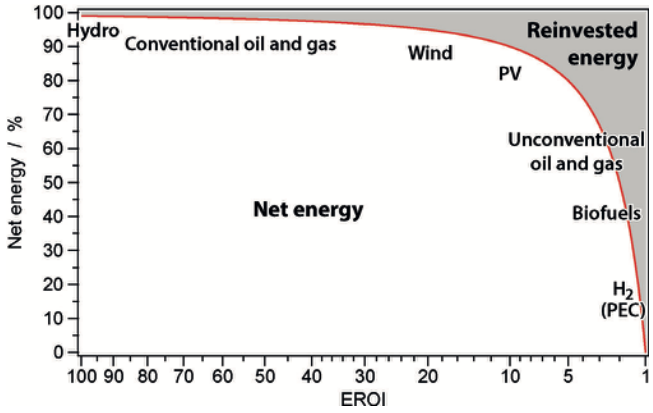

***Figure 1.3**. Relationship between net delivered energy and decreasing EROI. A qualitative indication of net energy obtainable from some selected energy sources or technologies is shown. The grey portion represents the energy to be reinvested to convert primary energy into usable energy. Reproduced from Ref. 3 with permission from Wiley.*

It is possible to see from the plot that till around an EROI of 10 just a small percentage of energy has to be reinvested to produce other energy, then there is a deep drop and more and more energy is required while a small amount of it is produced.

Of course, the EROI value for the same energy source can change over time, for example EROI for oil in the USA has declined from about 20 in 1970 to about 11 in 2013, and EROI for source of oil difficult to extract (ultra-deep-water, oil shale) is even lower. An opposite trend should be observed for developing technologies, such as photovoltaics (PV): the higher the efficiency, the more power can be delivered and so the higher the EROI. PV is already in a good range, in fact in the last decades the price for PV energy has dropped and it is now competitive with other sources. The worst source from this plot seems to be hydrogen made with PhotoElectrochemical cells (PEC), but it should be emphasized that this is a completely new technology, with all the limitations of emerging technologies. An improvement can be expected for sure when more and more examples of this devices will be available, so the present very low EROI should not be seen as a limitation but as a stimulus to focus research in this field.

1.1.3 Looking for clean energy

It is clear that energy is essential to live in acceptable conditions, but it is mandatory to produce it in a clean way to avoid pollution and a further increase in global temperature. Renewable energy exists since long ago, wind mills and water mills can be considered one of the first examples, but also electricity has been produced since the XIX century employing water. The first hydroelectric plant was put into operation on September 30, 1882 at Appleton, Wisconsin, with an output of 12.5 kW. It was called the Vulcan Street Plant and it was the first Edison hydroelectric power plant. Later on, many other plants were built, and Italy hosts many of them. Besides water, there are other sources for clean energy, such as sun, geothermical, wind, and many of them would be enough to cover the global energy need.

Figure 1.4 sketches the potentially available energy for each renewable source and the technically exploitable portion with the present technology. In that plot, the current primary energy consumption has been assumed as 1, and energy sources have been calculated as multiples of it.[6]

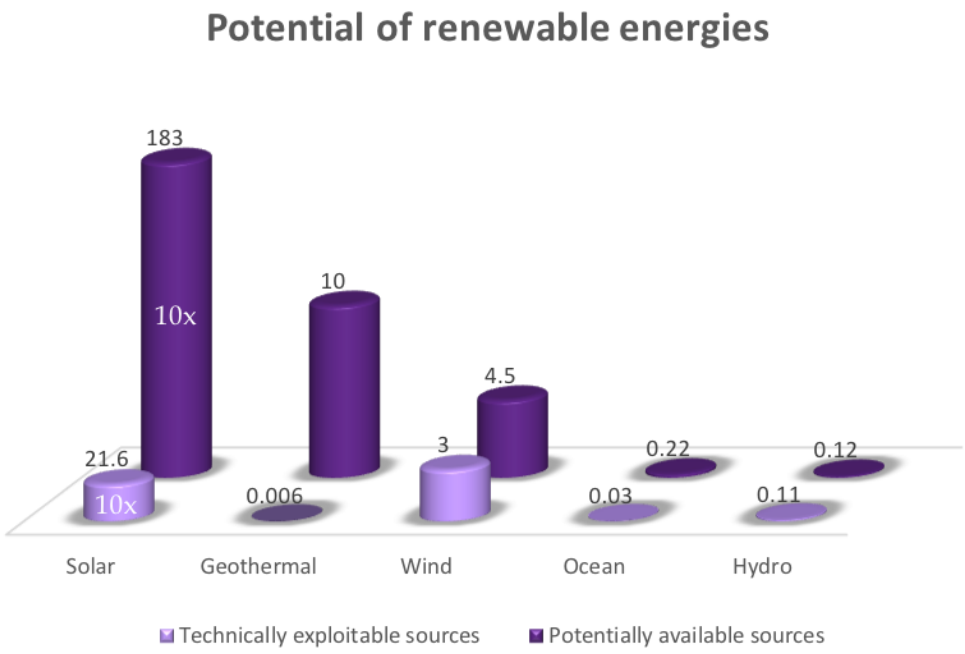

Figure 1.4. *Schematic representation of the relative amounts of potentially available (light colour) and technically exploitable (dark colour) renewable energies, compared to the world current primary energy consumption assumed as 1. Solar energy bars have been reduced to 1/10 for better readability.*

The plot clearly shows that it would be possible to rely on renewable sources alone even today, since either wind and solar energy would be enough to fulfil our needs; other sources instead could be interesting with an improved technology to collect them.

The most promising energy source is sun, since the power coming from it is orders of magnitude higher than our needs, even considering that they are going to grow in the future due to the developing countries demand (in the last decade, the global primary energy consumption has grown at an average 2.1% per year).[7] According to British Petroleum, in 2014 the average rate of consumption has been 17.2 TW, while 90 PW are coming from sun on Earth's surface every year, so it would be enough to cover 0.16% of Earth with 10% efficient solar panels and our needs would be satisfied.[8]

Unfortunately, at present, renewable energy has just a small share in the world energy production. **Figure 1.5** shows data about the global final energy

consumption: the biggest part is generated by fossil fuels, renewable energies account for the 10.4%, and solar power is just a small portion of that percentage. The good news is that during 2017 the total capacity of photovoltaics (PV) increased by nearly one-third, going from 302 GW to 404 GW,[9] mostly thanks to new installations in China (50% of the market) and India. Developing countries investing in this technology is a good hint of their will to satisfy their energy demand without increasing pollution and CO_2 emissions.

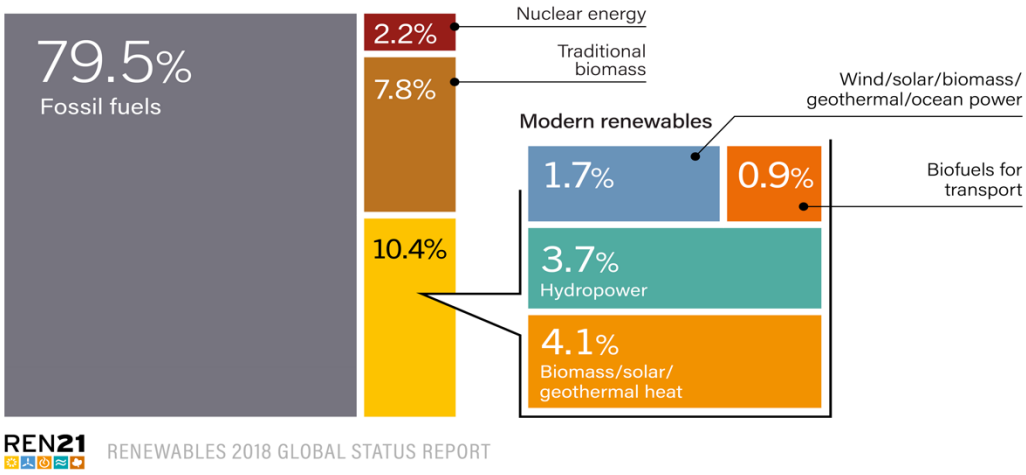

Figure 1.5. *Estimated renewable share of total final energy consumption, 2016, from REN21 Global Status Report, 2018.*

One of the drawbacks of PV energy is that its production is discontinuous, i.e. PV panels do not work in the night and in cloudy days, and another one is that electricity storage is not straightforward. At present, these limitations are overcome by using batteries to directly store electricity and electrolysers to transform electricity in solar fuels such as Hydrogen. Both these solutions mean a further transformation of solar electricity in another device, and this means an efficiency loss for the whole process from sun to energy storage. A more efficient way to obtain the same result would thus be a single device that transforms solar light in solar fuels, exactly as it happens in natural photosynthesis, where leaves transform light and water in carbohydrates for plants feeding. This process is

called artificial photosynthesis and, even if at present time its efficiency is very low, it is a very promising technology for the future.
In this work both the traditional solar cell approach and the innovative artificial photosynthesis one have been afforded, in order to have a wider view of eco-friendly and green solutions for the energetic issue.

1.2 Photovoltaic energy

One fifth of the Total Final Energy Consumption in 2015 was constituted by electricity, and very interestingly 25% of it was produced from renewable sources. The biggest part came from hydroelectric plants (16.4%), then from wind, from Bio-power and 1.9% came from solar photovoltaic (PV).

PV is a very promising technology that could potentially fulfil high energy needs thanks to the very high amount of solar energy hitting Earth everyday, as it was stated in the previous section. 90 PW of solar light arrive every year on almost every part of the Earth, so that electricity could be produced anywhere without the limit of geographic concentration of fields, as it happens with oil, with solar plants where needed. This widespread distribution of an energy source would avoid wars and almost monopolistic price variations, if cheap and abundant-materials-based solar panels were employed.

Sun has an emission spectrum that can be approximated with a 5800 K black-body, but its spectrum recorded on Earth surface is different: some wavelengths in fact are absorbed by our atmosphere, mainly by O_2, H_2O, N_2, CO_2 and O_3, that cuts off the biggest part of the UV portion; furthermore, particulate present in the atmosphere scatters light, particularly the higher frequency blue light (**Figure 1.6**).

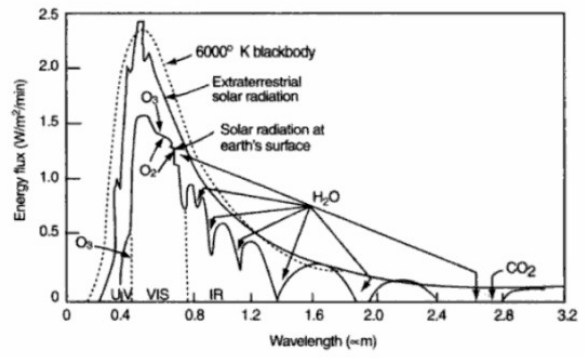

Figure 1.6. *Solar spectrum at the sea level compared with the one outside atmosphere and the black-body emission one. From Krondratjev, K Y., Radiation in the Atmosphere, Academic Press, New York, 1969.*

Of course, these effects are different according to the thickness of the atmosphere that sunlight has to cross, that is lower if it comes perfectly perpendicularly to the ground (Zenith angle = 0°, at the Equator) and increases depending on the latitude, and in the same place it varies with time of the day and with seasons.
In order to have a standard indication for the solar spectrum at a certain latitude, air mass coefficient (AM) has been introduced, and it is defined as follows:

$$AM = \frac{L}{L_0} = \frac{1}{\cos z}$$

where L is the path length through the atmosphere, L_0 is the zenith path length (the path normal to the Earth surface) and z is the zenith angle in degrees.
Outside the atmosphere the AM is set equal to 0, and it is used to characterize devices that have to work in spatial applications such as on satellites. AM 1 means that z = 0°, so it represents the solar path at the Equator. The most used AM value is 1.5, since it is the standard to characterize solar cells working in temperate latitudes, and it corresponds to z = 48.5° (just to give an idea, Italy lies between 35° N in Lampedusa and 47° N in Alto Adige, while Europe spreads from 34° N in Gavdos, Greece, to 71° N in Knivskjellodden, Norway). At that latitude, AM is lower that 1.5 in summertime, but it is higher at dawn and sunset and in winter, so 1.5 is an average over the year.
Varying the AM, also the power density reaching the ground changes: at AM 0, the power density is 1367 W m^{-2}, while at AM 1.5 it is 1000 W m^{-2}.[10] In this way, between 1000 and 2000 kWh hit every square meter of our planet every year, and even low-efficiency solar panels could produce current enough to fulfil a high percentage of our power needs.

1.2.1 Photovoltaic overview

The French physicist Edmond Becquerel first discovered the photovoltaic effect in 1839 while studying electrolytic cells. In 1883 the American inventor Charles

Fritts built the first solar cell, consisting of a junction of selenium and gold, with a 1% efficiency. To have a significant growth in efficiency and thus commercially applicable solar cells it was necessary to wait until the '50s: in 1954 at Bell Labs the first silicon solar cell with a 6% efficiency was announced,[11] and from then efficiency kept on growing and many other materials have been investigated. Technologic improvements allowed a dramatic decrease of solar panel cost: the price of silicon solar modules in 1977 was 76 $ per watt, while in 2018 it is only 0.27 $ per watt.[12]

It is possible to divide solar cells into three generations, according to different degrees of technological advancement and their availability in terms of costs and materials. The first and the second generations employ inorganic semiconductor materials; the first generation is constituted by both monocrystalline and polycrystalline silicon based solar cells that were firstly studied and commercialized and they are the most widespread installed even nowadays since they are very efficient (around 15% efficiency) and very stable (usually they have a 25-years-long life). Thin-film devices instead belong to the second generation, they require smaller quantities of active material than standard silicon cells to reduce costs and use both amorphous silicon and different semiconductors, such as CdTe and CIGS (Copper Indium Gallium Selenide), the efficiency is a little lower (10-15%) but, since the active layer is very thin, they can be a little bit flexible; unfortunately, the production includes expensive steps (such as high vacuum deposition) and they contain scarce and toxic elements, so that they have a limited market. The most recent types of solar cells are included in the third generation, that comprises several devices, both organic and inorganic. The inorganic ones are mainly expensive high performance experimental multi-junction solar cells which hold the world record in solar cell performance, that can be applied only in solar concentrators or in spatial applications due to the high cost. The other solar cells belonging to the third generation instead aim to give a low cost and often portable solution to produce

energy everywhere and comprise organic solar cells (OPV), dye-sensitized solar cells (DSSC), perovskite solar cells (PSC), quantum dot solar cells and also multijunction of these novel categories with silicon solar cells, for example. At the research level there are institutions that certify the advancement in efficiency reached for each existing technology of solar cells; a commonly used example is the NREL chart published by the US National Renewable Energy Laboratory (**Figure 1.7**).[13]

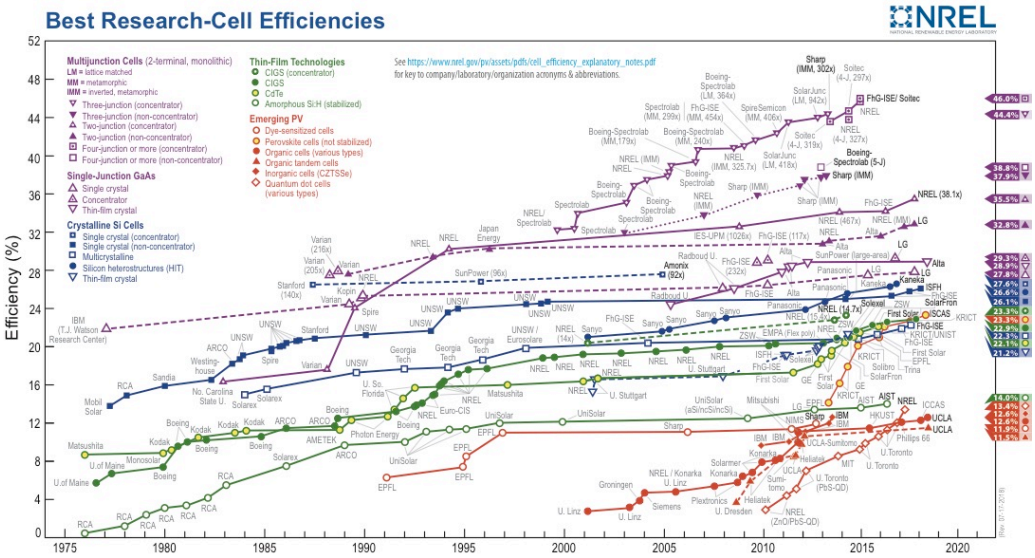

Figure 1.7. *Efficiencies of certified best cells in research conditions from National Renewable Energy Laboratory (NREL) updated to 2018.*

This work will focus on DSSCs since the research group had already gained the know-how both for the synthesis of dyes and for the device assembly. It is worth noting that, even if DSSC efficiency is lower than c-Si one, they have a big advantage, that is the possibility to work even in low-light environment. In fact, while silicon solar cells efficiency is very low when light intensity is low, DSSCs efficiency remains the same or it can even increase (**Figure 1.8**).[14-15] The main possible application for this technology is in fact for indoor solar panels, for example to supply energy to IoT (internet of things) devices.

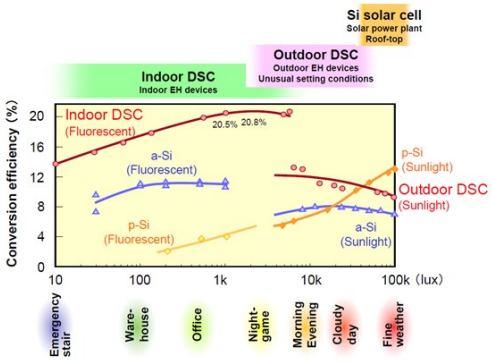

Figure 1.8. *Graph of the efficiency of DSSC modules optimized for indoor applications in comparison with crystalline and amorphous silicon. From Fujikura catalogue (www.fujikura.co.uk/products/energy-and-environment/dye-sensitized-solar-cell).*

The history of DSSCs dates back to the early '80s when the first dyes-sensitizers in the form of organometallic ruthenium complexes with bi-pyridines bi-carboxylated were used to activate the titanium oxide[16] and their development continued in the second half of the '80s using ruthenium complexes with three bi-pyridines bi-carbossilate.[17] A milestone was the famous publication on Nature magazine in 1991 from Brian O'Regan and Michael Grätzel, where they presented for the first time a photovoltaic device based on titanium dioxide functionalized with a trimeric ruthenium complex using bi-pyridines bi-carboxylated as ligands.[18] Since then, various complexes of ruthenium have been tested and, in 1993, Grätzel reported as sensitizers a series of mononuclear ruthenium complexes, the best performing of which was N3, where ruthenium shows two thiocyanate ligands and two bi-pyridines substituted in position 4, 4' with carboxylic acid units.[19] Carboxyl groups are very important because they allow the anchoring of the dye to titanium dioxide and for their conjugation to the pyridine groups. In the ground state electron density is concentrated onto the metal center, but in the excited state, resulting from the absorption of electromagnetic radiation, such density is concentrated on carboxylate groups linked to TiO_2. The thiocyanate groups are electron-donors which increase the absorption coefficient of the complex. Nazeeruddin and coworkers have tested different forms of protonated N3: N712 has four carboxylate groups with tetra-

butyl ammonium salt, N719 has two carboxylate groups and two carboxylic acids.[20-21] The carboxylic acids allow a better anchorage of titanium oxide and higher current, but carboxylates increase the voltage of the cells. Up to now, the best performing cells with ruthenium complexes make use of N719 dye and the redox couple I^-/I_3^- as the electrolyte (12% efficiency). It is now normal practice for each new tested dye, to use N719 as reference. Changes on the molecular structure allowed synthesizing many other photo-sensitizers. For example it was synthesized the Z907, in which a bi-pyridine bi-carboxylate substituent is replaced by a nonyl-4,4'-bipyridine.[22] The presence of alkyl hydrophobic chains makes the molecular structure more stable. The cell constructed making use of hexa-decyl-phosphonic acid as co-absorbent showed efficiency around 7%, which is also maintained when subjected to thermal stress. The structure of the two references dye, N719 and Z907, is shown in **Figure 1.9**.

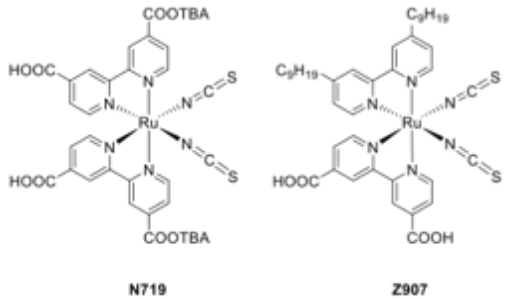

Figure 1.9. *Structure of the two references dye, N719 and Z907, presented by Nazeeruddin in 1999 and Wang in 2003.*

With the aim of improving the optical properties of such complexes, in the following years, many new ruthenium-based complexes have been synthesized, in which one of the two bi-pyridine ligands has been replaced with more conjugated systems. All these derivatives have showed improved optical properties, but lower efficiencies than those obtained with the reference dyes.[23-28]

Also metal free organic dyes have been deeply investigated. These new dyes with a dipolar donor-acceptor molecular structures such as D-π-A, in which the

acceptor is also linked to the anchoring group that is generally a unit vinyl-cyano-acetic. As donor groups, different electro-rich donor moieties have been investigated and different π-spacers have been bonded on each. As for the latter, generally the most efficient are the thiophenic or poly-thiophenic ones. Among the different investigated donors groups, the most performing were found to be coumarin, indolines, tetrahydroquinoline, carbazoles, dialkylaniline, and especially triphenylamine. Further structural modifications, followed by an optimization of the devices have allowed obtaining results comparable with those of the organometallic reference dyes.[29-34] The literature on these compounds is very extensive (**Figure 1.10**), since it is simple from the synthetic point of view to obtain a great variety of molecules. In particular, using as spacers 3-hexyl-thiophen unit, a 8.5% efficiency has been obtained.[35] The best efficiencies with organic dyes using triphenylamine as donor group have been obtained with alkoxy-triphenylamine linked to thieno-thiophene spacers. In particular, the C217, in which a tri-phenylamine is conjugated to a EDOT and a thieno-thiophene, has allowed a record efficiency of 9.8%.[36]

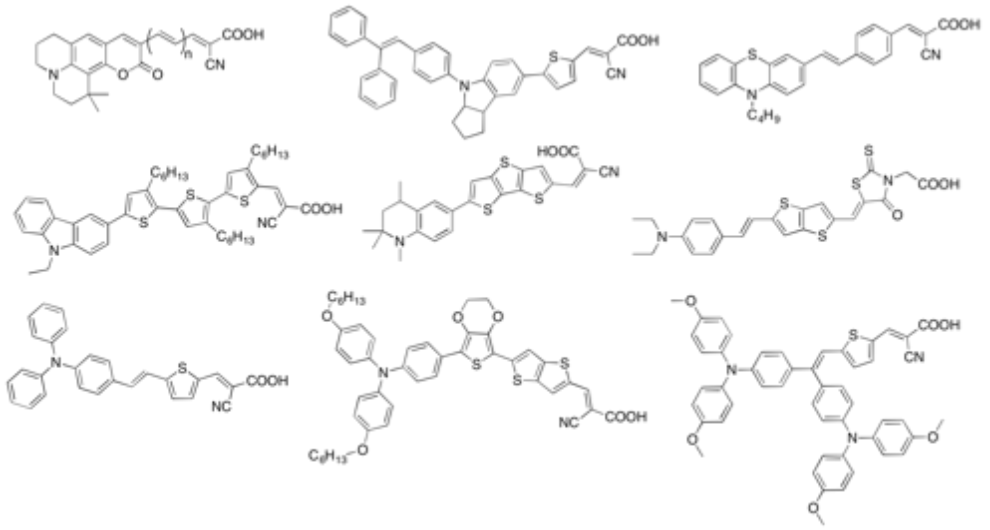

Figure 1.10. *Examples of linear organic dyes.*

More recently, Abbotto and co-workers have published a major work on a new class of multibranched triphenylamine based derivatives.[37] These derivatives

present a structure of the type D-(π-A)$_2$, where a single triphenylamine donor is connected to two conjugated π-spacers and, as a result, two anchor groups. This configuration allows to obtain a longer time stability compared to the corresponding linear system. Another important development of this class of compounds was subsequently proposed by synthesizing a system in which the two branches exhibited different structures connected to a more complex donor centre with the objective of improving the optical properties.[38-39] The validity of this approach (**Figure 1.11**) has been demonstrated by many other works published in the following years.[40]

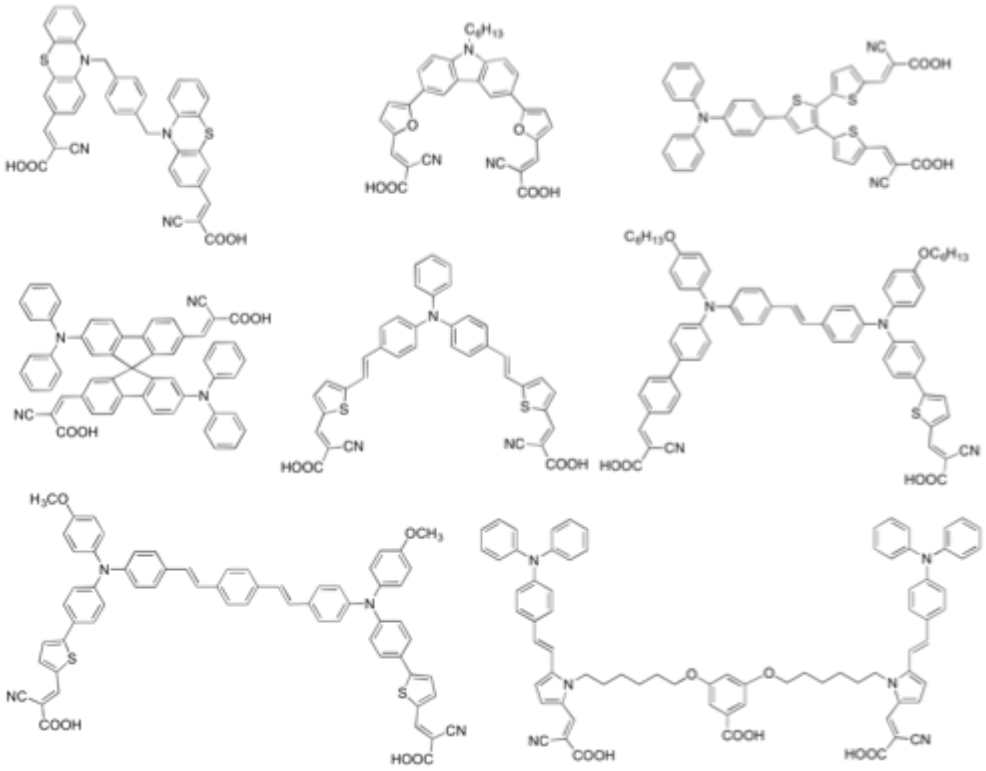

Figure 1.11. *Examples of multibranched organic dyes.*

After such a strong development of sensitizers, the focus has shifted to the development of the device to make it more commercially attractive. Indeed, a weak point of traditional DSSC technology not to be neglected is the presence of a liquid electrolyte containing iodine. Up to now, such an electrolyte is the best

redox mediator in order to obtain high efficiencies. There have been some attempts to replace iodine with more efficient redox systems such as the redox couple Co^{2+}/Co^{3+} with which, using a zinc porphyrin YD2-o-C8, Yella and coworkers have reached and exceeded the previous record efficiency bringing the value 12.7%.[41] Hanaya and coworkers hold the current record efficiency reported in literature of 14.7% using a cosensitized photoanode with an alkoxysilyl-anchor dye ADEKA-1 and a carboxy-anchor organic dye LEG4 in presence of a cobalt based electrolyte.[42] This outstanding result, however, was not enough to push the commercialisation of this type of devices because, once again, made with sensitizers with a complex synthesis and in the presence of a liquid electrolyte particularly toxic due to the presence of cobalt salts. In order to make these devices attractive to the market, it was necessary to develop solid state systems, thus eliminating the risk related to the presence of electrolytes containing solvents and toxic or corrosive components,[43-44] or to develop new eco-friendly electrolytes, for example using water as a solvent. At the beginning of studies on DSSCs, water was seen as a poisoner to be completely avoided because it was considered to be responsible of the performance decay of cells along time, even if in the '80s it was a commonly used solvent in DSSC ancestors (also the aforementioned work from Grätzel of 1988 used a water based electrolyte). A study from Lindquist in 1998 verified the effect of water contamination in a iodine-based organic electrolyte solution and proposed some hypothesis: water could coordinate with the TiO_2 surface Ti atoms, thus limiting the I_3^- recombination with TiO_2 conduction band and increasing the open circuit voltage (V_{oc}), but at the same time water significantly reduced the short circuit current (J_{sc}) due to a possible desorption of the dye from the semiconductor surface following the hydrolysis of carboxylate anchoring moieties, resulting in the carboxylic acid form of the free dye.[45] After a paper by O' Reagan published in 2010 in which water was added in different proportions to an organic electrolyte with little decay in the performance the trend has been reversed, and

many researchers are now working on aqueous DSSC. Many works followed a similar path of mixing water and organic solvents, often adding surfactants for a better compatibility, but there are also many examples of electrolytes that adopt only water as solvent.[45-47] The efficiencies unfortunately are usually very low, ranging from less than 1% to a record of 6%.[48]

A problem to address when considering aqueous electrolyte solutions is the hydrophilicity of the dye, that is responsible of the very important aspect of photoanode/electrolyte interface. Three main approaches have been proposed in literature to avoid dye desorption in water due to carboxylic bond hydrolysis: one is to use traditional ruthenium complexes in strongly acidic pH conditions, but these cells are not stable for a long time,[49] or to protect the dye with an inorganic coating using atomic layer deposition (ALD), improving the stability, but this is a very expensive technique.[50] Another possibility is to employ hydrophobic organic dyes, but the hydrophobicity hinders the electrolyte penetration in the cavities of the mesostructured photoelectrode, limiting the photocurrent of the cell. The third possible approach is to use hydrophilic dyes specifically designed to work in an aqueous environment that offer a good wettability of the electrode;[51] it is also possible to protect the TiO_2 anchoring group using an hydrophobic one, but the stability is short.[52] C. Barolo and coworkers carried out an exhaustive work testing nine sensitizers of very different nature, changing the anchoring unit, the polarity of the molecular backbone, the absorption region within the visible spectrum, and the presence of metal centers, to correlate the molecular structure to stability in water. Indolenine sensitizers gave the best results, even if the photovoltaic efficiencies were very low (0.12 to 0.20%).[53]

Once the dye has been chosen, it is necessary to optimize the electrolyte components: usually, if a completely aqueous cell is considered, inorganic salts are a common choice, because of their good solubility in water and also because they are not toxic like ionic liquids and they are cheaper. The common choice is

thus among iodine salts (NaI, KI, LiI), in variable concentrations and proportions to I_2, adding in some cases other components such as guanidinium thiocyanate (GuSCN) and chenodeoxycholic acid (CDCA).[47, 51] The efficiencies reported are usually lower than 2%. Ionic liquids have been compatibilized with water in various dilutions by adding surfactants like Triton X-100, resulting in similar efficiency.[46] Finally, good results have been obtained using cobalt based electrolyte solutions, with efficiency over 5%, but cobalt salts are very toxic, so they are in contrast with the eco-friendly aim of aqueous DSSC.[54-55]

Some improvements can be obtained when changing the counter electrode, switching from classical platinum to PEDOT over the conductive glass. Both these materials show total wetting upon deposition of water on the surface, therefore the increased photocurrent recorded cannot be ascribed to a better wettability. This improvement has thus been attributed to the high surface area of PEDOT due to a leaf-like structure that increases the catalytic activity. Also a reduced dye desorption has been reported when using PEDOT counter electrodes, ascribed to the ability of PEDOT to include ions in its matrix, that in this way cannot absorb on TiO_2. Efficiency reached 4.04% at 0.5 sun.[51] Finally, PEDOT counter electrodes are cheaper and more eco-friendly than platinum, as they are fabricated from cheap materials and can be electropolymerized at room temperature, in deionized water.[56]

A new frontier for a longer stability of aqueous solar cells is to make more solid the electrolyte. For example, a recent work employed eco-friendly carboxymethylcellulose hydrogels containing both NaI and I_2 with promising electrochemical characteristics on charge diffusion and ionic mobility. Even if they had not outstanding PV properties (the efficiency was 0.72%), they lost only 7% of the efficiency after 29 days of ageing in dark.[57]

1.2.2 Working principles of DSSC

A DSSC is a multi-component device comprising: a) a dye-sensitizer S; b) a n-type semiconductor metal oxide (typically TiO_2); c) a p-type semiconductor or a redox electrolyte (typically a redox couple); d) a transparent working anode and a counter electrode (based on fluorine-doped tin oxide, FTO). Under light irradiation the sensitizer S is excited to state S* from which an electron is injected into the conduction band (CB) of TiO_2, leaving the dye in its oxidized state S^+. The electrons collected at the photoanode are then transferred through the external circuit to the counter electrode where, via Pt catalysis, they reduce the electrolyte that then regenerates the sensitizer ($S+ \rightarrow S$). If a p-type semiconductor is used in place of the electrolyte (solid state devices), dye-regeneration occurs via hole transfer from S^+ to the HOMO of the hole transporter (**Figure 1.12**).[58-59] A DSSC is a very efficient device where, formally, one photon is converted into one electron without permanent modification of any component. In addition to the main processes, a number of undesired pathways and losses are present including recombination of injected electrons from TiO_2 to either S^+ or the oxidized form of the electrolyte, incomplete light harvesting, and inefficient electron transfer from S*. The main source of loss-in potential of a DSSC is the high overpotential needed to regenerate the dye, which strongly limits the maximum attainable photovoltage.[60]

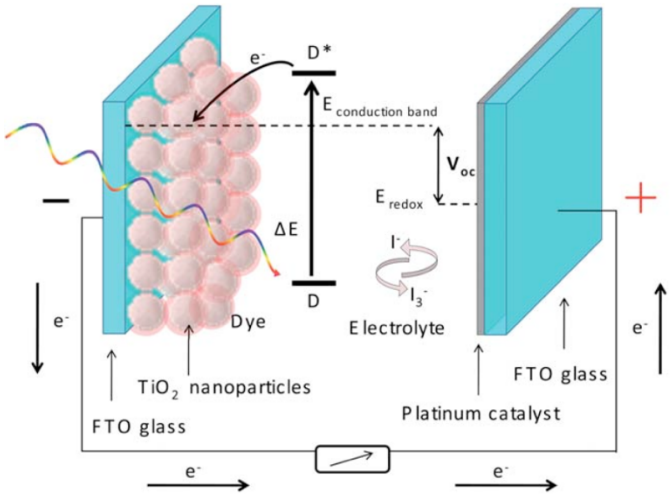

Figure 1.12. *Scheme of a dye sensitized solar cell. Reproduced from Ref. 59 with permission from The Royal Society of Chemistry.*

The performance of a DSSC, or in general of a PV cell, is determined by measuring the overall power conversion efficiency (sometimes referred to as PCE) from the ratio of maximum output power density (P_{out}, in W m^{-2}) and the input light irradiance (P_{in}, in the same units) as shown below. Under standard reporting conditions the light intensity P_{in} is 1000 W m^{-2}, the sun spectrum is AM 1.5 G,[10] and the sample temperature is 25 °C.[61-62]

$$\eta = PCE = \frac{P_{out}}{P_{in}}$$

According to the Shockley-Queisser model, the maximum theoretical efficiency for a single junction device under non-concentrated sunlight is ~30%.[63] The maximum power point P_{out} of a cell is given by the following equation where J_{mp} and V_{mp} represent the current density and voltage at the maximum power point.

$$P_{out} = V_{mp}J_{mp}$$

By defining the fill factor FF as the ratio (values between 0 and 1) of P_{out} and the product of the maximum attainable voltage (open circuit conditions) V_{oc} (in V) and current density (short circuit conditions) J_{sc} (in mA cm^{-2}), the efficiency

relationship can be rewritten as follows, which is used to determine the cell performance.

$$FF = \frac{P_{out}}{V_{oc}J_{sc}}$$

$$\eta = \frac{V_{oc}J_{sc}FF}{P_{in}}$$

The J_{sc}, V_{oc}, and FF values are measured by plotting the current density as the bias voltage is varied while irradiating the PV cell by means of a calibrated solar simulator. A typical diode current/voltage characteristic is shown in **Figure 1.13**. DSSC researchers usually report J and V as positive values, but other J/V curve notations are used as well.

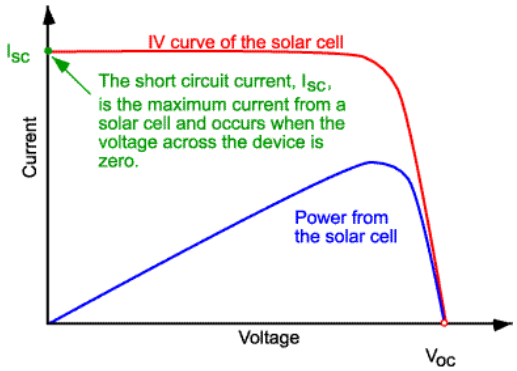

Figure 1.13. *Current-voltage characteristics of a DSSC under irradiation.*

An additional PV parameter, which is routinely employed to determine the quality of a PV device, is the external quantum efficiency (EQE), usually referred to as the incident photon-to-current conversion efficiency (IPCE) by the DSSCs community. IPCE(λ) is defined as the number of collected electrons under short circuit conditions per number of incident photons at a given excitation wavelength λ and gives the ability of a cell to generate current as a function of the wavelength of the incident monochromatic light. IPCE is calculated by measuring the short-circuit photocurrent as a function of the monochromatic photon flux.

$$IPCE(\lambda) = \frac{J_{sc}(\lambda)/_{e}}{P_{in}(\lambda)/_{h\nu}} = \frac{hc}{\lambda e} \times \frac{J_{sc}(\lambda)}{P_{in}(\lambda)} = \frac{1240}{\lambda} \times \frac{J_{sc}(\lambda)}{P_{in}(\lambda)}$$

IPCE is determined by the sensitizer light harvesting efficiency at λ (LHE), the quantum yield for electron injection from S* to the semiconductor oxide (Φ_{inj}), and the charge collection efficiency (η_{coll}), the product of the latter two parameters giving the absorbed photon-to-current efficiency (APCE) or internal quantum efficiency.

$$IPCE(\lambda) = APCE(\lambda) \times LHE(\lambda)$$

The integral of IPCE with the AM 1.5 G spectrum gives the photocurrent, which should match the one measured under the solar simulator. Therefore higher IPCE and broader spectra correspond to higher J_{sc}.

1.3 Artificial photosynthesis and Photoelectrochemical Cell

As already mentioned in the previous sections, the need to leave oil and to look for a clean energy source is demanding and cannot be further delayed. Photovoltaics can be a good approach to produce electric current, but it represents only 20% of the world final energy consumption, while transportation uses 32% of it. Unfortunately, if for electricity we already have a 25% renewable share, for transport it is only 3%, with a 2.8% of biofuels and 0.3% of renewable electricity. The problem is that it is not easy to store electrons, so electric cars need big and heavy (and expensive) batteries instead of a 40-60 L fuel tank, and they however have a limited autonomy; the ideal solution would be to efficiently employ solar light to produce a fuel that can be easily distributed and stored, with a fast car refilling. A good chance is represented by hydrogen, that, in principle, could be obtained from the most harmless of reagents: water.

Current transport situation

In Italy, in 2015 petrol was responsible of 91.9% of transport energy consumption; methane covered 2.8% of the consumption, biofuels 3.0% and electricity 2.4% (from elaborazione Gestore Servizi Energetici su dati Eurostat). As of 1st January 2017, 7.8% of Italian car fleet made use of alternative fuels, with a bigger part (5.2%) using LPG, a 2.3% using methane and only 0.3% was represented by hybrid or full electric vehicles (source ACI).

Biofuels are at the moment the principal renewable alternative to fossil fuels for transportation. Biofuels can come from appositely cultivated biomasses (first generation system), that thus compete for land with food cultivation, or they can be obtained from agriculture wastes, such as shells, husks, wood chips or fruit peels (second generation). The latter approach partly solves the competition for farmland, but the "Sun to wheels" conversion efficiency is extremely low, just 0.03%.[3] Chlorophyll photosynthesis has a very low efficiency, around 1%, on the

contrary of what is commonly believed, and the transformation process from biomass to biofuel has an even lower efficiency, so this explains such a small overall value (**Figure 1.14**).[64] On the contrary, photovoltaic panels offer far higher efficiencies, and the transfer of power from panel to car suffers from very little losses.

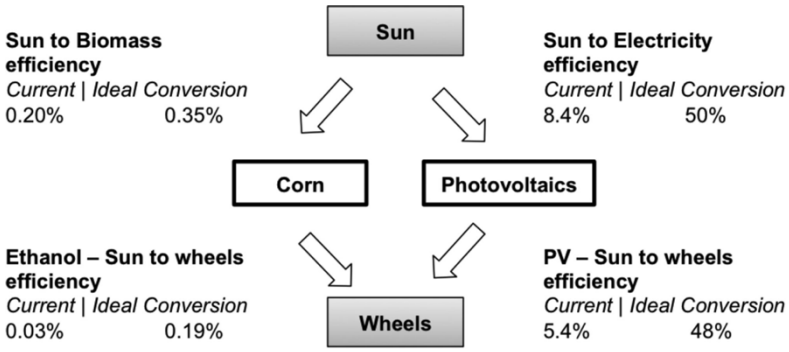

Figure 1.14. *Biofuel and photovoltaic sun-to-wheels pathways and efficiencies. Reprinted with permission from Ref. 64. Copyright 2015 American Chemical Society.*

An electric engine is thus order of magnitudes more efficient than a biofuels combustion one, 5.4% versus 0.03%. It is clear that a sustainable transport system cannot reckon on biofuels, but it has to look at more efficient solutions based on an electric engine.

All over the world, in 2015 more than 1.2 millions hybrid cars have been sold, around 220 000 plug-in hybrids and 325 000 full electric cars, with a constant increase with respect to previous years (data from IEA). Plug-in and electric cars together represented 0.85% of sold cars.

In Italy, in the first half-2018 hybrid and full electric vehicles market had a consistent improvement with respect to the previous year; in particular, 42 308 hybrid cars have been registered (+29.5%), 2 119 plug-in hybrids (+60.3%) and 2 249 full-electric cars, that showed an impressive 123.8% increase. Globally, 3.9% of the market is constituted by hybrid cars while 0.2% is made of electric cars (data from UNRAE).

The best seller full-electric car has been the Smart ForTwo (627 units, price from 23 920 €), followed by Nissan Leaf (457 units, price from 29 885 €), Renault Zoe (426 units, price from 23 300 €) and Tesla Model S (156 units, price from 72 640 €) and Model X (103 units, price from 94 480 €; price data from: Quattroruote). These selling data show that nowadays electric cars of every category are available with affordable prices, spanning from city cars, to saloon cars and to top line cars as Tesla; furthermore, the steep sell increase suggests that Italian population is willing to move to a clean transport system, even bearing the actual limitations of full-electric cars.

Their main drawbacks are due to the battery. First of all, it represents half of the price of the vehicle, and it is subject to ageing in a few years, so that a substitution has to be taken into account.[65] Furthermore, lithium price had a steep increase in the last years: in the six months ending in May 2016, the price of pure lithium being exported to China increased of 42%. Limited reserves, that are mainly localized in single areas, represent an important issue, and they involve the risk of monopolism like what has happened with oil. For instance, approximately 70% of global lithium brine (a mineral mixture, usually found in salt-lake basins, that is the main source for lithium production) resources are located in just four countries, Argentina, Bolivia, Chile and China, even if other lithium sources can be exploited.[66] Li-ion batteries have an high power density and are lighter than other batteries, but they however increase the weight of the car, require space and reduce the performance.[67] Finally, batteries offer a limited autonomy to cars (usually about 200-300 km, even if Tesla Model S reaches 600 km of possible distance covered) and require far more time to recharge than oil refilling, usually between 2 and 6 hours for a full charge.

A not-too-futuristic solution to these problems could be represented by fuel cell vehicles employing hydrogen as a fuel: some models already exist, such as Toyota Mirai, Hyundai IX-35 Fuel Cell and many buses for public

transportation, working for example in Milan and in Bolzano, where the first Italian public hydrogen filling station has been built in 2015.

Already in 1874, the day-dreamer writer Jules Verne published the novel "The mysterious island" where he already imagined a future where water would have been a fuel: "*I believe that water will one day be employed as fuel, that hydrogen and oxygen which constitute it, used singly or together, will furnish an inexhaustible source of heat and light, of an intensity of which coal is not capable.... Water will be the coal of the future*".

Not long after that, at the beginning of the twentieth century, hydrogen was used for street lighting in a mixture called "town gas", obtained from coal and water, and combined with carbon monoxide.[68] Hydrogen as a fuel was then forgotten until the 1970s,[69-71] when people started to be aware of the expected depletion of oil reserves and anthropogenic global warming, which is related to excessive emissions of CO_2.

Hydrogen is one of the most abundant elements on Earth, but the problem is that it is not present in a free form, it is just 1 ppm of the atmosphere because of its light weight (it can escape gravitational attraction), it has to be produced from hydrogen-rich compounds, and it thus requires energy. This is why hydrogen is not considered a fuel but an energy carrier, because it is a secondary form of energy, like electricity. It also has some drawbacks: it is highly flammable and burns in air at a very wide range of concentrations. At room temperature, uncompressed hydrogen occupies 11 250 L kg^{-1}; in a high-pressure (35.5 MPa or 350 atm) steel tank the volume reduces to 56 L kg^{-1}. Hydrogen liquefies at -253 °C (20 K). Liquefied hydrogen occupies only 14.1 L kg^{-1}. Hydrogen energy content is very high, 120 MJ kg^{-1} (33.3 kWh kg^{-1}), compared to 44.4 MJ kg^{-1} (12.4 kWh kg^{-1}) for gasoline.[72]

At the moment, the cheapest way to produce hydrogen is by steam reforming of methane:

$$CH_4 + 2H_2O \rightarrow 4H_2 + CO_2$$

This is a multi-step reaction that leads to carbon dioxide as a side product. When produced in this way, hydrogen cannot be considered a renewable source, since it does not solve the problem of oil running out and CO_2 emission. Only about 4% of hydrogen is now produced by electrolysis of water, that in principle is the only clean way to obtain it. Water can be split into its components, hydrogen and oxygen, when enough energy is supplied, exactly as it happens for example during photosynthesis:

$$2H_2O + h\nu \rightarrow 2H_2 + O_2$$

The challenge is to find a clean way to let this reaction happen, either as clean electricity or with innovative devices directly transforming water and photons into hydrogen.

Nowadays, the main alternatives to fossil fuels to produce electricity are nuclear power, hydroelectric power, wind power and photovoltaics. The first one is clearly an option to be discarded; in fact, even if nuclear plants do not release carbon dioxide, they produce a lot of radioactive wastes that can just be stored for centuries and millennia as long as they are not toxic anymore. Furthermore, to produce energy enough to obtain hydrogen only from electrolysis, more and more nuclear plants than currently present should be built, something like twice the world nuclear capacity only to fulfil USA needs for transport.

Luckily, in many countries hydroelectric power is already widespread employed, but it is already almost at its limit: in USA and Europe 70% of the potential sites are already exploited; more possibilities are present in Asia and Africa, but dams construction would mean serious damages for the environment.[73]

Photovoltaics state-of-the-art and perspectives have been previously illustrated; wind power is at the moment the "king" of renewables, so in the near future it is the most promising candidate for massive electric power production.

Once resolved the problem of the production of hydrogen, there are still many issues to be solved, such as the storage. Hydrogen is currently used in its

compressed form in vehicles, usually hold under 350 or 700 atm (35.5 or 71 MPa) in tanks made of very expensive innovative light-weight materials, such as carbon fibre with metal (aluminium or steel) or polymer (thermoplastic) liners. Even at 700 atm, hydrogen has a per-volume energy content that is 4.6 times lower than gasoline, which means that the hydrogen tank must be much larger, and it cannot use any shape, it has to be cylindrical to apply an uniform pressure all over the container. Furthermore, it has to be insulated and to assure that no leaks are present, since hydrogen is dangerous and explosive. And even with the best insulation possible, hydrogen is so small that it will however be able to evaporate, with a 1-5% loss daily from the tank, and this is a serious issue when considering car parked in the same close place for long periods.

Another issue, only partially solved, is how to use hydrogen as a fuel. It could be employed in internal combustion engines, but its density is so low that the car would have a very limited autonomy, or, as it is already happening, in fuel cell electric cars. A fuel cell is an electrochemical cell that produces electricity from the reaction of a reductant (fuel), in this case hydrogen, with an oxidant (usually oxygen coming from air) in the presence of an electrolyte, converting chemical energy into electric energy.[74-75] As long as reactants flow in the cell, it can work virtually continuously. The working mechanism is completely different from a combustion engine, and, since no conversion of heat is involved, fuel cell efficiency is not limited by the Carnot cycle. For hydrogen fuel cells, the theoretical efficiency limit is 83%, but the working efficiency depends on the amount of power they have to supply. If working between 0.6 and 0.8 V, hydrogen fuel cells efficiency is between 45 and 65%. In cars, the efficiency is about 50%, and the other 50% is dissipated as heat (fuel cells usually operate at 70-85 °C).

Of course, a cell filled with a liquid electrolyte would not be suitable for practical application outside a laboratory, so the electrolyte is replaced by a proton exchange membrane (PEM), made of a polymer electrolyte saturated with water

(usually a perfluorosulfonic acid) that allows only proton migration.[74] In this way, hydrogen is split into electrons and protons at the anode side of the fuel cell by a platinum catalyst; protons migrate through the PEM while electrons are forced to go into the external circuit, generating electric power; protons and electrons recombine with oxygen at the cathode thanks to another platinum catalyst and produce only water as a waste (**Figure 1.15**). A fuel cell driven hydrogen car is thus a really eco-friendly vehicle, releasing only aqueous vapor in the environment. The major limitation to this technology, apart from the production and distribution of hydrogen, is the high cost of fuel cells, since both platinum and PEM are really expensive. Furthermore, platinum can be poisoned even by extremely low concentrations of CO, that is commonly present in hydrogen made by steam reforming.

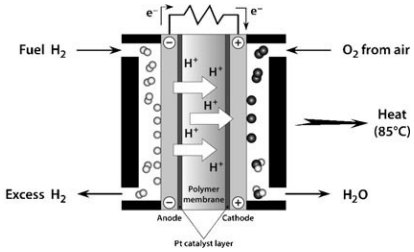

Figure 1.15. *Scheme of a proton exchange membrane (PEM) fuel cell. Reproduced with permission from Ref. 72.*

1.3.1 Photoelectrochemical cell and dye-sensitized water splitting

It is possible to split water into hydrogen and oxygen applying a potential higher than 1.23 V, that is the potential of water decomposition reaction, and it corresponds to a radiation of approximatively 1 000 nm. The first example of a device able to exploit this idea is the photoelectrochemical cell (PEC) of Fujishima and Honda, published on Nature in 1972.[76] Their active material was a single crystal wafer of titanium dioxide, so it could only absorb UV photons; a photocurrent a little higher than 1 mA cm^{-2} was reported. After this paper, many efforts have been made all around the world to find an active material that could absorb visible photons, usually employing other inorganic oxides such as bismuth vanadate ($BiVO_4$), tungsten oxide (WO_3) and hematite (Fe_2O_3),[77-79] or

more efficient multijunction electrodes,[80] but generally they absorb only wavelengths shorter than 500 nm, exhibit poor hole transport properties, and require large bias voltages. Instead, anchoring a dye to an oxide such as TiO_2 allows a fine tuning of absorbance and electrochemical properties in order to match both solar spectrum and the other components of the device. The final aim is to assemble a system mimicking the natural photosynthesis in plants, a very complex process whose function is not an efficient energy conversion, but to let plants survive and reproduce. The photosynthesis efficiency in full light is in fact only 1-3%.[81-84] The dye-sensitizing approach resembles what has been done also in DSSC, decoupling light absorption, catalytic and transport functions of the electrode. Actually, DSSCs can be considered a particular class of PEC, where the anode reaction is simply the reverse of the cathode reaction and the cell generates electricity; in fact, DSSCs are known also as regenerative PEC. In a water splitting PEC instead, the anodic reaction is different from the cathodic one and oxygen and hydrogen respectively are produced. A PEC is constituted by two electrodes, anode and cathode, that can in principle be both photoactive, made of a semiconductor absorbing a proper dye (ideally, two dyes with complementary absorption spectra should be used); on the electrode or in the aqueous electrolyte solution of each compartment a proper catalyst is present, either a Water Oxidation Catalyst (WOC) or a Hydrogen Evolution Catalyst (HEC). The device is completed by wires connecting the electrodes and the compartments are separated by a proton exchange membrane (PEM) or by a glass frit that allow only proton transmission. A scheme of a dye-sensitized PEC (DS-PEC) is depicted in **Figure 1.16**.

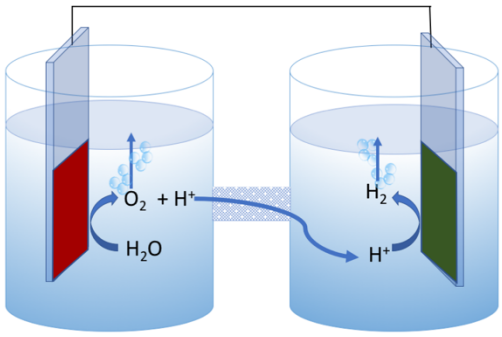

***Figure 1.16**. Scheme of a dye sensitized photoelectrochemical cell.*

The overall reaction taking place in a DS-PEC is the water splitting:

$$H_2O \rightarrow H_2 + \frac{1}{2}O_2 \qquad E=1.23\ V$$

When exposed to sunlight, the dye absorbed onto the photoanode is excited, the excitation is transferred to the conduction band of the semiconductor, and electrons flow from anode to cathode through the external circuit. The WOC oxidizes water producing oxygen and protons and transfers electrons to the dye, while protons generated by water oxidation migrate through the PEM to the cathode. There, the process is symmetric with an opposed charge flow, so the dye, upon absorption of light, transfers electrons to the HEC and returns to its ground state thanks to electrons coming from the semiconductor and the electric circuit. The HEC than uses electrons to oxidize protons and evolve hydrogen.

The working mechanism is similar to a DSSC, the difference is that in DSSCs the dye, after excitation following light absorption, is regenerated by a redox shuttle that completes the photoelectrochemical circuit, while in DS-PEC, if dyes are coupled to proper catalysts, water can serve as an electron source, and protons as electron acceptors for regenerating the oxidized dyes.

Solar-driven PEC water splitting would provide a chemical solution to the intermittency of PV devices, since a large amount of energy could be stored in the chemical bonds of hydrogen or hydrocarbon fuels that could be later released and utilized in fuel cells or internal combustion engines.[85] But PEC can

go beyond water splitting: they can be used to produce value-added chemicals, such as H_2O_2 or $H_2S_2O_8$,[86-87] or biomass-derived chemicals,[88] whose economical values are higher than hydrogen one due to challenges in production or transportation.

n-type organic dyes for DS-PEC photoanode

Light harvesting in natural photosynthesis is accomplished by a hierarchical assembly of accessory pigments that funnel their excitation energy to chlorophyll molecules. Aiming to mimic this natural phenomenon, it is necessary a dye acting as a sensitizer that absorbs visible light, injects an electron into the conduction band of a metal oxide semiconductor, usually TiO_2, and is then re-reduced by the water oxidation catalyst, which oxidizes water to give molecular oxygen and protons. The ideal dye should absorb a significant fraction of visible spectrum, convert all absorbed photons to electron–hole pairs, bind persistently to the surface, and have the appropriate redox potential to drive the catalytic oxidation of water at a WOC. Moreover, the dye should be as cheap as possible: the requirements are almost the same as DSSCs dyes, so ruthenium polypyridyl sensitizers and some porphyrins similar to the ones already tested in DSSCs have been used in DS-PECs,[89] but they often use rare elements, while earth-abundant catalysts and sensitizers will be needed for large-scale deployment of artificial photosynthesis.[90] This suggests that research should focus the attention on the development of fully organic dyes, that are terrestrially-abundant and can thus be low cost, just like what has happened in the extensive research for better DSSCs dyes; a few purely organic sensitizers have been published.[91-94] Some examples both of metal complexes and of metal-free dyes are depicted in **Figure 1.17**.

The chemical bonding of the dye to the high surface area of the semiconductor oxide is an important and subtle issue. Carboxylic acids are the most frequently used linking groups in dye-sensitized solar cells (DSSCs), but photoanodes for water splitting necessarily operate in solutions that contain water, making

hydrolysis of the carboxylic acid–metal bond a significant problem. Under the aqueous conditions, phosphonate linkers provide a more robust linkage to the oxide surface.[95-97] The performance of phosphonate-functionalized dyes is generally comparable or better than that of carboxylate analogues under non-aqueous conditions because of reduced dye desorption, and in aqueous environment it is possible to reduce it by using multiple phosphonic functionalities, even if this leads to a decrease in the electron injection efficiency of the dye.[98]

After choosing the right anchoring group, the dye molecule has to be designed so that: (a) the photosensitizer absorbs visible light as much as possible, and even the near-infrared (NIR) part; (b) the LUMO level of the photosensitizer is more negative than the CB edge of the n-type semiconductor (SC) to facilitate efficient electron injection after photoexcitation; the HOMO level of the photosensitizer, on the other hand, has to be positive compared to the catalytic onset potential of the WOC for oxygen evolution; (c) the photosensitizer is photo and electrochemically stable.

Another aspect that has to be taken into account is how much hydrophilic the dye should be. A hydrophobic dye, in fact, could keep the water far from the SC surface, but on that surface usually there is also the WOC that has to be close to water in order to work. On the other hand, a very hydrophilic dye could prefer to detach from the surface and dissolve into the water, thus making the photoanode useless. Much attention has to be paid in balancing these opposite behaviours.

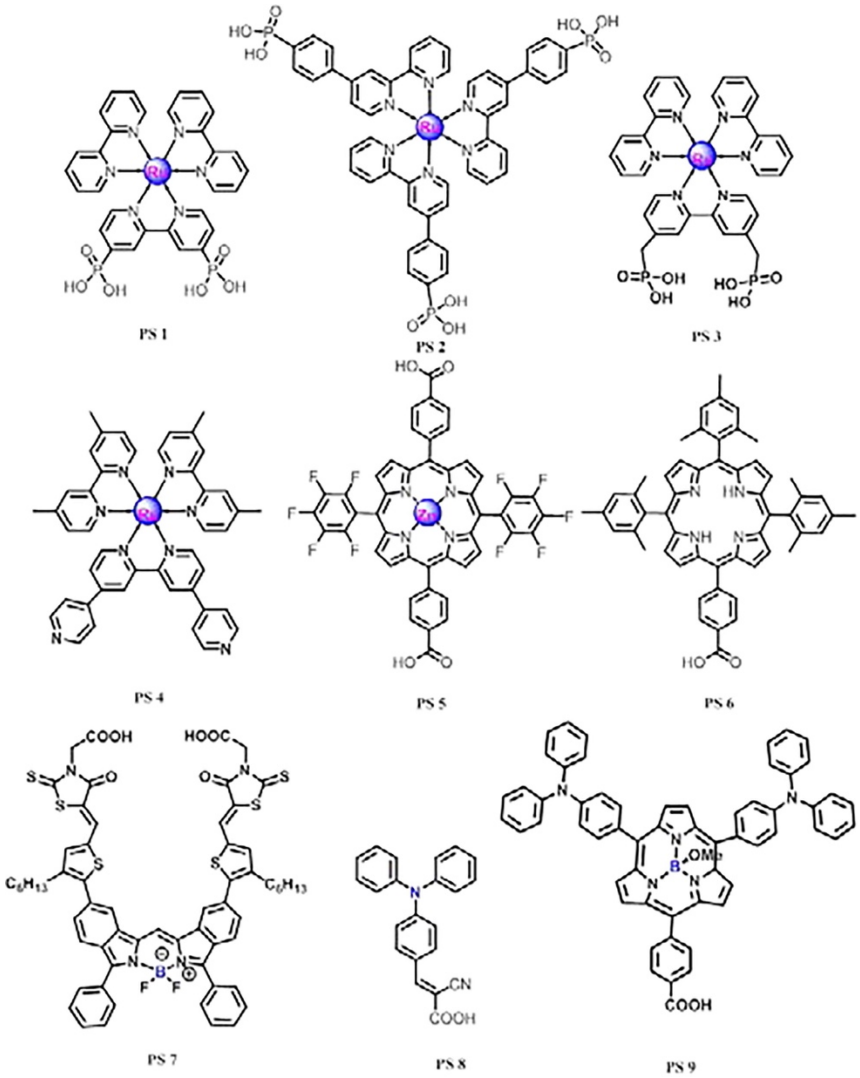

Figure 1.17. *Structures of different dyes tested on photoanodes in DS-PECs. Reprinted from Ref. 89, Copyright 2018, with permission from Elsevier.*

WOC for the anodic compartment

The preparation of a photoanode for a PEC device is pretty similar to the one used to prepare the photoanode in DSSC cells. The big difference is that, besides the dye, it is necessary to load a proper catalyst on the SC surface, in particular a WOC. An ideal WOC must collect four oxidizing equivalents per oxygen molecule generated, facilitate the formation of molecular oxygen, and be

chemically stable. Literature suggests us several routes and several catalysts. As for the dyes, the catalyst should be a cheap compound, such as an organic molecule. Up to now, the most used catalysts are crystalline IrO_2,[90, 93, 99-100] Ir[101-102] or Ru complexes,[89, 103-104] polyoxometalates (POM) based on Ru, Co or Mo,[105-106] but there are also some examples of purely organic molecules.[107] Some published molecules are depicted in **Figure 1.19**.

Unfortunately, heterogeneous WOCs are usually not very simple to synthetize, because purification and characterization of metallo-organic compounds can be challenging. One of the most commonly used WOC in literature is the $Ru(bpa)pic_2$ (Ru(II)(2,2'-bipyridine-6,6'-dicarboxylic acid, bpa; 4-picoline, pic)) depicted in **Figure 1.18**, firstly synthetized by L. Sun and coworkers,[108] and from this molecule many others can be derived.[109-111] It is evident that this molecule does not have any anchoring group, so it can be employed only dissolved in the electrolyte solution of the PEC, even if in this way the efficiency of the catalytic process is lower. If carboxylic or phosphonic acid groups are integrated in the same or in similar complexes, it is possible to chemisorb them onto the TiO_2 layer simply soaking the electrode in a WOC solution. After this, electrodes are soaked in the dye solution as for DSSCs.

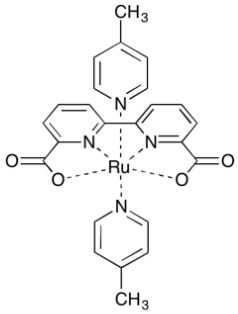

Figure 1.18. *Structure of reference WOC $Ru(bpa)pic_2$.*

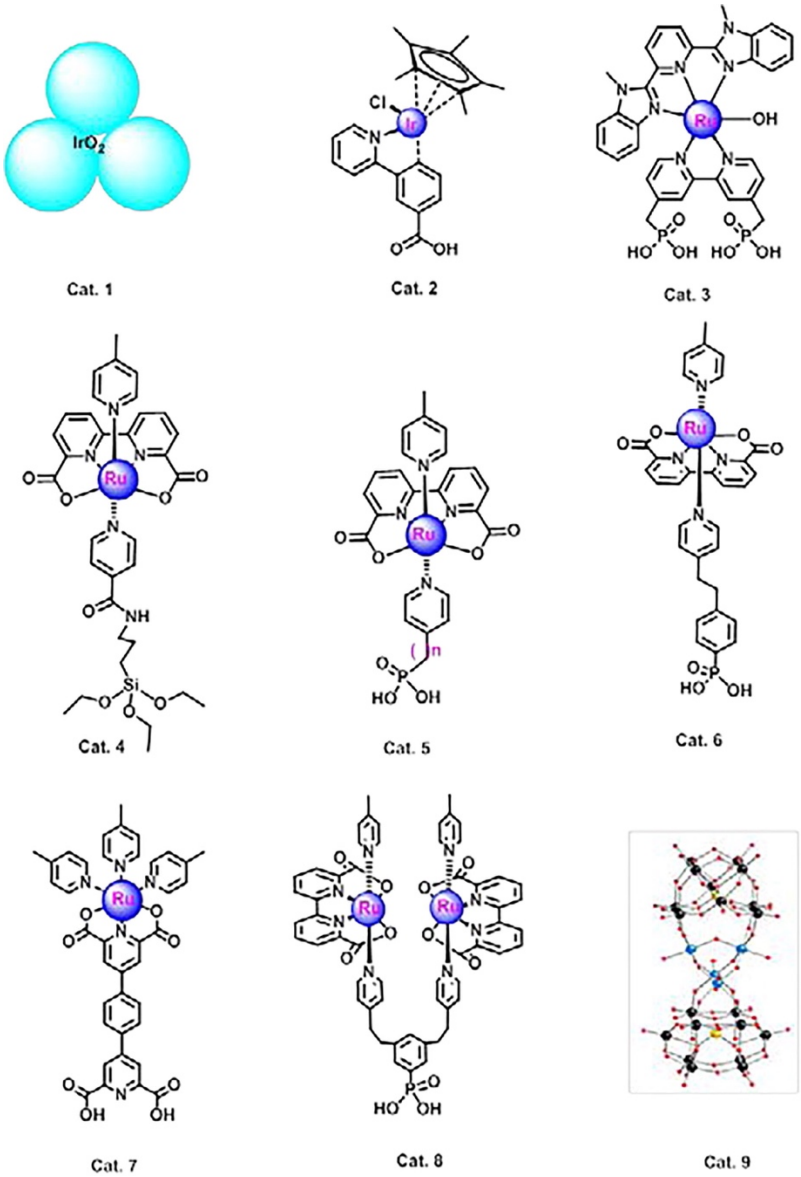

Figure 1.19. *Structures of some water oxidation catalysts published for using in DS-PEC. Reprinted from Ref. 89, Copyright 2018, with permission from Elsevier.*

Dye-catalyst dyad: one molecule makes it all

It is possible to covalently attach the dye with the anchoring group and the WOC in one single molecule. This follows the hypothesis that a covalent linkage will ensure that the WOC is always in close proximity to the dye-sensitizer. This should lead to rapid electron transfer from the WOC to the dye after its photo-

oxidization due to electron injection into the TiO_2 CB. In fact, charge recombination reactions are usually much faster than the difficult multi-electron water oxidation process, so that charges generated by light absorption are lost before electrons can be transferred to the CB of TiO_2 and holes to the WOC. The use of a dyad would also simplify the realization of the device since just one molecule has to be absorbed onto the semiconductor surface, but the synthesis of such a system is far more complex than that of the two single molecules of dye and WOC. Up to now, few examples of dyad for water oxidation are present in the literature. Several molecules employ Ru complex as sensitizers.[112] For example, Youngblood et al. reported in 2009 a dyad with various ruthenium complexes as a light absorber and IrO_2 as a catalyst (PS-Cat. 1 in **Figure 1.20**).[113] Iridium oxide capped with dicarboxylate ligands has been covalently coupled to a variety of ruthenium poly(pyridyl) dyes that contained malonate or succinate linkers. The dye underwent rapid photodegradation and the quantum yield was poor (~1%), but it was a proof of concept that this was a feasible way. Yamamoto et al. reported in 2016 a covalently-linked ruthenium-based WOC–zinc porphyrin (ZnP) sensitizer dyad; the DS-PEC performance was better than the reference systems with coadsorption of individual Ru(bda) and ZnP as well as with ZnP solely, corroborating the advantage of the covalent linking approach over the noncovalent one (**Figure 1.21**).[114] In the same year, Sherman et al. reported a Ru(II) polypyridyl- based chromophore−catalyst assemblies, with particularly good performances on SnO_2/TiO_2 core−shell electrodes (PS-Cat. 4 in **Figure 1.20**).[115] Lindquist et al. published in 2016 a dyad employing an organic sensitizer (a perylene derivative, **Figure 1.22**).[116]

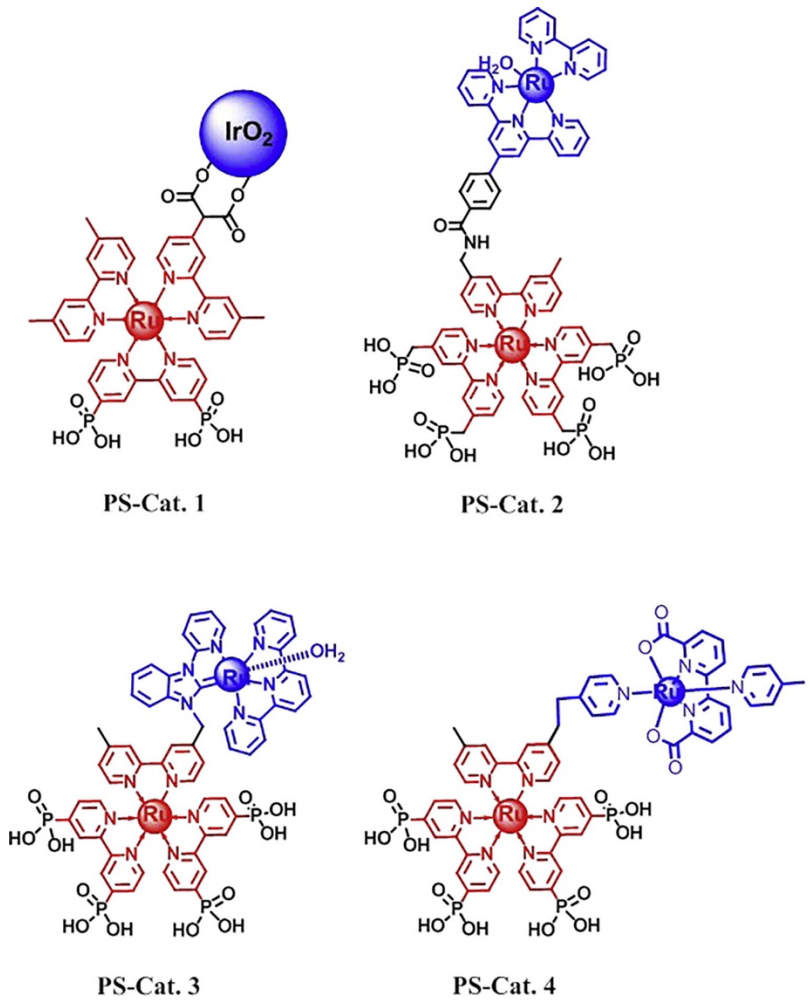

Figure 1.20. *Examples of dyads with Ru-based sensitizers. Reprinted from Ref. 89, Copyright 2018, with permission from Elsevier.*

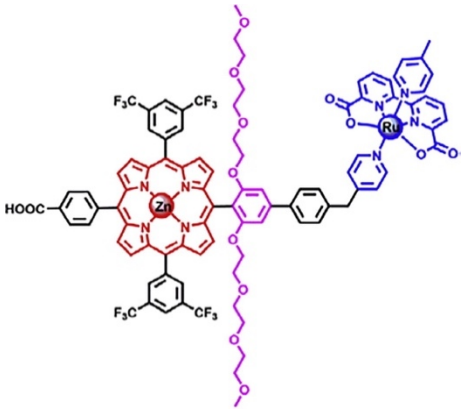

Figure 1.21. *Dyad with a Zn-porphyrin designed by Yamamoto et al. Reprinted from Ref. 89, Copyright 2018, with permission from Elsevier.*

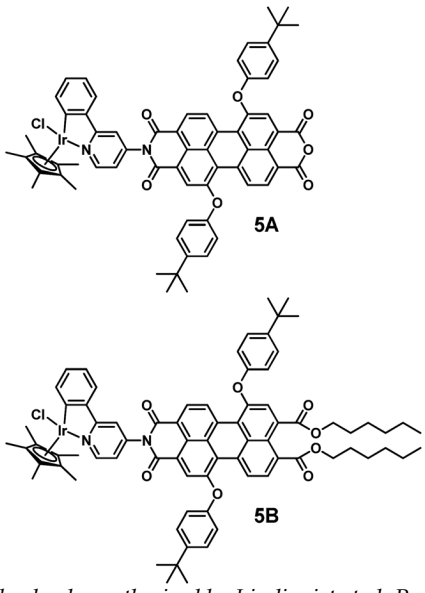

Figure 1.22. *Structures of the dyads synthesized by Lindiquist et al. Reproduced from Ref. 116 with permission from The Royal Society of Chemistry.*

In order to overcome the issues related to the difficult synthesis of dyads, some self-assembly systems have been purposed.[117-118] A very interesting approach is the use of host-guest systems, such as a cyclodextrin functionalized dye and a proper Ru-catalyst with hydrophobic functionalities, reported by L. Sun and coworkers in 2016 (**Figure 1.23**).[119] This implies major flexibility, since many

combinations of adducts can be tested in DS-PEC starting from a limited number of different molecules.

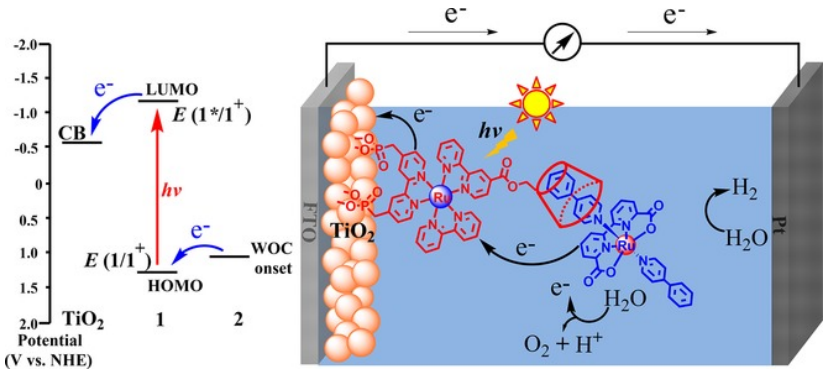

Figure 1.23. *DS-PEC cell consisting of a photoanode based on a dye-sensitized TiO_2 film, a Ru–bda water oxidation catalyst, and a Pt cathode for visible-light-driven water splitting. The dye–catalyst assembly forms on the surface of TiO_2 through the host–guest interaction (right). The energy diagram of the photoanode is shown on the left. Reproduced from Ref. 119, copyright 2016, with permission from Wiley.*

p-type organic dyes for DS-PEC photocathode

The requirements for a dye working in a p-type photocathode for a PEC are somehow similar to the ones for photoanodes dyes. Of course, it has to absorb the visible light, it should be cheap, it needs proper energy levels to match both semiconductor valence band and the redox potential of the catalyst, it needs an anchoring group to bind onto the surface of the semiconductor (usually NiO). So it is possible to use a properly designed p-type push-pull molecule composed by an electron acceptor, a linker and an electron donor with the binding moiety. To design a working photocathode for hydrogen production, a favourable match of the reduction potentials between a dye and a H_2-evolving catalyst is critical. More specifically, the catalytic onset reduction potential of a HER has to be more positive than the reduction potential E(D/D-) of the dye in order to keep the photo-induced electron transfer occurring from the dye to the catalyst. Besides this, the HOMO level of the sensitizer has to be more positive than the valence band of NiO, so that the dye can inject holes into the VB of the semiconductor.

Photoelectrode stability for water splitting is another challenge. Ideally, low pH is favourable for improving kinetics of hydrogen production on the deficient photocathode side and allowing proton conducting membranes to be used to separate each half cell. Thus it is crucial that the photocathode side is stable in acidic conditions because local pH changes from the water oxidation reaction can cause dye degradation and desorption even at neutral pH. Y. Wu and coworkers reported an innovative dye inspired by the natural membrane-enabled subcellular compartmentation: they used an organic donor−acceptor dye that prevents both dye desorption and semiconductor degradation by mimicking the hydrophobic/hydrophilic properties of lipid bilayer membranes.[120] The molecule, denoted as BH4, is an organic push-double-pull dye (D−π−2A) that consists of a triphenylamine (TPA) donor moiety connected to two perylenemonoimide (PMI) acceptor groups by head-to-tail oligio-3-hexylthiophene-conjugated π-linker groups. The donor group layer, which contains the carboxylic acid functional group for loading onto NiO, is protected from the highly protic aqueous electrolyte (1 M HCl, pH 0) by the canopy of hydrophobic hexyl groups above it in the thiophene linkers. The PMI groups are located above the canopy of hydrophobic hexyl groups and act as the head layer whereby the aqueous electrolyte can interact. Upon photoexcitation, an electron can move from the donor (TPA) to the acceptors (PMI) whereby the charge-separated state is protected from charge recombination with NiO by the length of oligothiophene π linker, which is between the donor and acceptor. Coupled with a cubane molybdenum sulphide cluster, $[Mo_3S_4]^{4+}$, dissolved in the electrolyte solution as the hydrogen evolving catalyst, this system shows great stability and impressive current densities (about 180 μA/cm^2, one order of magnitude higher than the usually reported ones). This suggests to use bulky hydrophobic sensitizers in order to obtain the best results both in stability and efficiency of the photocathode.

HEC for the cathodic compartment

As for photoanodes for DS-PECs, photocathodes preparation is similar to active photocathodes for DSSCs. Unfortunately, this field had been less investigated than the anodic counterpart, so not much literature is present for this argument. Also in this case it is necessary to adsorb on a semiconductor (usually NiO) both the dye and the catalyst.

In order to see if the system could work as a photocathode, it is possible to use a sacrificial electron donor such as triethanolamine (TEOA) in a homogeneous system with the dye and the catalyst dissolved in a proper solvent. If light driven H_2-evolution is detected, the preparation of a photocathode with immobilized dye and catalyst is feasible.

The photocathode can be realized by incorporating the dye and the catalyst into a nanostructured NiO-based photoactive cathode. The photocathode can be assembled first by sensitization of a prepared nano-structured NiO film on conducting glass with the dye, followed by direct deposition of a solution of the catalyst. The photocathode can then be explored as a working electrode in a standard three-electrode cell with a proper reference electrode (e.g. Ag/AgCl) and a counter electrode (e.g. a platinum wire).

The tandem DS-PEC: integration of photoanode and photocathode in the same device

Up to now, research has focused on PEC devices with a DS-photoanode and a passive Pt-wire as cathode; platinum is a noble metal, so this is of course an expensive system, the ideal solution would be to replace platinum with an active photocathode. In this way, the device would be cheaper and, in principle, it could show better performances and efficiency: both electrodes would contain a dye and a catalyst, so they would both actively participate to the water splitting process by absorbing different portions of the solar spectrum. A few example are present in the literature of such a device, but they employ metallo-organic dyes or inorganic oxides.[121-122]

L. Sun et al. recently demonstrated that a device with both anode and cathode sensitized by purely organic dyes is feasible, with a design similar to tandem

pn-DSSCs (**Figure 1.24**).[123] They used a meso-TiO_2 cosensitized by an organic dye and a Ru-based catalyst as photoanodic active material and a NiO layer cosensitized by another organic dye and a Co-based catalyst as photocathodic active material. The photocathode acted as the working electrode in the cell while the photoanode was the counter electrode. Different configurations are possible to illuminate the cell and the best one is, of course, lighting simultaneously both sides of the system, but good results can also be obtained illuminating from the thinner electrode side, so that more light can pass through and reach the other electrode. In this way they obtained a working tandem DS-PEC cell with IPCE of 25% at 380 nm under neutral pH conditions without applying any bias. The main drawbacks of this system are due to the photocathode: it is known that NiO has a poor hole mobility as a p-type semiconductor and short hole diffusion length, leading to fast charge recombination. At the same time, it is difficult to prepare thicker NiO films to load more dye and catalyst. The IPCE data indicated that the photoanode could convert more light into electrons than the photocathode, so the latter is the bottleneck of this device.

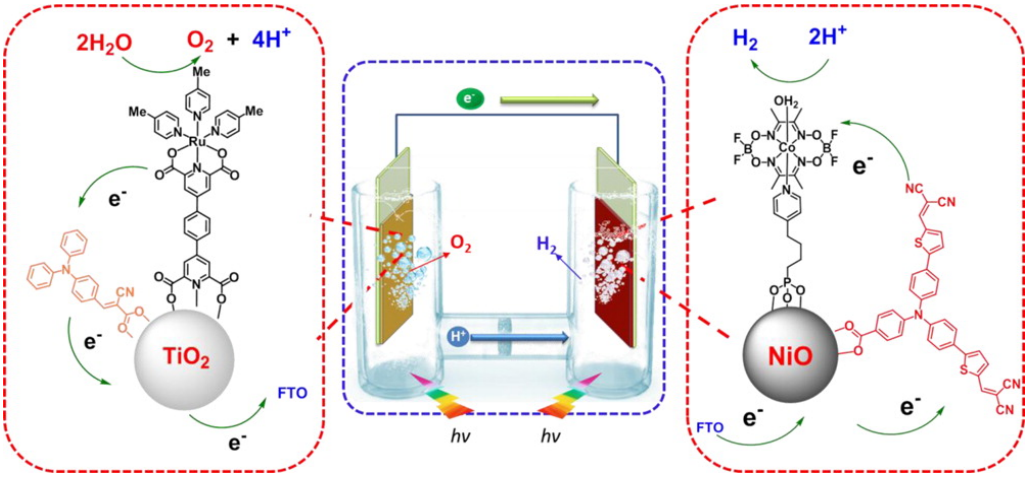

Figure 1.24. *The only example of organic Dye-Sensitized Tandem Photoelectrochemical Cell for water splitting developed by L. Sun and coworkers. Reprinted with permission from J. Am. Chem. Soc.,* **2015**, *137* (28), pp 9153–9159. *Copyright 2015 American Chemical Society.*

1.3.2 Working principles and characterization of a DS-PEC

The standard potential ΔE° of water splitting or water electrolysis to H_2 and O_2 is 1.23 V at any pH.

$$H_2O \rightarrow H_2 + \frac{1}{2}O_2$$

From the reaction stoichiometry, the volume of produced hydrogen is twice that of oxygen. In energetic terms, water splitting requires a free energy $\Delta G° = -nF\Delta E°$ (where F is the Faraday constant, 96485.3365 C mol^{-1}). For the splitting of 1 mol of H_2O to 1 mol of H_2 and 0.5 mol of O_2, n is equal to 2 electrons and $\Delta G° = -2 \times 96485$ C $mol^{-1} \times -1.23$ J $C^{-1} = 237$ kJ mol^{-1} H_2O or $\Delta G° = 2.46$ eV mol^{-1} H_2O (with 1 eV = 96.48 kJ mol^{-1}). Accordingly, for each electron involved in the redox reaction, the free energy is 1.23 eV. Water splitting is a multi-electronic (2 electrons per each molecule of hydrogen and 4 electrons per each molecule of oxygen evolved), multi-atomic thermodynamic energy demanding, and kinetically hampered process with a high activation barrier. Thermodynamic losses and overpotentials associated to the reaction kinetics increase the voltage required for water splitting to higher values, up to 1.8 - 2.0 V, the typical voltage at which commercial electrolysers operate.[124]

In order to let the water splitting reaction happen, it is possible to use a photoelectrochemical cell employing both photoanode and photocathode (tandem configuration) or focusing only on one electrode. In the following work only active photoanodes have been tested, assembled in a PEC like the one sketched in **Figure 1.25**. The photoanode is the working electrode (WE) of the cell, the counter electrode (CE) is a platinum wire where protons are reduced to hydrogen and the pseudo-reference electrode (RE) is a Ag/AgCl electrode. The cell is filled with a phosphate buffer solution (PBS) containing the sacrificial electron donor or the water oxidation catalyst. Anodic and cathodic compartments are separated by a proton exchange membrane (PEM) made with Nafion® membrane, that allows only protons to move from the anode to the cathode.

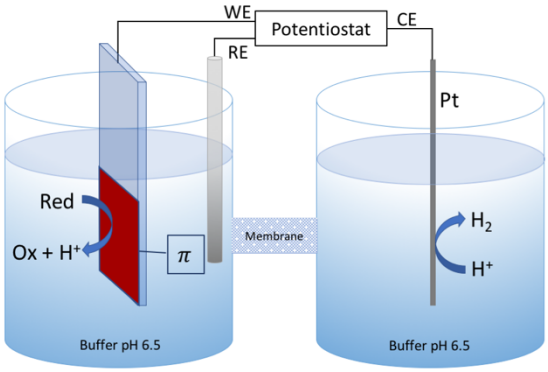

Figure 1.25. *Scheme of a DS-PEC with active photoanode. "Red" can be either a sacrificial electron donor (SED) or water, "Ox" is the oxidized SED or O_2, respectively. π is the organic sensitizer absorbed on the photoelectrode.*

Water splitting reaction, as already mentioned above, is a complex process that involves four electrons and four protons:

$$2H_2O \rightarrow O_2 + 4H^+ + 4e^-$$

$$4H^+ + 4e^- \rightarrow 2H_2$$

$$2H_2O \rightarrow 2H_2 + O_2$$

In order to test dyes on photoanodes in a simpler process, it is possible to use a sacrificial electron donor (SED) that allows the cell to work, for example hydroquinone that is oxidized to quinone, according to the scheme in **Figure 1.26**.

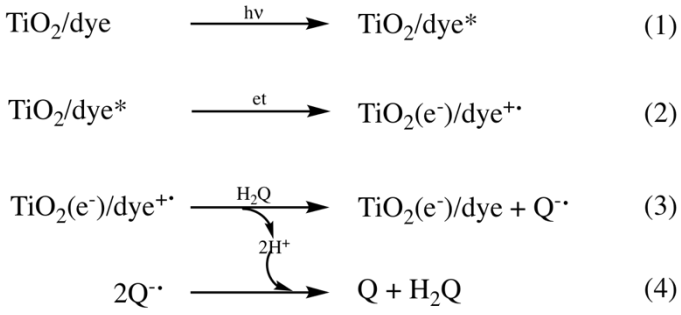

Figure 1.26. *Photocatalytic process in presence of H_2Q as SED.*

Upon photoexcitation, the adsorbed dye TiO_2/dye goes from its ground to excited state TiO_2/dye* (1), from which an electron is injected to the TiO_2 conduction band generating a radical-cation species ($TiO_2(e^-)$/$dye^{+\bullet}$) (2). The adsorbed $dye^{+\bullet}$ is restored to its starting state by reaction with H_2Q in solution, which is thus oxidized to a quinone radical-anion ($Q^{-\bullet}$, 3).[125] This process generates two protons which are included to the rapid disproportionation process (one electron transfer) of two molecules of quinone radical-anion to quinone (Q) and H_2Q.[126]

Testing a sensitized photoanode with a H_2Q solution in the PEC allows to see if the dye is able to collect light and to transfer electrons to the circuit, simplifying the process that happens in water spitting reaction. If the molecule gives good results, then it is worth proceeding with the more complex catalysed water splitting reaction.

To let the system work, the WOC has to accept four electrons before being able to oxidize water and produce one molecule of oxygen and four protons, that then move to the cathode through the PEM. It is intuitive that a transition metal with many possible oxidation states is needed, but such a high oxidation number is not so easy to be obtained without side reactions. Once four electrons are collected by the WOC and oxygen is produced, the catalyst goes back to the starting point and is ready for another cycle.

The measurements carried out in both the configurations are the same. First of all, a linear sweep voltammetry (LSV) is run onto the DS-PEC; it consists of an electric measurement where the potential applied on the circuit spans over a fixed range and the resulting current is recorded (**Figure 1.27**, left). The LSV is measured both in dark and in light, in order to verify that the system effectively responds to light. The expected result is to have almost zero current when the DS-PEC is in dark and a clear signal when it is lightened by the solar simulator (using a UV filter, otherwise the signal would be given by the TiO_2 layer onto which the dye is absorbed). Through the LSV results it is possible to determine

the potential where the light/dark ratio is maximized, so that at that value a chronoamperometry (CA) can be run (**Figure 1.27**, right). Also in this case, the current flowing in the circuit is recorded both in dark and in light, carrying on also long term measurements under illumination in order to evaluate the stability of the system and the gas evolution. At the end of the CA, the atmosphere of cathodic compartment (when working with SED) or of both compartments (when working with WOC) is analysed through a gas-chromatograph (GD), where the peak of hydrogen can be clearly identified and also oxygen can be evaluated. With the quantified gas evolved and the total charge flown in the circuit it is eventually possible to calculate the Faradaic efficiency for both hydrogen and oxygen, defined as follows:

$$FE = \frac{n_{H_2,op}}{n_{H_2,theor}}$$

where $n_{H2,op}$ is the hydrogen amount measured and $n_{H2,theor}$ the amount calculated according to Faraday's law.

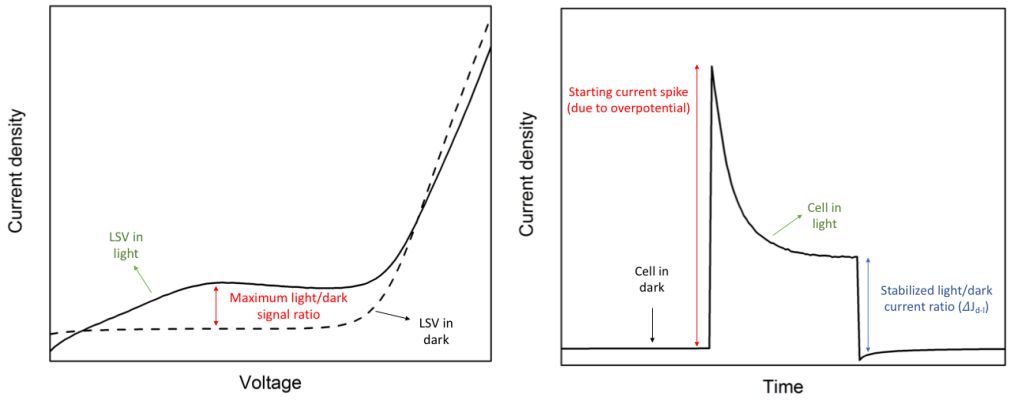

Figure 1.27. *LSV (left) and CA (right) curves of a PEC in measurement conditions.*

1.4 Bibliography

1. Grätzel, M., "Photoelectrochemical cells". *Nature* **2001,** *414*, 338, doi: 10.1038/35104607

2. Chiras, D. D., *Environmental Science*. 9 ed.; Jones & Bartlett Publishers: 2012.

3. Armaroli, N.; Balzani, V., "Solar Electricity and Solar Fuels: Status and Perspectives in the Context of the Energy Transition". *Chem. Eur. J.* **2016,** *22*, 32-57, doi: 10.1002/chem.201503580

4. Webber, M. E., "More Food, Less Energy". *SciAm* **2012,** *306*, 74-79, doi: 10.1038/scientificamerican0112-74

5. Murphy, D. J.; Hall, C. A. S.; Dale, M.; Cleveland, C., "Order from Chaos: A Preliminary Protocol for Determining the EROI of Fuels". *Sustainability* **2011,** *3*, doi: 10.3390/su3101888

6. Nicola Armaroli, V. B., *Energy for a Sustainable World: From the Oil Age to a Sun-Powered Future*. Wiley-VCH Verlag GmbH & Co. KGaA 2011.

7. "British Petroleum, BP Statistical Review of World Energy 2015". http://www.bp.com.

8. Service, R. F., "Is It Time to Shoot for the Sun?". *Sci* **2005,** *309*, 548, doi:

9. REN21, *Renewables 2018 Global Status Report*. 2018 ed.; 2018.

10. NREL American Society for Testing.2010."Terrestrial Reference Spectra for Photovoltaic Performance Evaluation (ASTM G-173-03)". http://rredc.nrel.gov/solar/spectra/am1.5/.

11. Chapin, D. M.; Fuller, C. S.; Pearson, G. L., "A New Silicon p-n Junction Photocell for Converting Solar Radiation into Electrical Power". *JAP* **1954,** *25*, 676-677, doi: 10.1063/1.1721711

12. EnergyTrend TrendForce Corp. ."PV Price Quotes". https://pv.energytrend.com/pricequotes.html (accessed September 2018).

13. NREL, Best Research-Cell Efficiencies. http://www.nrel.gov, 2018.

14. Lee, C.-P.; Lin, C.-A.; Wei, T.-C.; Tsai, M.-L.; Meng, Y.; Li, C.-T.; Ho, K.-C.; Wu, C.-I.; Lau, S.-P.; He, J.-H., "Economical low-light photovoltaics by using the Pt-free dye-sensitized solar cell with graphene dot/PEDOT:PSS counter electrodes". *Nano Energy* **2015,** *18*, 109-117, doi: https://doi.org/10.1016/j.nanoen.2015.10.008

15. Rasheduzzaman, M.; Pillai, P. B.; Mendoza, A. N. C.; Souza, M. M. D. In *A study of the performance of solar cells for indoor autonomous wireless sensors*, 2016 10th International Symposium on Communication Systems, Networks and Digital Signal Processing (CSNDSP), 20-22 July 2016; 2016; pp 1-6.

16. Desilvestro, J.; Graetzel, M.; Kavan, L.; Moser, J.; Augustynski, J., "Highly efficient sensitization of titanium dioxide". *J. Am. Chem. Soc.* **1985,** *107*, 2988-2990, doi: 10.1021/ja00296a035

17. Vlachopoulos, N.; Liska, P.; Augustynski, J.; Graetzel, M., "Very efficient visible light energy harvesting and conversion by spectral sensitization of high surface area polycrystalline titanium dioxide films". *J. Am. Chem. Soc.* **1988,** *110*, 1216-1220, doi: 10.1021/ja00212a033

18. O'Regan, B.; Grätzel, M., "A low-cost, high-efficiency solar cell based on dye-sensitized colloidal TiO2 films". *Nature* **1991,** *353*, 737-740, doi:

19. Nazeeruddin, M. K.; Kay, A.; Rodicio, I.; Humphry-Baker, R.; Mueller, E.; Liska, P.; Vlachopoulos, N.; Graetzel, M., "Conversion of light to electricity by cis-X2bis(2,2'-bipyridyl-4,4'-dicarboxylate)ruthenium(II) charge-transfer sensitizers (X = Cl-, Br-, I-, CN-, and SCN-) on nanocrystalline titanium dioxide electrodes". *J. Am. Chem. Soc.* **1993,** *115*, 6382-6390, doi: 10.1021/ja00067a063

20. Nazeeruddin, M. K.; Zakeeruddin, S. M.; Humphry-Baker, R.; Jirousek, M.; Liska, P.; Vlachopoulos, N.; Shklover, V.; Fischer, C.-H.; Grätzel, M., "Acid−Base Equilibria of (2,2′-Bipyridyl-4,4′-dicarboxylic acid)ruthenium(II) Complexes and the Effect of Protonation on Charge-Transfer Sensitization of Nanocrystalline Titania". *Inorg. Chem.* **1999,** *38*, 6298-6305, doi: 10.1021/ic990916a

21. Nazeeruddin, M. K.; Humphry-Baker, R.; Liska, P.; Grätzel, M., "Investigation of Sensitizer Adsorption and the Influence of Protons on Current and Voltage of a Dye-Sensitized Nanocrystalline TiO2 Solar Cell". *J. Phys. Chem. B* **2003,** *107*, 8981-8987, doi: 10.1021/jp022656f

22. Wang, P.; Zakeeruddin, S. M.; Moser, J. E.; Nazeeruddin, M. K.; Sekiguchi, T.; Grätzel, M., "A stable quasi-solid-state dye-sensitized solar cell with an amphiphilic ruthenium sensitizer and polymer gel electrolyte". *Nature Materials* **2003,** *2*, 402, doi: 10.1038/nmat904

23. Abbotto, A.; Barolo, C.; Bellotto, L.; Angelis, F. D.; Grätzel, M.; Manfredi, N.; Marinzi, C.; Fantacci, S.; Yum, J.-H.; Nazeeruddin, M. K., "Electron-rich heteroaromatic conjugated bipyridine based ruthenium sensitizer for efficient dye-sensitized solar cells". *Chem. Commun.* **2008**, 5318-5320, doi: 10.1039/B811378E

24. Abbotto, A.; Sauvage, F.; Barolo, C.; De Angelis, F.; Fantacci, S.; Graetzel, M.; Manfredi, N.; Marinzi, C.; Nazeeruddin, M. K., "Panchromatic ruthenium sensitizer based on electron-rich heteroarylvinylene π-conjugated quaterpyridine for dye-sensitized solar cells". *Dalton Transactions* **2011,** *40*, 234-242, doi: 10.1039/C0DT01190H

25. Chen, C.-Y.; Wu, S.-J.; Wu, C.-G.; Chen, J.-G.; Ho, K.-C., "A Ruthenium Complex with Superhigh Light-Harvesting Capacity for Dye-Sensitized Solar Cells". *Angew. Chem. Int. Ed.* **2006,** *45*, 5822-5825, doi: 10.1002/anie.200601463

26. Coluccini, C.; Manfredi, N.; Calderon, E. H.; Salamone, M. M.; Ruffo, R.; Roberto, D.; Lobello, M. G.; De Angelis, F.; Abbotto, A., "Photophysical and Electrochemical Properties of Thiophene-Based 2-Arylpyridines". *Eur. J. Org. Chem.* **2011,** *2011*, 5587-5598, doi: 10.1002/ejoc.201100651

27. Sauvage, F.; Decoppet, J.-D.; Zhang, M.; Zakeeruddin, S. M.; Comte, P.; Nazeeruddin, M.; Wang, P.; Grätzel, M., "Effect of Sensitizer Adsorption Temperature on the Performance of Dye-Sensitized Solar Cells". *J. Am. Chem. Soc.* **2011,** *133*, 9304-9310, doi: 10.1021/ja110541t

28. Shi, D.; Pootrakulchote, N.; Li, R.; Guo, J.; Wang, Y.; Zakeeruddin, S. M.; Grätzel, M.; Wang, P., "New Efficiency Records for Stable Dye-Sensitized Solar Cells with Low-Volatility and Ionic Liquid Electrolytes". *J. Phys. Chem. C* **2008,** *112*, 17046-17050, doi: 10.1021/jp808018h

29. Hagfeldt, A.; Boschloo, G.; Sun, L.; Kloo, L.; Pettersson, H., "Dye-Sensitized Solar Cells". *Chem. Rev.* **2010,** *110*, 6595-6663, doi: 10.1021/cr900356p

30. Hao, Y.; Yang, X.; Cong, J.; Tian, H.; Hagfeldt, A.; Sun, L., "Efficient near infrared D–π–A sensitizers with lateral anchoring group for dye-sensitized solar cells". *Chem. Commun.* **2009**, 4031-4033, doi: 10.1039/B908396K

31. Mishra, A.; Fischer, M. K. R.; Bäuerle, P., "Metal-Free Organic Dyes for Dye-Sensitized Solar Cells: From Structure: Property Relationships to Design Rules". *Angew. Chem. Int. Ed.* **2009,** *48*, 2474-2499, doi: 10.1002/anie.200804709

32. Wang, Z.-S.; Cui, Y.; Dan-oh, Y.; Kasada, C.; Shinpo, A.; Hara, K., "Thiophene-Functionalized Coumarin Dye for Efficient Dye-Sensitized Solar Cells: Electron Lifetime Improved by Coadsorption of Deoxycholic Acid". *J. Phys. Chem. C* **2007,** *111*, 7224-7230, doi: 10.1021/jp067872t

33. Wang, Z.-S.; Koumura, N.; Cui, Y.; Takahashi, M.; Sekiguchi, H.; Mori, A.; Kubo, T.; Furube, A.; Hara, K., "Hexylthiophene-Functionalized Carbazole Dyes for Efficient Molecular Photovoltaics: Tuning of Solar-Cell Performance by Structural Modification". *Chem. Mater.* **2008,** *20*, 3993-4003, doi: 10.1021/cm8003276

34. Hagberg, D. P.; Yum, J.-H.; Lee, H.; De Angelis, F.; Marinado, T.; Karlsson, K. M.; Humphry-Baker, R.; Sun, L.; Hagfeldt, A.; Grätzel, M.; Nazeeruddin, M. K., "Molecular Engineering of Organic Sensitizers for Dye-Sensitized Solar Cell Applications". *J. Am. Chem. Soc.* **2008,** *130*, 6259-6266, doi: 10.1021/ja800066y

35. Choi, H.; Baik, C.; Kang, S. O.; Ko, J.; Kang, M.-S.; Nazeeruddin, M. K.; Grätzel, M., "Highly Efficient and Thermally Stable Organic Sensitizers for Solvent-Free Dye-Sensitized Solar Cells". *Angew. Chem. Int. Ed.* **2007,** *47*, 327-330, doi: 10.1002/anie.200703852

36. Zhang, G.; Bala, H.; Cheng, Y.; Shi, D.; Lv, X.; Yu, Q.; Wang, P., "High efficiency and stable dye-sensitized solar cells with an organic chromophore featuring a binary π-conjugated spacer". *Chem. Commun.* **2009**, 2198-2200, doi: 10.1039/B822325D

37. Abbotto, A.; Manfredi, N.; Marinzi, C.; De Angelis, F.; Mosconi, E.; Yum, J.-H.; Xianxi, Z.; Nazeeruddin, M. K.; Gratzel, M., "Di-branched di-anchoring

organic dyes for dye-sensitized solar cells". *Energy Environ. Sci.* **2009,** *2*, 1094-1101, doi: 10.1039/B910654E

38. Abbotto, A.; Leandri, V.; Manfredi, N.; De Angelis, F.; Pastore, M.; Yum, J.-H.; Nazeeruddin, M. K.; Grätzel, M., "Bis-Donor–Bis-Acceptor Tribranched Organic Sensitizers for Dye-Sensitized Solar Cells". *Eur. J. Org. Chem.* **2011,** *2011*, 6195-6205, doi: 10.1002/ejoc.201100821

39. Leandri, V.; Ruffo, R.; Trifiletti, V.; Abbotto, A., "Asymmetric Tribranched Dyes: An Intramolecular Cosensitization Approach for Dye-Sensitized Solar Cells". *Eur. J. Org. Chem.* **2013,** *2013*, 6793-6801, doi: 10.1002/ejoc.201300962

40. Manfredi, N.; Cecconi, B.; Abbotto, A., "Multi-Branched Multi-Anchoring Metal-Free Dyes for Dye-Sensitized Solar Cells". *Eur. J. Org. Chem.* **2014,** *2014*, 7069-7086, doi: 10.1002/ejoc.201402422

41. Yella, A.; Lee, H.-W.; Tsao, H. N.; Yi, C.; Chandiran, A. K.; Nazeeruddin, M. K.; Diau, E. W.-G.; Yeh, C.-Y.; Zakeeruddin, S. M.; Grätzel, M., "Porphyrin-Sensitized Solar Cells with Cobalt (II/III)–Based Redox Electrolyte Exceed 12 Percent Efficiency". *Sci* **2011,** *334*, 629, doi:

42. Kakiage, K.; Aoyama, Y.; Yano, T.; Oya, K.; Fujisawa, J.-i.; Hanaya, M., "Highly-efficient dye-sensitized solar cells with collaborative sensitization by silyl-anchor and carboxy-anchor dyes". *Chem. Commun.* **2015,** *51*, 15894-15897, doi: 10.1039/C5CC06759F

43. Wu, J.; Lan, Z.; Lin, J.; Huang, M.; Huang, Y.; Fan, L.; Luo, G., "Electrolytes in Dye-Sensitized Solar Cells". *Chem. Rev.* **2015,** *115*, 2136-2173, doi: 10.1021/cr400675m

44. Yun, S.; Freitas, J. N.; Nogueira, A. F.; Wang, Y.; Ahmad, S.; Wang, Z.-S., "Dye-sensitized solar cells employing polymers". *Prog. Polym. Sci.* **2016,** *59*, 1-40, doi: https://doi.org/10.1016/j.progpolymsci.2015.10.004

45. Liu, Y.; Hagfeldt, A.; Xiao, X. R.; Lindquist, S. E., "Investigation of influence of redox species on the interfacial energetics of a dye-sensitized nanoporous TiO2 solar cell". *Sol. Energy Mater. Sol. Cells* **1998,** *55*, 267-281, doi: 10.1016/s0927-0248(98)00111-1

46. Bella, F.; Gerbaldi, C.; Barolo, C.; Grätzel, M., "Aqueous dye-sensitized solar cells". *Chem. Soc. Rev.* **2015,** *44*, 3431-3473, doi: 10.1039/C4CS00456F

47. Bella, F.; Galliano, S.; Falco, M.; Viscardi, G.; Barolo, C.; Grätzel, M.; Gerbaldi, C., "Unveiling iodine-based electrolytes chemistry in aqueous dye-sensitized solar cells". *Chem. Sci.* **2016**, doi: 10.1039/C6SC01145D

48. Lin, R. Y.-Y.; Wu, F.-L.; Li, C.-T.; Chen, P.-Y.; Ho, K.-C.; Lin, J. T., "High-Performance Aqueous/Organic Dye-Sensitized Solar Cells Based on Sensitizers Containing Triethylene Oxide Methyl Ether". *ChemSusChem* **2015,** *8*, 2503-2513, doi: 10.1002/cssc.201500589

49. Kaneko, M.; Nomura, T.; Sasaki, C., "Photoinduced Charge Separation in an Aqueous Phase Using Nanoporous TiO2 Film and a Quasi-Solid Made of Natural Products". *Macromol. Rapid Commun.* **2003,** *24*, 444-446, doi: 10.1002/marc.200390059

50. Kim, D. H.; Losego, M. D.; Hanson, K.; Alibabaei, L.; Lee, K.; Meyer, T. J.; Parsons, G. N., "Stabilizing chromophore binding on TiO2 for long-term stability of dye-sensitized solar cells using multicomponent atomic layer deposition". *Phys. Chem. Chem. Phys.* **2014,** *16*, 8615-8622, doi: 10.1039/C4CP01130A

51. Leandri, V.; Ellis, H.; Gabrielsson, E.; Sun, L.; Boschloo, G.; Hagfeldt, A., "An organic hydrophilic dye for water-based dye-sensitized solar cells". *Phys. Chem. Chem. Phys.* **2014,** *16*, 19964-19971, doi: 10.1039/C4CP02774D

52. Choi, H.; Jeong, B.-S.; Do, K.; Ju, M. J.; Song, K.; Ko, J., "Aqueous electrolyte based dye-sensitized solar cells using organic sensitizers". *New J. Chem.* **2013,** *37*, 329-336, doi: 10.1039/C2NJ40577F

53. Galliano, S.; Bella, F.; Gerbaldi, C.; Falco, M.; Viscardi, G.; Grätzel, M.; Barolo, C., "Photoanode/Electrolyte Interface Stability in Aqueous Dye-Sensitized Solar Cells". *Energy Technology* **2016,** *5*, 300-311, doi: 10.1002/ente.201600285

54. Xiang, W.; Huang, F.; Cheng, Y.-B.; Bach, U.; Spiccia, L., "Aqueous dye-sensitized solar cell electrolytes based on the cobalt(ii)/(iii) tris(bipyridine) redox couple". *Energy Environ. Sci.* **2013,** *6*, 121-127, doi: 10.1039/C2EE23317G

55. Dong, C.; Xiang, W.; Huang, F.; Fu, D.; Huang, W.; Bach, U.; Cheng, Y.-B.; Li, X.; Spiccia, L., "Controlling Interfacial Recombination in Aqueous Dye-Sensitized Solar Cells by Octadecyltrichlorosilane Surface Treatment". *Angew. Chem. Int. Ed.* **2014,** *53*, 6933-6937, doi: 10.1002/anie.201400723

56. Ellis, H.; Vlachopoulos, N.; Häggman, L.; Perruchot, C.; Jouini, M.; Boschloo, G.; Hagfeldt, A., "PEDOT counter electrodes for dye-sensitized solar cells prepared by aqueous micellar electrodeposition". *Electrochim. Acta* **2013,** *107*, 45-51, doi: http://dx.doi.org/10.1016/j.electacta.2013.06.005

57. Bella, F.; Galliano, S.; Falco, M.; Viscardi, G.; Barolo, C.; Grätzel, M.; Gerbaldi, C., "Approaching truly sustainable solar cells by the use of water and cellulose derivatives". *Green Chem.* **2017,** *19*, 1043-1051, doi: 10.1039/C6GC02625G

58. Kalyanasundaram, K., *Dye-sensitized Solar Cells*. EFPL Press: 2010.

59. Calogero, G.; Calandra, P.; Irrera, A.; Sinopoli, A.; Citro, I.; Di Marco, G., "A new type of transparent and low cost counter-electrode based on platinum nanoparticles for dye-sensitized solar cells". *Energy Environ. Sci.* **2011,** *4*, 1838-1844, doi: 10.1039/C0EE00463D

60. Snaith, H. J., "Estimating the Maximum Attainable Efficiency in Dye-Sensitized Solar Cells". *Adv. Funct. Mater.* **2009,** *20*, 13-19, doi: 10.1002/adfm.200901476

61. Christoph Joseph Brabec, V. D., Jürgen Parisi, Niyazi Serdar Sariciftci, *Organic Photovoltaics*. Springer-Verlag Berlin Heidelberg: Berlin, 2003.

62. Green, M. A.; Emery, K.; Hishikawa, Y.; Warta, W., "Solar cell efficiency tables (version 36)". *Progr. Photovolt: Res. Appl.* **2010,** *18*, 346-352, doi: 10.1002/pip.1021

63. Shockley, W.; Queisser, H. J., "Detailed Balance Limit of Efficiency of p-n Junction Solar Cells". *JAP* **1961,** *32*, 510-519, doi: 10.1063/1.1736034

64. Williams, E.; Sekar, A.; Matteson, S.; Rittmann, B. E., "Sun-to-Wheels Exergy Efficiencies for Bio-Ethanol and Photovoltaics". *Environ Sci Technol* **2015,** *49*, 6394-6401, doi: 10.1021/es504377b

65. Narins, T. P., "The battery business: Lithium availability and the growth of the global electric car industry". *The Extractive Industries and Society* **2017,** *4*, 321-328, doi: https://doi.org/10.1016/j.exis.2017.01.013

66. Vikström, H.; Davidsson, S.; Höök, M., "Lithium availability and future production outlooks". *ApEn* **2013,** *110*, 252-266, doi: https://doi.org/10.1016/j.apenergy.2013.04.005

67. Tarascon, J. M.; Armand, M., "Issues and challenges facing rechargeable lithium batteries". *Nature* **2001,** *414*, 359, doi: 10.1038/35104644

68. Smil, V., *Energy at the Crossroads: Global Perspectives and Uncertainties* MIT press: Cambridge, MA, 2003.

69. Hammond, A. L., "Solar Energy: The Largest Resource". *Sci* **1972,** *177*, 1088, doi:

70. Dawson, J. K., "Prospects for hydrogen as an energy resource". *Nature* **1974,** *249*, 724, doi: 10.1038/249724a0

71. Balzani, V.; Moggi, L.; Manfrin, M. F.; Bolletta, F.; Gleria, M., "Solar Energy Conversion by Water Photodissociation". *Sci* **1975,** *189*, 852, doi:

72. Armaroli, N.; Balzani, V., "The Hydrogen Issue". *ChemSusChem* **2010,** *4*, 21-36, doi: 10.1002/cssc.201000182

73. Stone, R., "Three Gorges Dam: Into the Unknown". *Sci* **2008,** *321*, 628, doi:

74. *Handbook of Fuel Cells*. Wiley-VCH: Weinheim, 2009; Vol. 3.

75. "Fuel Cell Basics". http://www.fchea.org/fuelcells/ (accessed September 2018).

76. Fujishima, A.; Honda, K., "Electrochemical Photolysis of Water at a Semiconductor Electrode". *Nature* **1972,** *238*, 37-38, doi:

77. Liu, X.; Wang, F.; Wang, Q., "Nanostructure-based WO3 photoanodes for photoelectrochemical water splitting". *Phys. Chem. Chem. Phys.* **2012,** *14*, 7894-7911, doi: 10.1039/C2CP40976C

78. Abdi, F. F.; van de Krol, R., "Nature and Light Dependence of Bulk Recombination in Co-Pi-Catalyzed BiVO4 Photoanodes". *J. Phys. Chem. C* **2012,** *116*, 9398-9404, doi: 10.1021/jp3007552

79. Sivula, K.; Le Formal, F.; Grätzel, M., "Solar Water Splitting: Progress Using Hematite (α-Fe2O3) Photoelectrodes". *ChemSusChem* **2011,** *4*, 432-449, doi: 10.1002/cssc.201000416

80. Licht, S.; Wang, B.; Mukerji, S.; Soga, T.; Umeno, M.; Tributsch, H., "Over 18% solar energy conversion to generation of hydrogen fuel; theory and experiment for efficient solar water splitting". *Int. J. Hydrogen Energy* **2001,** *26*, 653-659, doi: https://doi.org/10.1016/S0360-3199(00)00133-6

81. Nelson, N.; Yocum, C. F., "STRUCTURE AND FUNCTION OF PHOTOSYSTEMS I AND II". *Annual Review of Plant Biology* **2006,** *57*, 521-565, doi: 10.1146/annurev.arplant.57.032905.105350

82. Beadle, C. L.; Long, S. P., "Photosynthesis — is it limiting to biomass production?". *Biomass* **1985,** *8*, 119-168, doi: https://doi.org/10.1016/0144-4565(85)90022-8

83. Beale, C. V.; Long, S. P., "Can perennial C4 grasses attain high efficiencies of radiant energy conversion in cool climates?". *Plant, Cell & Environment* **1995,** *18*, 641-650, doi: 10.1111/j.1365-3040.1995.tb00565.x

84. Chrispeels, M. J. S., David E. , *Plants, genes, and crop biotechnology*. 2nd ed.; Jones and Bartlett Publisher: Boston, 2002.

85. Jin, S., "What Else Can Photoelectrochemical Solar Energy Conversion Do Besides Water Splitting and CO2 Reduction?". *ACS Energy Letters* **2018,** *3*, 2610-2612, doi: 10.1021/acsenergylett.8b01800

86. Mase, K.; Yoneda, M.; Yamada, Y.; Fukuzumi, S., "Efficient Photocatalytic Production of Hydrogen Peroxide from Water and Dioxygen with Bismuth Vanadate and a Cobalt(II) Chlorin Complex". *ACS Energy Letters* **2016,** *1*, 913-919, doi: 10.1021/acsenergylett.6b00415

87. Sayama, K., "Production of High-Value-Added Chemicals on Oxide Semiconductor Photoanodes under Visible Light for Solar Chemical-Conversion Processes". *ACS Energy Letters* **2018,** *3*, 1093-1101, doi: 10.1021/acsenergylett.8b00318

88. Cha, H. G.; Choi, K.-S., "Combined biomass valorization and hydrogen production in a photoelectrochemical cell". *Nature Chemistry* **2015,** *7*, 328, doi: 10.1038/nchem.2194
https://www.nature.com/articles/nchem.2194#supplementary-information

89. Ding, X.; Zhang, L.; Wang, Y.; Liu, A.; Gao, Y., "Design of photoanode-based dye-sensitized photoelectrochemical cells assembling with transition metal complexes for visible light-induced water splitting". *Coord. Chem. Rev.* **2018,** *357*, 130-143, doi: https://doi.org/10.1016/j.ccr.2017.10.020

90. Swierk, J. R.; Mallouk, T. E., "Design and development of photoanodes for water-splitting dye-sensitized photoelectrochemical cells". *Chem. Soc. Rev.* **2013,** *42*, 2357-2387, doi: Doi 10.1039/C2cs35246j

91. Yamamoto, M.; Nishizawa, Y.; Chabera, P.; Li, F.; Pascher, T.; Sundstrom, V.; Sun, L.; Imahori, H., "Visible light-driven water oxidation with a subporphyrin sensitizer and a water oxidation catalyst". *Chem. Commun.* **2016,** *52*, 13702-13705, doi: 10.1039/C6CC07877J

92. Wee, K.-R.; Sherman, B. D.; Brennaman, M. K.; Sheridan, M. V.; Nayak, A.; Alibabaei, L.; Meyer, T. J., "An aqueous, organic dye derivatized SnO2/TiO2 core/shell photoanode". *J. Mater. Chem. A* **2016**, doi: 10.1039/C5TA06678F

93. Swierk, J. R.; Méndez-Hernández, D. D.; McCool, N. S.; Liddell, P.; Terazono, Y.; Pahk, I.; Tomlin, J. J.; Oster, N. V.; Moore, T. A.; Moore, A. L.; Gust, D.; Mallouk, T. E., "Metal-free organic sensitizers for use in water-splitting dye-sensitized photoelectrochemical cells". *Proc. Natl. Acad. Sci. U.S.A.* **2015,** *112*, 1681-1686, doi: 10.1073/pnas.1414901112

94. Suryani, O.; Higashino, Y.; Mulyana, J. Y.; Kaneko, M.; Hoshi, T.; Shigaki, K.; Kubo, Y., "A near-infrared organic photosensitizer for use in dye-sensitized photoelectrochemical water splitting". *Chem. Commun.* **2017,** *53*, 6784-6787, doi: 10.1039/C7CC02730C

95. Gillaizeau-Gauthier, I.; Odobel, F.; Alebbi, M.; Argazzi, R.; Costa, E.; Bignozzi, C. A.; Qu, P.; Meyer, G. J., "Phosphonate-Based Bipyridine Dyes for Stable Photovoltaic Devices". *Inorg. Chem.* **2001,** *40*, 6073-6079, doi: 10.1021/ic010192e

96. Bae, E.; Choi, W.; Park, J.; Shin, H. S.; Kim, S. B.; Lee, J. S., "Effects of Surface Anchoring Groups (Carboxylate vs Phosphonate) in Ruthenium-Complex-Sensitized TiO2 on Visible Light Reactivity in Aqueous Suspensions". *J. Phys. Chem. B* **2004,** *108*, 14093-14101, doi: 10.1021/jp047777p

97. Park, H.; Bae, E.; Lee, J.-J.; Park, J.; Choi, W., "Effect of the Anchoring Group in Ru−Bipyridyl Sensitizers on the Photoelectrochemical Behavior of Dye-Sensitized TiO2 Electrodes: Carboxylate versus Phosphonate Linkages". *J. Phys. Chem. B* **2006,** *110*, 8740-8749, doi: 10.1021/jp060397e

98. Hanson, K.; Brennaman, M. K.; Luo, H.; Glasson, C. R. K.; Concepcion, J. J.; Song, W.; Meyer, T. J., "Photostability of Phosphonate-Derivatized, RuII Polypyridyl Complexes on Metal Oxide Surfaces". *ACS Appl. Mater. Interfaces* **2012,** *4*, 1462-1469, doi: 10.1021/am201717x

99. Lee, S.-H. A.; Zhao, Y.; Hernandez-Pagan, E. A.; Blasdel, L.; Youngblood, W. J.; Mallouk, T. E., "Electron transfer kinetics in water splitting dye-sensitized solar cells based on core-shell oxide electrodes". *Faraday Discuss.* **2012,** *155*, 165-176, doi: 10.1039/C1FD00083G

100. Zhao, Y.; Swierk, J. R.; Megiatto, J. D.; Sherman, B.; Youngblood, W. J.; Qin, D.; Lentz, D. M.; Moore, A. L.; Moore, T. A.; Gust, D.; Mallouk, T. E., "Improving the efficiency of water splitting in dye-sensitized solar cells by using a biomimetic electron transfer mediator". *Proc. Natl. Acad. Sci. U.S.A.* **2012,** *109*, 15612-15616, doi: 10.1073/pnas.1118339109

101. Thomsen, J. M.; Huang, D. L.; Crabtree, R. H.; Brudvig, G. W., "Iridium-based complexes for water oxidation". *Dalton Transactions* **2015,** *44*, 12452-12472, doi: 10.1039/C5DT00863H

102. Moore, G. F.; Blakemore, J. D.; Milot, R. L.; Hull, J. F.; Song, H.-e.; Cai, L.; Schmuttenmaer, C. A.; Crabtree, R. H.; Brudvig, G. W., "A visible light water-splitting cell with a photoanode formed by codeposition of a high-potential porphyrin and an iridium water-oxidation catalyst". *Energy Environ. Sci.* **2011,** *4*, 2389-2392, doi: 10.1039/C1EE01037A

103. Chen, Z.; Concepcion, J. J.; Meyer, T. J., "Rapid catalytic water oxidation by a single site, Ru carbene catalyst". *Dalton Transactions* **2011,** *40*, 3789-3792, doi: 10.1039/C0DT01178A

104. Joya, K. S.; Joya, Y. F.; Ocakoglu, K.; van de Krol, R., "Water-Splitting Catalysis and Solar Fuel Devices: Artificial Leaves on the Move". *Angew. Chem. Int. Ed.* **2013,** *52*, 10426-10437, doi: 10.1002/anie.201300136

105. Gao, J.; Miao, J.; Li, Y.; Ganguly, R.; Zhao, Y.; Lev, O.; Liu, B.; Zhang, Q., "Dye-sensitized polyoxometalate for visible-light-driven photoelectrochemical cells". *Dalton Transactions* **2015,** *44*, 14354-14358, doi: 10.1039/C5DT01769F

106. Bofill, R.; García-Antón, J.; Escriche, L.; Sala, X., "Chemical, electrochemical and photochemical molecular water oxidation catalysts". *Journal of Photochemistry and Photobiology B: Biology* **2015,** *152*, 71-81, doi: https://doi.org/10.1016/j.jphotobiol.2014.10.022

107. Tachan, Z.; Hod, I.; Zaban, A., "The TiO2–Catechol Complex: Coupling Type II Sensitization with Efficient Catalysis of Water Oxidation". *Adv Energy Mater* **2014,** *4*, 1301249-n/a, doi: 10.1002/aenm.201301249

108. Duan, L.; Fischer, A.; Xu, Y.; Sun, L., "Isolated Seven-Coordinate Ru(IV) Dimer Complex with [HOHOH]− Bridging Ligand as an Intermediate for Catalytic Water Oxidation". *J. Am. Chem. Soc.* **2009,** *131*, 10397-10399, doi: 10.1021/ja9034686

109. Duan, L.; Bozoglian, F.; Mandal, S.; Stewart, B.; Privalov, T.; Llobet, A.; Sun, L., "A molecular ruthenium catalyst with water-oxidation activity comparable to that of photosystem II". *Nat Chem* **2012,** *4*, 418-423, doi: http://www.nature.com/nchem/journal/v4/n5/abs/nchem.1301.html#supplementary-information

110. Jiang, Y.; Li, F.; Zhang, B.; Li, X.; Wang, X.; Huang, F.; Sun, L., "Promoting the Activity of Catalysts for the Oxidation of Water with Bridged Dinuclear Ruthenium Complexes". *Angew. Chem. Int. Ed.* **2013,** *52*, 3398-3401, doi: 10.1002/anie.201209045

111. Xue, L.-X.; Meng, T.-T.; Yang, W.; Wang, K.-Z., "Recent advances in ruthenium complex-based light-driven water oxidation catalysts". *Journal of*

Photochemistry and Photobiology B: Biology **2015,** *152*, 95-105, doi: https://doi.org/10.1016/j.jphotobiol.2015.07.005

112. Gao, Y.; Duan, L.; Yu, Z.; Ding, X.; Sun, L., "Artificial photosynthesis: photosensitizer/catalyst supramolecular assemblies for light driven water oxidation". *Faraday Discuss.* **2014,** *176*, 225-232, doi: 10.1039/C4FD00127C

113. Youngblood, W. J.; Lee, S.-H. A.; Maeda, K.; Mallouk, T. E., "Visible Light Water Splitting Using Dye-Sensitized Oxide Semiconductors". *Acc. Chem. Res.* **2009,** *42*, 1966-1973, doi: Doi 10.1021/Ar9002398

114. Yamamoto, M.; Wang, L.; Li, F.; Fukushima, T.; Tanaka, K.; Sun, L.; Imahori, H., "Visible light-driven water oxidation using a covalently-linked molecular catalyst-sensitizer dyad assembled on a TiO2 electrode". *Chem. Sci.* **2016,** *7*, 1430-1439, doi: 10.1039/C5SC03669K

115. Sherman, B. D.; Xie, Y.; Sheridan, M. V.; Wang, D.; Shaffer, D. W.; Meyer, T. J.; Concepcion, J. J., "Light-Driven Water Splitting by a Covalently Linked Ruthenium-Based Chromophore–Catalyst Assembly". *ACS Energy Letters* **2016**, 124-128, doi: 10.1021/acsenergylett.6b00661

116. Lindquist, R. J.; Phelan, B. T.; Reynal, A.; Margulies, E. A.; Shoer, L. E.; Durrant, J. R.; Wasielewski, M. R., "Strongly oxidizing perylene-3,4-dicarboximides for use in water oxidation photoelectrochemical cells". *J. Mater. Chem. A* **2016**, doi: 10.1039/C5TA05790F

117. Ding, X.; Gao, Y.; Zhang, L.; Yu, Z.; Liu, J.; Sun, L., "Visible Light-Driven Water Splitting in Photoelectrochemical Cells with Supramolecular Catalysts on Photoanodes". *Acs Catal* **2014,** *4*, 2347-2350, doi: 10.1021/cs500518k

118. Ma, D.; Bettis, S. E.; Hanson, K.; Minakova, M.; Alibabaei, L.; Fondrie, W.; Ryan, D. M.; Papoian, G. A.; Meyer, T. J.; Waters, M. L.; Papanikolas, J. M., "Interfacial Energy Conversion in RuII Polypyridyl-Derivatized Oligoproline Assemblies on TiO2". *J. Am. Chem. Soc.* **2013,** *135*, 5250-5253, doi: 10.1021/ja312143h

119. Li, H.; Li, F.; Wang, Y.; Bai, L.; Yu, F.; Sun, L., "Visible-Light-Driven Water Oxidation on a Photoanode by Supramolecular Assembly of Photosensitizer and Catalyst". *Chempluschem* **2016,** *81*, 1056-1059, doi: 10.1002/cplu.201500539

120. Click, K. A.; Beauchamp, D. R.; Huang, Z.; Chen, W.; Wu, Y., "Membrane-Inspired Acidically Stable Dye-Sensitized Photocathode for Solar Fuel Production". *J. Am. Chem. Soc.* **2016,** *138*, 1174-1179, doi: 10.1021/jacs.5b07723

121. Fan, K.; Li, F.; Wang, L.; Daniel, Q.; Gabrielsson, E.; Sun, L., "Pt-free tandem molecular photoelectrochemical cells for water splitting driven by visible light". *Phys. Chem. Chem. Phys.* **2014,** *16*, 25234-25240, doi: 10.1039/C4CP04489D

122. Tong, L.; Iwase, A.; Nattestad, A.; Bach, U.; Weidelener, M.; Gotz, G.; Mishra, A.; Bauerle, P.; Amal, R.; Wallace, G. G.; Mozer, A. J., "Sustained solar hydrogen generation using a dye-sensitised NiO photocathode/BiVO4 tandem photo-electrochemical device". *Energy Environ. Sci.* **2012,** *5*, 9472-9475, doi: 10.1039/C2EE22866A

123. Li, F.; Fan, K.; Xu, B.; Gabrielsson, E.; Daniel, Q.; Li, L.; Sun, L., "Organic Dye-Sensitized Tandem Photoelectrochemical Cell for Light Driven Total Water Splitting". *J. Am. Chem. Soc.* **2015,** *137*, 9153-9159, doi: 10.1021/jacs.5b04856

124. Kudo, A.; Miseki, Y., "Heterogeneous photocatalyst materials for water splitting". *Chem. Soc. Rev.* **2009,** *38*, 253-278, doi: 10.1039/B800489G

125. Rodenberg, A.; Orazietti, M.; Mosberger, M.; Bachmann, C.; Probst, B.; Alberto, R.; Hamm, P., "Quinones as Reversible Electron Relays in Artificial Photosynthesis". *Chemphyschem* **2016,** *17*, 1321-1328, doi: 10.1002/cphc.201501085

126. Becker, H.-D., "Photochemical Reactions with Phenols. IV. The Benzophenone-Sensitized Disproportionation of Hydroquinone Monoaryl Ethers". *J. Org. Chem.* **1967,** *32*, 2136-2140, doi: 10.1021/jo01282a601

2 Chapter 2: Eco-friendly dye-sensitized solar cells

Aim of this section

The first part of this PhD project has been dedicated to the study of dye-sensitized solar cells containing eco-friendly solvents in the electrolyte solution, namely Deep Eutectic Solvents (DES). Traditional organic solvents used for this scope (usually nitriles mixtures) have many drawbacks, such as volatility and often toxicity. This can be a problem if the cell is not perfectly sealed, because it would involve toxic vapours in the environment and also a fast deterioration of the performance of the cell, that cannot work without the liquid electrolyte.

Two different systems have been studied, an hydrophilic and an hydrophobic one, with proper dyes absorbed onto TiO_2. Many variables have been considered, such as different TiO_2 pastes and layer thickness, different iodides (both inorganic and ionic liquids, IL), different ions concentration, presence and absence of additives and of disaggregating agents.

The efficiency of the optimized cell was 1.9% at 0.5 sun for the hydrophilic system and 2.5% at 1 sun for the hydrophobic solvent, compatible with traditional organic-solvent-based cells.

2.1 Deep eutectic solvents (DES)

In this work, a new class of solvents in fast growth has been tested in DSSC, namely Deep Eutectic Solvents (DES). They meet the urgent need for eco-friendly and biodegradable solvents, officially stated first on 8 September 2000, when, after a three-day Millennium Summit of World leaders at the headquarters of the United Nations, the General Assembly adopted the Millennium Declaration; it contained eight chapters and the fourth objective was entitled "Protecting our common environment".[1] Solvents are everywhere in chemical industry and products, for example they are fundamental during synthesis (in 2005 they constituted more than 80% of non-aqueous materials used to make active medicine ingredient),[2] but also in products such as paints, coatings, adhesives.

Common volatile organic compounds (VOC) tend to accumulate in the atmosphere due to the low boiling point, and they are characterized by flammability, high toxicity, and non-biodegradability. They are however necessary to carry out organic reactions: for instance, they allow easy control over mass and heat transference, stabilization of transition states, and fast modification of reactivity.

Fluorinated solvents, that are thermally and chemically stable and nontoxic, could be a good alternative, but they are very expensive and they persist in the atmosphere.[3]

Some solvents can be derived from biomasses, such as ethanol, limonene, ethyl lactate,[4] glycerol,[5] 2-methyltetrahydrofuran,[6] but their properties are not tunable.

Intuitively, water would be a perfect solvent, being nontoxic, renewable, safe and cheap, but usually organic reagents and catalyst are not water-soluble, and water could even hinder some reaction by hydrolysis of some functionalities.

Finally, it is very hard to purify water contaminated by chemicals at the end of reactions.

The interest of scientific community then focused on ionic liquids (IL), composed by a combination of an organic cation (usually imidazolium-based cations) with a large variety of anions, the most common ones being Cl^-, BF_4^-, PF_6^-. Thanks to the wide choice of anions and cations that could be employed (it has been calculated that more than 10^{18} possible IL could be theoretically produced)[7], IL can show very different properties such as viscosity, melting point, conductivity, solubility, stability over 200 °C, so that they can be tailored for many different applications. The drawbacks are that they need very pure components (even small impurities can change their properties), they are expensive, poorly biodegradable, and they require big quantities of salts and solvents during preparation.[8-9]

Since the beginning of this century, a new class of solvents has gained more and more attention: eutectic mixtures in which it is possible to realize many reactions. When a mixture of two or more phase-immiscible solid components has one single composition and temperature where it has a transition to one liquid phase it is said to be an eutectic mixture, and the coordinates of composition and temperature define the eutectic point (**Figure 2.1**). This transition happens when a part of the component atoms are small and can move in interstitial spaces of the network created by larger atoms; the crystalline pattern is thus disrupted thanks to diminished electrostatic forces and this leads to a decrease of the freezing point of the eutectic mixture.[1]

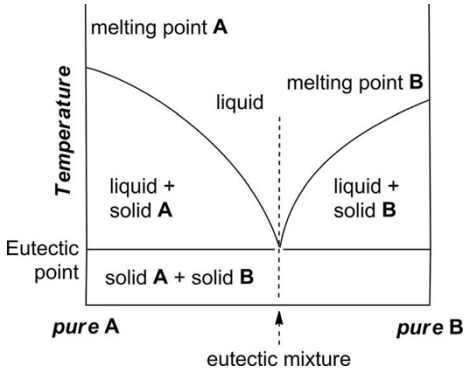

Figure 2.1. *Phase diagram of a mixture that shows an eutectic point.*

Deep Eutectic Solvents (DESs) are a particular case of eutectic mixtures, made of two or more solids that give a liquid solution at room temperature.[10] The formation of these DESs is simply obtained by mixing together two safe components in fixed proportions (cheap, renewable and biodegradable), until the mixture becomes liquid. Lately, DESs can be obtained also from a solid component and a liquid one, such as ethylene glycol or glycerol.[11]

Generally, a DES is composed by two or three components that associate with each other through hydrogen bond interactions, forming an eutectic mixture with a melting point far lower than that of both components (this explains the adjective "Deep" in the name). Usually, DESs are liquid at temperatures lower than 150 °C, and most of them are liquid between room temperature and 70 °C. In most cases, a DES is obtained by mixing a quaternary ammonium salt with metal salts or a hydrogen bond donor that has the ability to form a complex with the halide anion of the quaternary ammonium salt.[12] Many different components can be used, some example are reported in **Figure 2.2**.

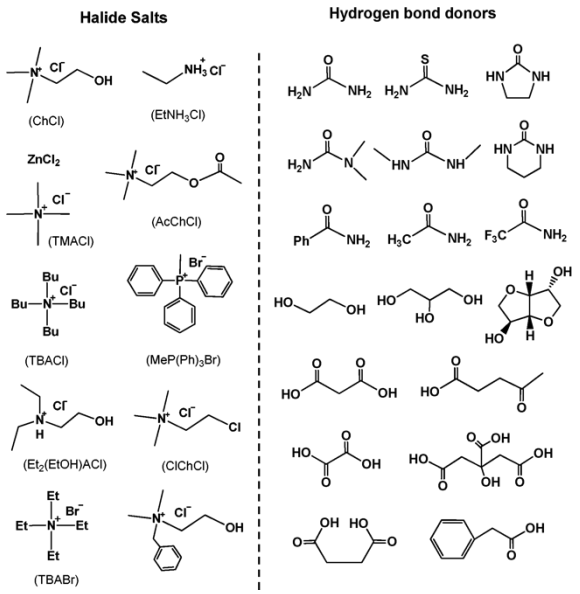

Figure 2.2. *Typical structures of the halide salts and hydrogen bond donors used for DES syntheses. Reproduced from Ref. 12 with permission from The Royal Society of Chemistry.*

One of the most common components present in DESs is choline chloride (ChCl), that is a very cheap, biodegradable and non-toxic quaternary ammonium salt which can be extracted from biomass or synthesized from fossil reserves, often used as an additive in chicken food for accelerating growth (it is also known as Vitamin B_4). In combination with safe hydrogen bond donors such as urea, renewable carboxylic acids (e.g. oxalic, citric, succinic or amino acids) or renewable polyols (e.g. glycerol, carbohydrates), ChCl can rapidly form a DES. The freezing point of the eutectic mixture is usually impressively lower than the melting temperature of the components; for example, the melting point of ChCl and glycerol is 302 and 17.8 °C respectively, while the freezing point of the DES composed by 1:2 ratio of them is as low as -40 °C.[13]

Although most of DESs are made from ChCl as an ionic species, DESs cannot be considered as ILs because DESs are not entirely composed of ionic species and they can also be obtained from non-ionic species.

When compared to traditional ILs, DESs derived from ChCl gather many advantages: they are cheap, chemically inert with water (that means easy

storage), easy to prepare since DESs are obtained by simply mixing two components, thus by-passing all problems of purification and waste disposal generally encountered with ILs, and most of them are biodegradable,[14] biocompatible[15] and nontoxic.[16]

These DESs are attractive since they have physico-chemical properties similar to traditional imidazolium-based ILs and thus can advantageously replace them in many applications. As compared to traditional organic solvents, DESs are not considered as volatile organic solvents and they are not flammable, making their storage convenient. Additionally, synthesis of DESs is characterized by a 100% atom economy, it is easy to handle and does not need any purification, thus making their large-scale use feasible.

Since it is possible to prepare DESs made of so many different components, their physicochemical properties can be widely tuned so that they can find many different applications. For example, density is usually higher than water, but the range can go from 1.04 to 1.63 g mL^{-1}.[12] Usually, DESs have a high viscosity, often attributed to the hydrogen bond network between the components, that causes a lower mobility of species inside the solution. At 20 °C, DESs viscosity ranges from 19 to 85 000 cP, while water is 1 cP.[12] Such high density and viscosity can be considered an important drawback for industrial scale or in continuous-flow applications, but adding another component such as water, a carboxylic acid or a halide frequently solves this problem and makes DESs even more versatile.

An impressive feature of DESs is their dissolving ability; for example, a ChCl/urea 1:2 DES can dissolve water-soluble inorganic salts (e.g. LiCl) but also scarcely water-soluble ones (e.g. AgCl), aromatic acids such as benzoic acid and amino acids,[17] and even various metal oxides, and this could lead to a green way for metal recycle process. [18]

Thanks to all the peculiar properties of these solvents, they are applied in many different fields, for example in extraction and separation processes,[19-21] for metal electrodeposition,[10] in polymerisation and material sciences,[22-23] but they have

recently gained increasing attention also in other hot fields of science such as metal-,[24-29] bio-,[30-34] and organocatalysis,[35-37] photosynthesis and electrochemistry,[38-39] and organometallics[26, 40-45] with surprising and unexpected results.

Among all of this variety of publications, also an application of DESs in DSSCs has been reported by Jhong et al. in 2009; using a DES composed by glycerol and choline iodide as electrolyte solvent, an efficiency of 3.88% has been obtained under 1 sun illumination.[46] To the best of our knowledge, no other examples of DES-based DSSCs are present in the literature, apart from the ones illustrated in this PhD work.

2.2 Aqueous-DES based DSSC

Among the alternative technologies for energy production free from fossil fuels, in the last two decades research focused the attention on third generation photovoltaics (PV), aiming to high-efficiency and low cost cells based on thin film technology, using both organic and inorganic materials.[47] The most studied devices in this class were dye-sensitized solar cells (DSSCs), that promised to be easy to fabricate, efficient and low cost.[48-50] One of the main drawbacks of this kind of cells is the electrolyte solution: they usually employ volatile organic solvents (VOCs), that are often toxic, such as acetonitrile. This is a serious issue to be afforded in order to have a widespread use of these devices. In order to overcome these problems, different electrolytes have been proposed as electrolyte media, such as ionic liquids (ILs),[51] liquid solutions adsorbed on polymeric matrix,[49, 52-54] and even solid state cells free from any solvent.[55-56] Each of these configurations carries some disadvantages: for example, the performance and the price of the cells are often negatively affected. Therefore, an easy-available, sustainable, low cost electrolyte media, retaining an efficiency comparable to VOCs, would give an important boost to a wider diffusion of DSSCs.

In the last years, many efforts have been made to employ a perfectly eco-friendly solvent in DSSCs: water.[57] Of course, it is abundant, non-toxic and cheap, but it is an atypical solvent for DSSCs. Usually, it was avoided because of its detrimental effects on DSSCs performance. For example, water negatively affects the stability of the covalent grafting of the sensitizer to the photoanode semiconductor oxide, typically TiO_2, leading to dye desorption and corresponding shutdown of the device. Furthermore, water can negatively shift the TiO_2 conduction band, interact with additives and salts present in the electrolyte solution, and inhibit the interfacial contact between the electrolyte phase and the dye-coated semiconductor surface when common hydrophobic

sensitizers are used. [58] Nevertheless, very exhaustive works have been recently published using water as the electrolyte solvent, but efficiencies are usually low, ranging from less than 1% to 4%.[57, 59-60]

In the last years, a new category of solvents has been proposed: the Deep Eutectic Solvents (DESs).[61] As described previously, DESs show many physico-chemical properties similar to ILs, such as density, viscosity, refractive index, conductivity, surface tension, chemical inertness, etc., but they also have some great advantages over ILs. In fact, DESs were studied to overcome some drawbacks of ILs, that are often expensive, toxic and poorly biodegradable, and their synthesis is not eco-friendly at all.

DESs are obtained by just mixing together two or three safe components that can form an eutectic mixture, liquid at room temperature. One of the most used component is choline chloride, also known as vitamin B_4, that is a very cheap (ca. 2 € kg^{-1}), biodegradable and non-toxic quaternary ammonium salt, and it is mixed with safe hydrogen bond donors such as urea, carboxylic acids (e.g. oxalic, citric, succinic or amino acids) or polyols (e.g. glycerol, carbohydrates). In this way a solvent is obtained that cannot be considered as ILs because DESs are not entirely composed of ionic species and they can also be obtained from non-ionic species. This kind of solvent is easy to prepare (it is just a mixture of the components), cheap, low volatile, non-flammable and, last but not least, they are biodegradable, biocompatible and non-toxic.

To the best of our knowledge, however, applications of DESs in electrochemistry and energy conversion are still limited.[62] The only example in the literature of exploitation of a DES [namely choline iodide–glycerol (1:3, mol mol^{-1})] in DSSCs has recently been reported by Wong and co-workers.[46] In combination with an organic sensitizer, these authors have reported a PCE of 3.9% vs a value of 4.9% of a control experiment in CH_3CN as the electrolyte solvent. However, in this case, the whole electrolyte solvent was constituted by a mixture of 1-propyl-3-methylimidazolium iodide (PMII) and the aforementioned DES (13:7, v v^{-1}),

which resembles more an adapted IL rather than a "pure" DES medium. Indeed, the same authors classify their work amongst IL-based DSSCs, and the reported efficiency is to be referred to IL-based devices where PCEs higher than in water are routinely achieved.

The present section of the PhD work combined the green aspects of both water and DES, using a healthy and safe electrolyte solvent, and employing a hydrophilic molecule developed in our research group as a dye. The efficiencies presented in this preliminary work are not high as an absolute value, but they are comparable to those known in literature for water-based solar cells.

2.2.1 Choice of materials

Since the aim of the present work was to prepare a DSSC working with a water-based electrolyte solvent, the dye acting as a sensitizer has been carefully chosen to offer good performance and good compatibility with an aqueous environment. Organic dyes usually show a molar extinction coefficient higher than metalorganic ones, such as the conventional Ru-based N719,[63] so less dye is needed and ultrathin TiO_2 layers (less than 5 μm) can be used. In order to improve the hydrophilicity of the dye, glycolic chains can be successfully employed.[59]

Both this requirements were met by two organic dyes already developed in our research group for photocatalytic hydrogen production.[64] The chosen sensitizers were thus a donor–acceptor phenothiazine (PTZ) molecule containing thiophene-based spacers and characterized by the presence of a terminal tris(ethylene glycol) monomethyl ether (TEG) substituent (**PTZ-TEG**) and a similar one characterized by the presence of a methyl α-D-glucopyranoside moiety (**PTZ-GLU**), **Figure 2.3**.

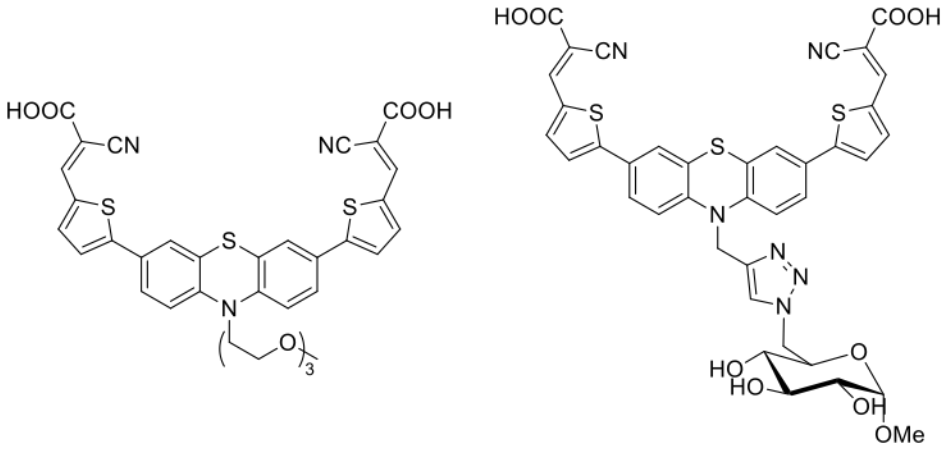

Figure 2.3. *Structure of the hydrophilic dyes used as DSSC sensitizers:* ***PTZ-TEG*** *(left) and* ***PTZ-GLU*** *(right).*

A first screening concerning the choice of the dye candidate to go on with this study and the proper dilution of the DES was carried out with a set of cells comparing different electrolytes (the traditional VOC-based Z960, the commercial IL-based Solaronix Mosalyte TDE-250, DES diluted with 20% water and with 40% water) and the two illustrated dyes. The results are reported in **Table 2.1** and in **Figure 2.4**.

Table 2.1. *Photovoltaic characteristics of DSSCs made with* ***PTZ-TEG*** *and* ***PTZ-GLU*** *varying different electrolytes.*

Dye	Electrolyte	Cell #	J_{sc} (mA cm^{-2})	V_{oc} (V)	FF (%)	η (%)
PTZ-TEG	Z960	1	7.95	0.620	73	3.6
	Mosalyte	2	5.8	0.575	72	2.3
	DES 20% water	3	2.65	0.381	61	0.6
	DES 40% water	4	2.45	0.355	59	0.5
PTZ-GLU	Z960	5	7.0	0.614	75	3.2
	Mosalyte	6	5.4	0.579	72	2.3

DES 20% water	7	3.9	0.361	60	0.8
DES 40% water	8	3.8	0.363	62	0.9

Dye absorbed on 5-µm thick TiO_2 transparent layer; co-absorbent: 1:50 CDCA with ***PTZ-TEG****, 1:50 glucuronic acid with* ***PTZ-GLU****; DES-based solutions with 4 M KI, 20 mM I_2.*

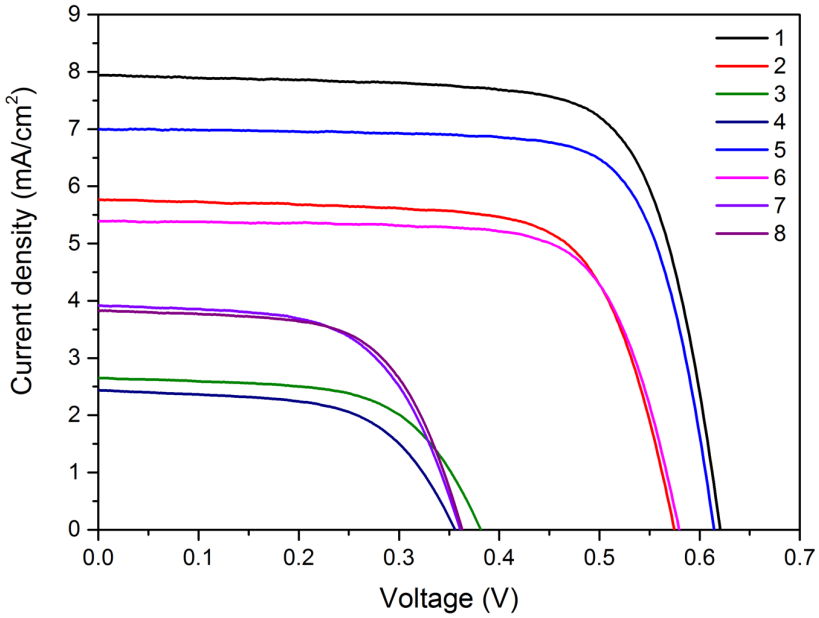

Figure 2.4. *J/V characteristics for DSSC described in* ***Table 2.1****.*

Since the DES diluted with 20% water was very viscous, it was immediately discarded from further study. Regarding the comparison between the dyes, **PTZ-GLU** performed a little better with DES, but its synthesis is very laborious and complex, so the difference in efficiency did not justify its choice, and the study was then carried out testing only **PTZ-TEG** dye.

The choice of an appropriate DES as electrolyte solvent was made following the main aspect of an eco-friendly material, so it has to be made of abundant, cheap, low-cost to synthesise, little viscous, non-toxic, and sustainable components. As a green solvent, constituted by cheap and widely used materials, a 1:2 choline chloride/glycerol DES was chosen (**Figure 2.5**); its eco-friendly nature has been

further improved and the viscosity has been reduced and adapted to an easy application in large area panels by adding a 40% w/w water to this DES.

An hydrophilic dye-sensitizer was then needed to maximize the compatibility between electrolyte and dye. In this way, dye regeneration was efficiently promoted (electron donation from the reduced form of the redox couple to the oxidized dye following photon absorption of the dye and electron injection to the CB of TiO_2).

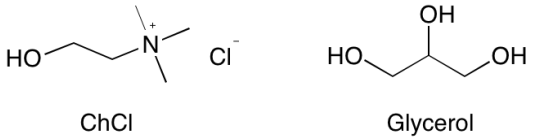

Figure 2.5. *Structures of choline chloride (ChCl) and glycerol.*

After choosing the dye and the DES, a short investigation was dedicated to the choice of the proper co-adsorbent. In DSSCs chenodeoxycholic acid (CDCA) is often used to reduce the formation of dye aggregates and the detrimental charge recombination, thus improving the cell performance.[65] Also other acids could act in a similar way by attaching on TiO_2 surface, so a more water-compatible acid was tested, namely glucuronic acid (GA), that has a simple structure and its polar nature favours interactions with polar media; finally, GA is widely available from natural sources (*e.g.* gum arabic) and is very cheap (**Figure 2.6**). To the best of our knowledge, it has never been employed before as a co-adsorbent in DSSC.

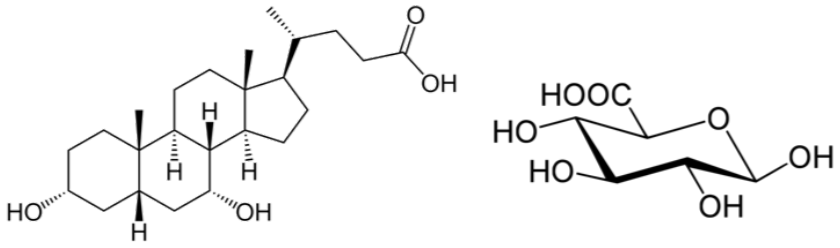

Figure 2.6. *Structures of the co-adsorbent agents tested in this study: CDCA (left) and GA (right).*

As illustrated in **Table 2.2**, the presence of CDCA basically does not affect neither the performance nor the dye loading with respect to not using a co-

adsorbent at all; very similar performances were obtained using the same ratio of GA (1:50 dye/acid), but the amount of dye adsorbed on the TiO_2 surface was one order of magnitude smaller. Different ratios of GA were then tested, with a dye loading always smaller than the one with CDCA.

***Table* 2.2.** *Photovoltaic characteristics of DES-based DSSC and dye loading upon variation of co-adsorbent*

Co-adsorbent	J_{sc} [mA cm^{-2}]	V_{oc} [V]	FF	η[%]	Dye loading [10^{-7} mol cm^{-2}]
No co-ads.	3.0	0.373	0.57	0.6	2.54
CDCA 1:50	2.5	0.384	0.62	0.6	2.64
GA 1:50	2.6	0.344	0.62	0.5	0.461
GA 1:10	2.5	0.355	0.60	0.5	1.37
GA 1:1	2.5	0.349	0.60	0.5	2.01

Electrolyte composition: 4 M KI, 20 mM I_2, DES with 40% water.

It is worth noting that, independently of the GA/dye ratio, the photovoltaic characteristics remain almost the same; to find an explanation to this behaviour further investigations were carried out, measuring the incident photon to current efficiency (IPCE), the light harvesting efficiency (LHE) and calculating the absorbed photon to current efficiency (APCE), see **Figure 2.7**. The IPCE measurements are very similar for all the investigated ratios, but LHE look different, as it could be expected. The higher the quantity of co-absorbent, the lower the quantity of absorbed dye and the lower the LHE (measured as the complementary to 1 of a transmittance spectrum), since a lower quantity of dye implies an higher transmittance. The APCE is then calculated as:

$$APCE(\lambda) = \frac{IPCE(\lambda)}{LHE(\lambda)}$$

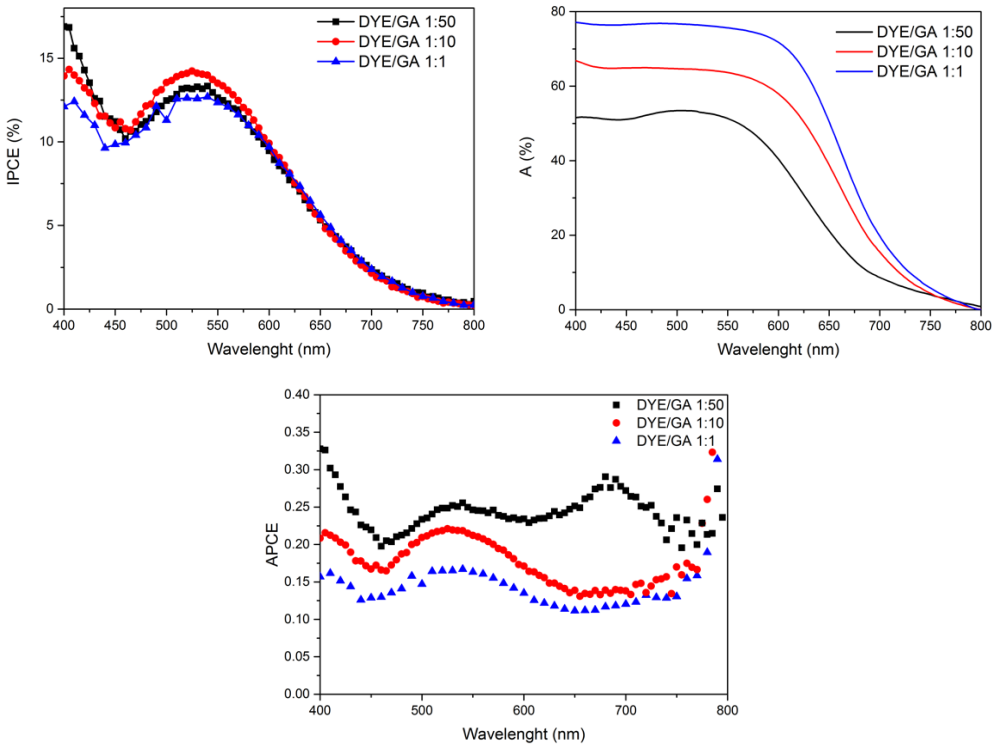

Figure 2.7. *Measured IPCE and LHE and calculated APCE for different dye/GA ratios.*

The APCE follows an opposite trend with respect to LHE, so electrodes with a lower quantity of dye are more efficient in transforming absorbed photons into electrons, likely due to an higher recombination occurring in electrodes with more dye. As a result, we chose the 1:10 ratio as a compromise.

2.2.2 Photovoltaic investigation

DSSC using water-based DES as an electrolyte solvent and an hydrophilic organic dye as a sensitizer have been investigated.

The electrolyte composition was varied both in quantity and type of iodide, testing an inorganic salt (KI 1 M, 2 M and 4 M) and several inorganic ones (1-Methyl-3-propylimidazolium iodide, 1-Butyl-3-methylimidazolium iodide and 1,3-Dimethylimidazolium iodide). Some additives routinely found in liquid DSSC were then added to the electrolyte solution, such as several pyridine-

derivatives and guanidinium thiocyanate. To enhance TiO_2 pore diffusion, thin transparent TiO_2 layers can be employed, so different transparent TiO_2 thicknesses (2.5 and 5 μm) have been tested; a blocking layer and/or a scattering layer was also investigated for a better comparison with conventional double-layer DSSCs. Finally, two different counter electrodes were used, namely Pt and PEDOT ones, since PEDOT counter electrodes have been reported to have better performances in aqueous environment.[59]

The results of the first set investigated are summarized in **Table 2.3** and the J/V curves are illustrated in **Figure 2.8**. Iodine concentration was kept equal to 0.02 M in agreement with the most common values used in conventional liquid DSSCs. At first, the cells were filled with an electrolyte based on 1 M and 2 M KI solutions, with the 2 M cells giving a little higher current than the 1 M ones. Also a 4 M KI solution has been tested, but it was more viscous and did not carry any big improvement in the PV performance, so it was not considered anymore in the study.

A significant improvement was recorded when using an ionic liquid as iodide source; as for KI, three concentrations of 1-Methyl-3-propylimidazolium iodide (PMII) solutions were tested, 1 M, 2 M and 4 M, with a good improvement in the photocurrent. 4 M cells showed the best performance, with a 1.7% efficiency, but it is worth noting that the biggest part of the solution was constituted by the ionic liquid with just a small quantity of aqueous DES (the concentration of pure PMII is 6 M), so DES could not be considered the solvent; thus, this result has been discarded.

Table 2.3. *Photovoltaic characteristics of DES-based DSSC upon variation of electrolyte composition*

Cell	Electrolyte	J_{sc} [mA cm^{-2}]	V_{oc} [V]	FF	η [%]
1	PMII 2M in CH_3CN	7.3	0.483	0.70	2.5
2	KI 1M	1.4	0.452	0.63	0.4
3	KI 2M	1.9	0.429	0.64	0.5
4	PMII 1M	1.1	0.467	0.70	0.4
5	PMII 2M	3.3	0.478	0.67	1.0
6	PMII 2M + GuSCN	4.1	0.495	0.65	1.3

I_2 concentration = 20 mM

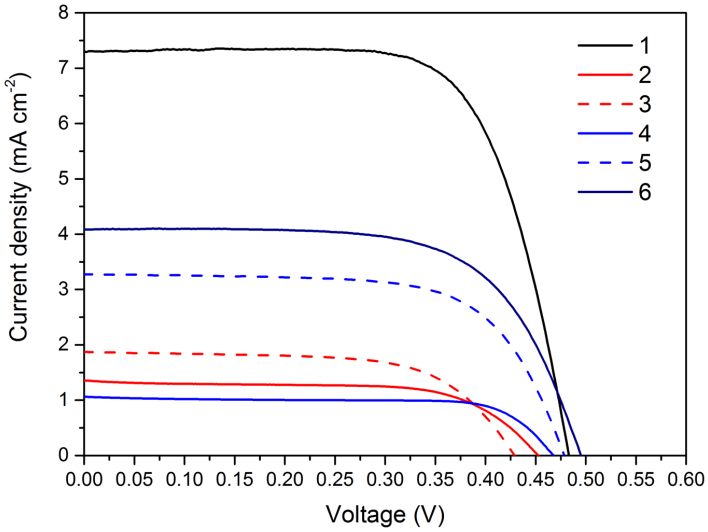

Figure 2.8. *J/V characteristics for Des-based DSSC listed in* ***Table 2.3****.*

Since the best result had been reached with the 2 M PMII solution, other iodide imidazolium salts were tested to see if there would have been any difference. 1-Butyl-3-methylimidazolium iodide (BMII) and 1,3-Dimethylimidazolium iodide (DMII) were tested in 2 M concentration solutions in aqueous DES but the performances of BMII were analogous to the PMII cells, while DMII cells showed lower values for all the parameters (**Table 2.4** and **Figure 2.9**). PMII was then chosen for the following measurements.

Table 2.4. *Photovoltaic characteristics of DES-DSSC upon variation of organic (imidazolium) iodide.*

Electrolyte	J_{sc} [mA cm^{-2}]	V_{oc} [V]	FF	η [%]
PMII 2 M	3.3	0.478	0.67	1.0
BMII 2 M	3.3	0.454	0.66	1.0
DMII 2 M	2.5	0.435	0.63	0.7

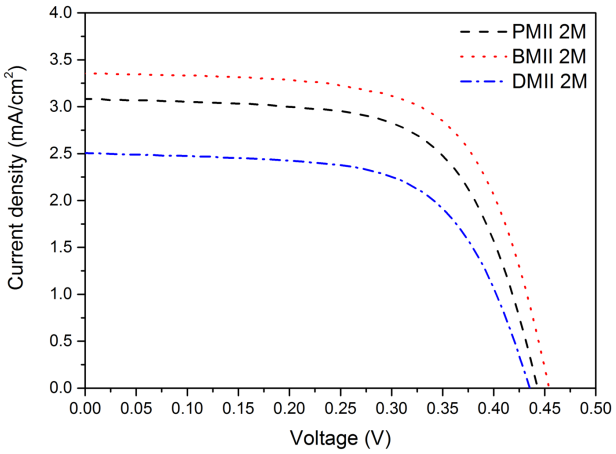

Figure 2.9. *J/V characteristics for Des-based DSSC listed in* ***Table 2.4****.*

In order to increase the V_{oc}, some pyridine-derivatives were added to either KI or PMII solutions.[66] 4-*tert*-Butylpyridine (TBP), 4-picoline and pyridine where tested with both 2 M KI and 2 M PMII solution, but the solubility of TBP in 2 M KI DES solution was too poor to perform any measurement, so the experiment with this solution was not carried out. Pyridine derivatives coordinate to the TiO_2 surface through their ring nitrogen lone pair, causing an up-shift of the energy of the CB and Fermi level of the semiconductor. This usually results in an increase of the photovoltage, which is proportional to the difference between the CB of the n-type semiconductor and the Nernst level of the redox couple.[49] Indeed, the solar cells containing the azine derivative showed an higher V_{oc}, with values increased from less than 0.5 to almost 0.7 V, but simultaneously in many cases a solid decrease of the current was observed. This was likely due to dye desorption from the titania surface (i.e., decrease of active dye concentration) due to the hydrolysis in basic aqueous media of the ester bonding

between the dye and TiO_2.[67-68] The measurements are reported in **Table 2.5** and in **Figure 2.10**; from **Figure 2.11** it is possible to notice the difference in the colour of the cell with and without pyridine derivative, an indication of the dye detachment from TiO_2. In order to get a proof of this phenomenon, a dye loading measurement was conducted on DSSCs containing PMMI and pyridine derivatives: the cell containing PMII alone had 1.67×10^{-7} mol cm^{-2} of dye onto the active layer, while all the cells where the electrolyte contained also the pyridines showed a lower dye loading, confirming the detachment of the dye. Considering these effects and the toxicity of pyridine derivatives, they were not further investigated during this study.

Table 2.5. *Photovoltaic characteristics of DES-DSSC upon addition of pyridine-based additives.*

Electrolyte	J_{sc} [mA cm^{-2}]	V_{oc} [V]	FF	η[%]	Dye loading [10^{-7} mol cm^{-2}]
KI 2 M, pyridine 0.5 M	2.1	0.628	66	0.9	/
KI 2 M, 4-picoline 0.5 M	1.3	0.646	70	0.6	/
PMII 2 M, TBP 0.5 M	1.5	0.642	73	0.7	1.11
PMII 2 M, pyridine 0.5 M	3.0	0.593	70	1.2	1.10
PMII 2M, 4-picoline 0.5 M	2.6	0.632	70	1.2	1.30

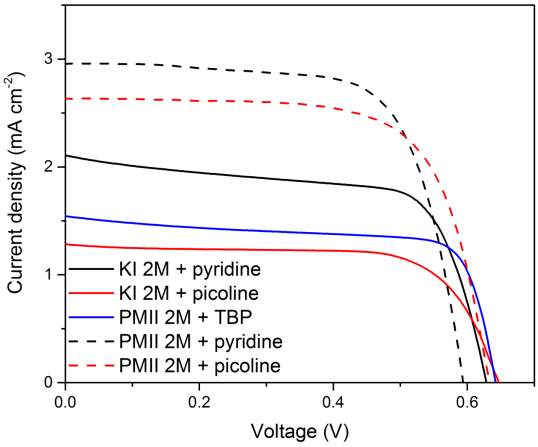

Figure 2.10. *J/V characteristics for DES-based DSSC listed in* ***Table 2.5****.*

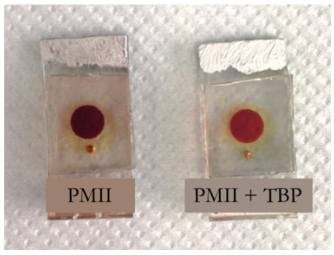

Figure 2.11. *Picture of a DSSC containing a PMII-DES based electrolyte (left) and one with the same electrolyte with added TBP (right).*

The effect of iodine concentration in the electrolyte solution was also evaluated both with KI and PMII DES based solutions. Besides the concentration commonly used in electrolytes, 0.02 M, also 0.01, 0.05 and 0.1 M have been tested, and the results are summarized in **Table 2.6** and in **Figure 2.12**. Since there were only little differences between the cells with different iodine concentration, the previously "reference" concentration 0.02 M was chosen for the subsequent experiments.

Table 2.6. *Photovoltaic characteristics of DES-DSSC upon variation of iodine concentration.*

Iodide	[I_2] [M]	J_{sc} [mA cm^{-2}]	V_{oc} [V]	FF	η [%]
KI 2M + pyridine 0.5 M	0.02	2.1	0.608	66	0.9
	0.01	1.9	0.614	68	0.8
	0.05	2.0	0.609	69	0.9
	0.10	1.9	0.582	66	0.8
PMII 2M + pyridine 0.5 M	0.02	3.0	0.593	70	1.2
	0.01	2.5	0.591	71	1.1
	0.05	2.7	0.605	71	1.2
	0.10	2.4	0.609	71	1.0

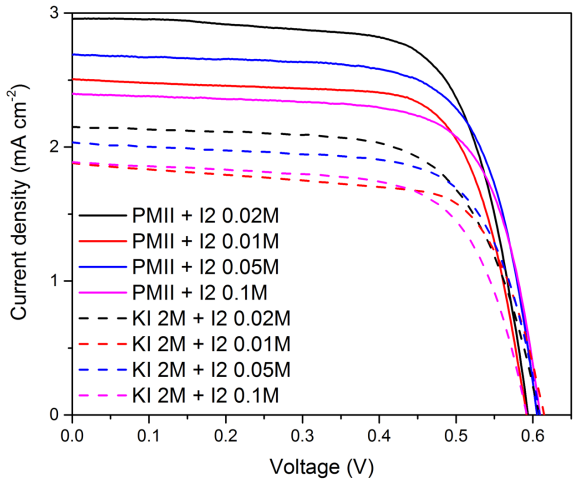

Figure 2.12. *J/V characteristics for DES-based DSSC listed in* ***Table 2.6****.*

A common additive of electrolyte solutions for organic DSSCs is guanidinium thiocyanate (GuSCN), and it has also been reported to act as a surfactant in aqueous cells.[69] For this reason, it was tested in 2 M PMMI DES solution, leading to an improvement in the photocurrent and the overall efficiency (more than twice higher than with KI), reaching 1.3% (cell 6 in **Table 2.3**).

After testing all of these variables in the electrolyte solution, also different TiO_2 substrates where evaluated, using the 2 M PMII solution as a standard for the electrolyte. In particular, the differences among photoanodes were in terms of

TiO_2 mono- (transparent) or double-layers (transparent+scattering), layer thickness and presence of a compact hole blocking layer (BL). The results are presented in **Table 2.7**.

At first, a 5-µm-thick scattering layer was screen-printed over the 5-µm transparent TiO_2 used for the previous experiments, since the double transparent+scattering layers has often been reported to afford higher photocurrents.[70-71] Unfortunately, this did not lead to any improvement, maybe because of the high recombination that is likely to happen (cell 3 of **Table 2.7**).

In order to exclude recombination effects, a blocking layer (BL) was deposited via spray-pyrolysis on FTO glass according to a standard procedure. The layer was deposited before proceeding with the TiO_2 active layer screen printing. In the case of BL+monolayer architecture, a very poor efficiency of 0.2% was recorded (cell 2 in **Table 2.7**); BL+double-layer cell instead gave a better result of 0.9% efficiency (cell 4 in **Table 2.7**), but it performed worse than without the BL. A possible explanation is the reduced charge transport induced by the presence of the compact layer.

In contrast, a net improvement was recorded by decreasing the semiconductor mesoporous transparent layer from 5 to 2.5 µm. The use of thinner films decreases the available surface for dye grafting but improves pore filling and charge transport to the electrode before recombination takes place. In this way, the cell photocurrent (cell 5 of **Table 2.7**) increases, with PCE reaching almost 1.5%.

Lastly, some tests were performed changing the material of the counter electrode, using PEDOT in place of Pt, according to literature suggestions.[59] PEDOT has been polymerised directly on pre-drilled FTO glass according to a modified standard procedure.[72] The PEDOT counter electrodes were tested with both 5 and 2.5 µm TiO_2 photoanodes (cells 6 and 7 in **Table 2.7**). PEDOT counter electrodes lead to a small improvement for 5-µm-thick cells, while the efficiency decreased for 2.5-µm-thick cells. It is then apparent that in DES-DSSCs the use

of PEDOT is not beneficial. A conventional Pt counter electrode thus appears as the best choice.

Table 2.7. *Photovoltaic characteristics of DES-based DSSC upon variation of working and counter electrode.*[a]

Cell #	TiO_2 layer1	TiO_2 layer2	TiO_2 thickness [µm]	Counter-electrode	J_{sc} [mA cm^{-2}]	V_{oc} [V]	FF	η [%]
1	Transparent	/	5	Pt	3.3	0.478	0.67	1.0
2	Transparent + BL	/	5	Pt	1.9	0.488	0.17	0.2
3	Transparent	Scattering	5+5	Pt	2.9	0.471	0.63	0.9
4	Transparent + BL	Scattering	5+5	Pt	2.9	0.498	0.62	0.9
5	Transparent	/	2.5	Pt	4.6	0.469	0.65	1.4
6	Transparent	/	5	PEDOT	4.2	0.427	0.59	1.1
7	Transparent	/	2.5	PEDOT	4.1	0.421	0.59	1.0

[a] *Electrolyte composition: 2 M PMII, 20 mM I_2, DES with 40% water.*

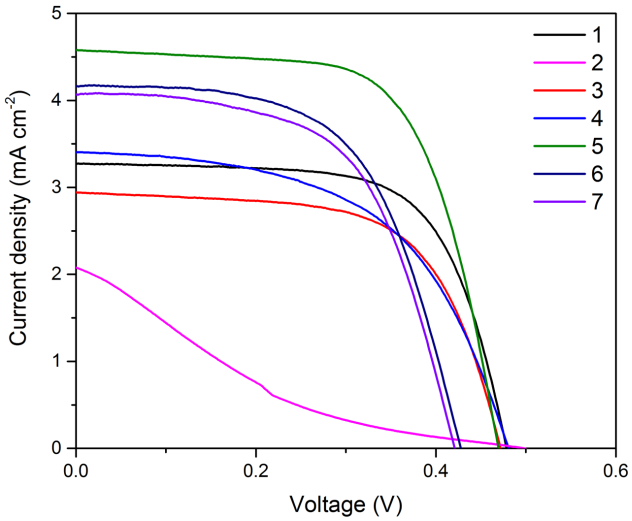

Figure 2.13. *J/V characteristics for DES-based DSSC listed in* ***Table 2.7****.*

Combining the results regarding the best TiO_2 layer (2.5-μm-thick transparent layer) and the best electrolyte composition (2 M PMMI + 0.1 M GuSCN aqueous DES solution) it was possible to design the optimal configuration for the system under examination. The best cell gave a photocurrent higher than 5 mA cm^{-2} and an overall PCE of 1.7%. This result was further improved at reduced irradiation (0.5 Sun), as those typically found under diffuse light conditions, reaching a conversion efficiency of almost 2% (**Table 2.8** and **Figure 2.14**). For the best cell, also the incident monochromatic photon-to-electric current conversion efficiency (IPCE) as a function of wavelength has been evaluated: the DES-DSSC shows IPCE values > 0 over the whole visible wavelength range, exceeding 40% from ca. 480 to 550 nm (**Figure 2.15**). This IPCE characteristics compare well with best performances of water-based DSSC.[57, 59-60] Finally, to check the effect of the co-adsorbent, a similar device prepared under the same conditions of the champion cell but without co-adsorbent GA has been tested. In this case the IPCE values were smaller (< 30%), although the shape is similar to that in presence of the co-adsorbent. It is therefore confirmed the aforementioned beneficial effects of the co-adsorbent on device performances.

Table 2.8. *Photovoltaic characteristics of best-performing DES-based DSSC.*[a]

Light power [Sun]	J_{sc} [mA cm^{-2}]	V_{oc} [V]	FF	η [%]
1	5.1	0.504	0.66	1.7
0.5	3.0	0.478	0.66	1.9

[a] *Electrolyte composition: 2 M PMII + 0.1 M GuSCN; transparent TiO_2 thickness: 2.5 μm.*

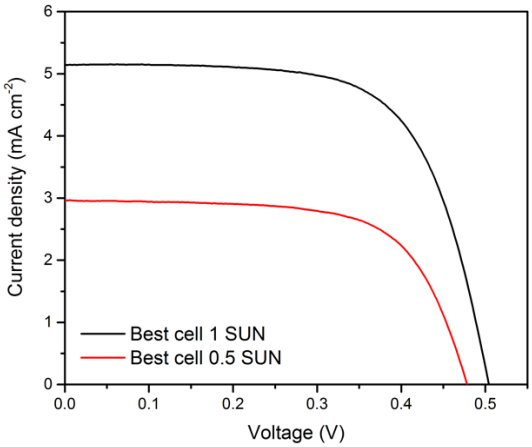

Figure 2.14. *J/V characteristics for the champion DES-based DSSC under 1 and 0.5 Sun illumination.*

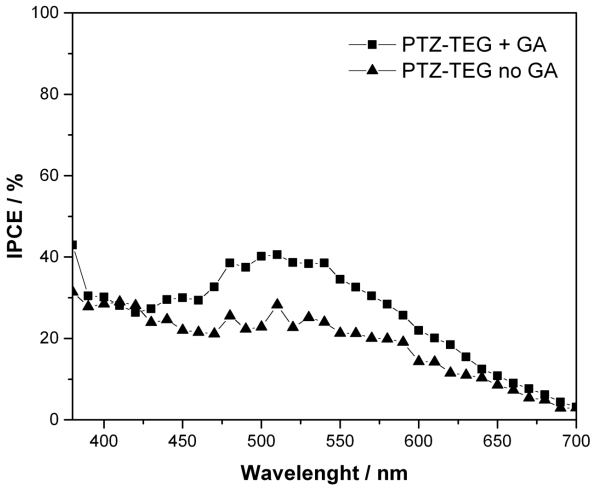

Figure 2.15. *IPCE plot of the champion cell and of the corresponding one without the co-absorbent (GA).*

In order to further investigate the different behaviour of the DSSCs when changing the semiconductor layer structure and thickness, an electrochemical impedance spectroscopy (EIS) investigation was carried out,[73-74] considering only Pt counter electrode devices (cells 1-3-4-5 in **Table 2.7**) since they gave the most interesting results (**Table 2.8**).

In a EIS experiment, a small sinusoidal voltage stimulus of a fixed frequency is applied to an electrochemical cell and its current response is measured. It is possible to investigate the ac behaviour of an electrochemical system by

sweeping the frequency over several orders of magnitude (generally from a few mHz to several MHz). The analysis of the impedance spectra is usually performed in terms of Nyquist plots where the imaginary part of the impedance is plotted as a function of the real part over the range of frequencies. The properties of the TiO_2/dye/electrolyte interface can be derived from the central arc in terms of recombination resistance (R_{rec}) and chemical capacitance for charge accumulation (C_μ). Both parameters are associated to charge transfer (recombination) phenomena representing detrimental back-processes between the injected electrons in the oxide and the oxidized form of the electrolyte. EIS analysis has been performed in dark condition to deeply investigate the charge-transfer phenomena at the TiO_2/dye/electrolyte interface. Charge recombination resistance (R_{rec}) and chemical capacitance for charge accumulation (C_μ) have been determined as a function of the bias potential (V_b) by fitting the experimental data with an equivalent electrical model.[75] The apparent electron lifetime in the oxide τ_n can be calculated from $\tau_n = R_{rec} \times C_\mu$. The results are illustrated in **Figure 2.16**. The EIS study clearly demonstrates the superior performance of the TiO_2 transparent monolayer (cells 1 and 5) compared to the double-layer geometry (cell 3 and 4). The higher electron lifetime of the former cells is mostly due to the higher recombination resistance, while there are not significant differences in the chemical capacitance. This higher resistance leads to a lower back-electron transfer, resulting in higher photocurrents and, eventually, higher efficiency of the DSSC. These data therefore suggest that the best semiconductors layer architecture in combination with the DES-based electrolyte is the monolayer and not the double layer geometry, the latter being typically used in combination with conventional liquid electrolytes in organic solvents. Different monolayer thickness did not lead to significant differences in terms of electron lifetime and recombination resistance (cells 1 and 5).

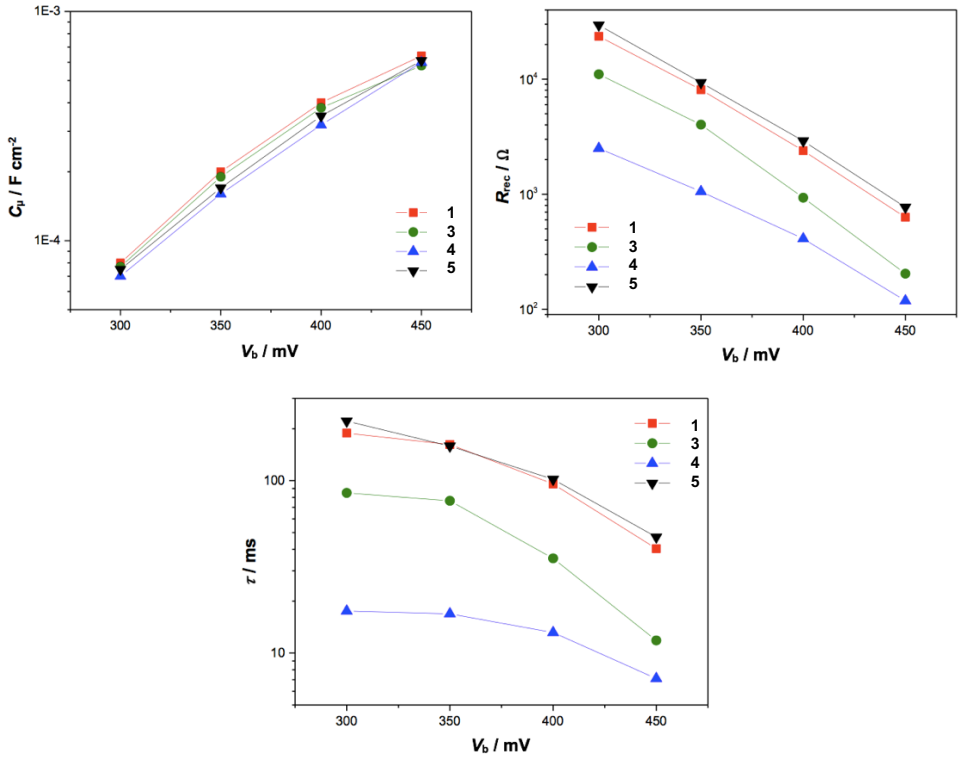

***Figure* 2.16.** *Recombination resistance, chemical capacitance, and electron lifetime determined as a function of the bias potential of devices 1,3, 4, 5 of* ***Table* 2.7**.

2.3 Hydrophobic-Eutectic-Solvent-based DSSC

The presence of volatile organic compounds (VOCs) as electrolyte media in dye-sensitized solar cells (DSSCs) limits their sustainable character and prevents widespread diffusion of this technology. This section reports, for the first time, the use of a hydrophobic eutectic solvent (HES) as truly eco-friendly electrolyte medium. The HES, consisting in a DL-menthol-acetic acid (1:1 molar ratio) mixture, has been tested in DSSCs in the presence of de-aggregating agents and a representative hydrophobic organic photosensitizer. The corresponding HES-based devices displayed relatively good power conversion efficiencies in very thin active layers. In particular, the highest cell photovoltage detected in comparison to VOC-based devices may stem from a more efficient interface interaction, as suggested by EIS studies showing the highest charge recombination resistance and electron lifetime among all of the tested DSSCs.

2.3.1 Introduction

The increase in energy demand requires the urgent development of alternative and renewable energy technologies.[76] In particular, in order to circumvent all of the issues deriving from the use of fossil fuels, such as climate crisis and shortage, a promising route is to foster new photovoltaic (PV) technologies aiming to easy-to-fabricate, efficient, and low-cost devices.[77] In the last two decades, much attention has been paid to hybrid organic-inorganic thin film systems, such as dye- sensitized solar cells (DSSCs)[49-50] and perovskite solar cells.[78] DSSCs are based on a photo-active anode, comprising an inorganic n-type semiconductor layer (typically TiO_2) sensitized by a molecular organic or organometallic dye, a counter electrode, and a liquid electrolyte solution that completes the circuit and allows dye regeneration. By using a liquid electrolyte, Hanaya et al. reported a 14.7% record efficiency.[79] Therefore, liquid DSSCs may be playing an important role in the future industrial development of low-cost solar cells with high power energy conversion efficiencies (PCEs).

One of the main drawbacks of liquid DSSCs, however, is the presence of a toxic and volatile organic compound (VOC) as an electrolyte medium, typically acetonitrile or a mixture of aliphatic nitriles. Indeed, leakage or evaporation of the VOC solvent produces a negative environmental impact and seriously limits the temporal stability of the PV efficiency. Thus, the presence of these VOCs is the most critical aspect from the standpoint of "greenness" as it hampers a truly sustainable development of the DSSC technology and prevents its widespread industrial use. The replacement of the liquid medium with a solid or quasi-solid[49, 52, 55-56] electrolyte or hole transporting material in a solid DSSC[80] circumvents this issue, but at the expenses of much lower PCEs. In the case of solid perovskite solar cells, high efficiency and the absence of liquid media have been usefully combined. The presence, however, of lead derivatives once again prevents us from defining this technology as genuinely and pervasively sustainable, both during and after its period of operational use.

Deep eutectic solvents (DESs) have been introduced in the past decade as cost-effective ionic liquid analogues because they are thermally stable, non-flammable, non-toxic, and biodegradable. Because of their minimal ecological footprint, and thus environmental friendliness, DESs are attractive substitutes for ionic liquids, and are also progressively replacing VOCs in several fundamental and applied processes.[1, 10, 81] They have been primarily investigated in extraction and separation processes,[19-21] for metal electrodeposition,[10] in polymerisation and material sciences,[22-23] but have recently gained increasing attention also in other hot fields of science such as metal-,[24-29] bio-,[30-34] and organocatalysis,[35-37] photosynthesis and electrochemistry,[38-39] and organometallics[26, 40-45] with surprising and unexpected results.

The vast majority of eutectic solvents described in the literature are hydrophilic, and thus unstable in water. Conversely, hydrophobic DESs have been developed only very recently. In 2015, Kroon et al. first reported the preparation and the usefulness of hydrophobic DESs, consisting of a fatty acid and a

quaternary ammonium salt, for the recovery of volatile fatty acids from diluted aqueous solution,[82] and for CO_2 capture.[83] Hydrophobic DESs consisting of decanoic acid and lidocaine in various proportions proved to be effective as well for the removal of metal ions from non-buffered water.[84] In parallel, Marrucho et al. synthesized and characterized novel cheap, biodegradable, and hydrophobic eutectic mixtures composed of DL-menthol and several, naturally occurring hydrophilic carboxylic acids, namely acetic acid, pyruvic acid, L-lactic acid, and lauric acid, and tested their extraction efficiencies towards biomolecules such as caffeine, triptophan, isophthalic acid, and vanillin.[85] Marrucho's group has also reported the successful use of this family of DESs for the extraction of pesticides from aqueous environment, and their reusability.[86] A tailor-made hydrophobic DES from methyl trioctyl ammonium chloride and 1-butanol (1:4 molar ratio) has also been recently set up by Su and co-workers, and showed the highest extraction yield of bioactive Artemisinin from *Artemisia annua* leaves.[87]

In the previous section, we have investigated the development of more environmentally friendly DSSCs, by combining a highly hydrophilic choline chloride-based DES with a specifically designed hydrophilic photosensitizer, which showed PCEs up to 1.9% at 0.5 sun, thereby comparable with the use of a conventional organic VOC medium or water under the same conditions.[88] Starting from these studies, the following work will focus on the first use in the field of solar energy of a menthol-based hydrophobic eutectic solvent as an alternative and promising eco-friendly and low-cost medium for liquid DSSCs exhibiting PV efficiency which well compares with VOC-based DSSCs. It is worth underlying that the employment of an hydrophobic, in place of the more common hydrophilic, DES allows the use of conventional, hydrophobic dyes as DSSC sensitizers, including the most efficient systems reported in the literature.[79] This obviates the need to both adapt the molecular structure and to design new dyes for the aqueous media.

2.3.2 Choice of materials

We have selected as a representative sensitizer a phenotiazine-based hydrophobic dye containing a terminal 8-carbon atom alkyl chain (**PTZ-Th**, **Figure 2.17**) that has been previously employed both in DSSCs[89] and in the photocatalytic production of hydrogen.[90] The DL-menthol-acetic acid (1:1 molar ratio) eutectic mixture has been selected as a representative HES because it displays very low viscosity compared to the other menthol-based eutectic mixtures developed (**Figure 2.18**).[85]

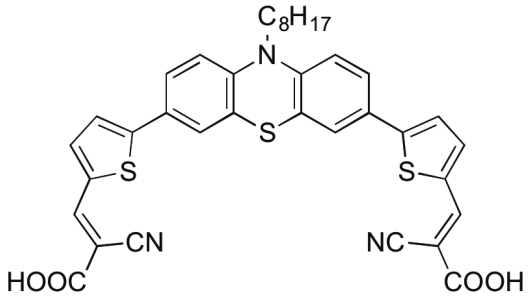

Figure 2.17. *Structure of molecule* ***PTZ-Th****.*

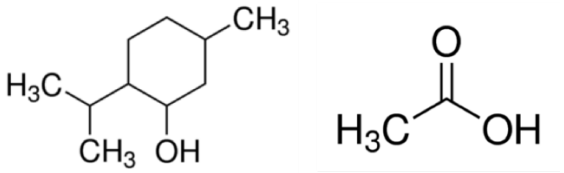

Figure 2.18. *Structure of HES components:* DL*-menthol (left) and acetic acid (right).*

DSSC cells have been prepared using **PTZ-Th** as a sensitizer in the presence of chenodeoxycholic acid (CDCA) as a disaggregating co-adsorbent.[65] Different types of TiO_2 layers have been investigated including transparent and opaque active layers with different thicknesses to find the best operative conditions. The electrolyte medium is a DL-menthol-acetic acid (1:1) eutectic mixture, which has been further diluted with 10% v/v EtOH (one of the recommended eco-friendly solvents) to improve solubility of the electrolyte components and to reduce the

viscosity of the solution. The EtOH addition simplifies device preparation without altering the nature of the HES, as confirmed by FT-IR spectra performed both on pure and diluted HES (**Figure 2.19**). As shown by Marrucho and co-workers, the formation of a network of hydrogen bonds between the carboxylic acid group (hydrogen bond donor) and the alcoholic group in DL-menthol (hydrogen bond acceptor), and thus of a eutectic mixture, is testified by a shift towards higher wavenumbers values of the carbonyl stretching absorption band.[85] Recently, Edler has also reported that DES nanostructure is retained up to 42 wt% water dilution. Further dilution produces an aqueous solution of DES components.[91] The perfect overlap of FT-IR spectra before and after ETOH dilution of the eutectic mixture is consistent with the solvophobic sequestration of EtOH into the eutectic mixture hydrogen bond network.

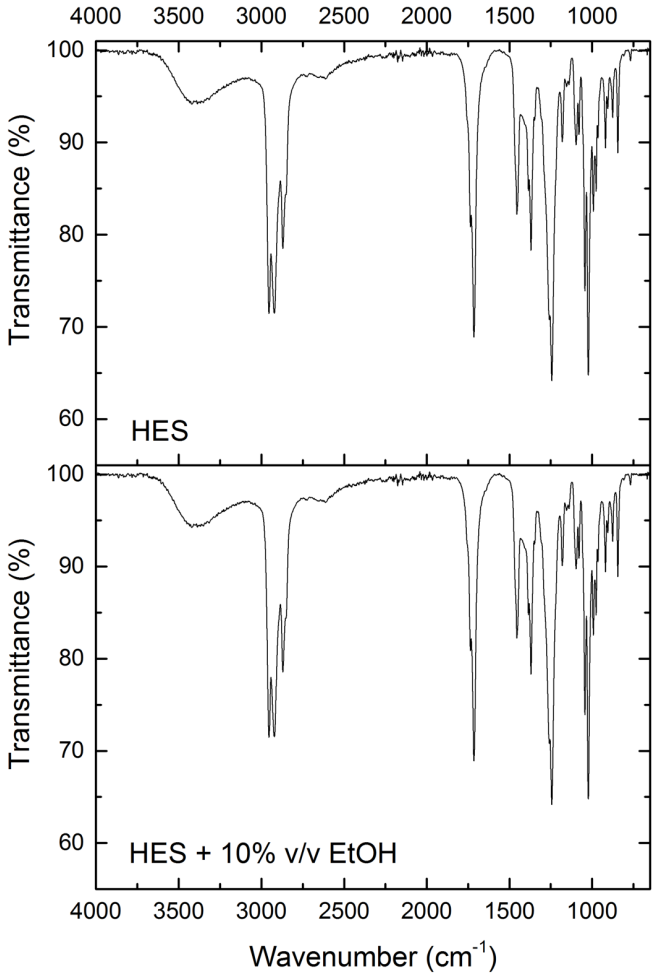

Figure 2.19. *FT-IR spectra recorded for the pure* DL*-menthol-acetic acid 1:1 HES and of the same HES diluted with 10% v/v EtOH.*

The Z960 electrolyte (see Experimental Section) has been used as a conventional reference system for its wide use in DSSCs.[92-96] The properties of HES-based DSSCs have been compared with DSSCs featuring the same components (semiconducting layer, sensitizers, electrolyte composition) but containing the conventional acetonitrile/valeronitrile 85:15 mixture as an electrolyte solvent.

2.3.3 Photovoltaic investigation

Firstly, we have focused on the nature (transparency and thickness) of the TiO_2 layer. We have tested two different thicknesses for transparent TiO_2 (2.5 and 5 μm) as well as a 5-μm-thick opaque TiO_2 layer. The results are summarized in **Table 2.9** and in **Figure 2.20**. The efficiency of HES-based cells was similar for all of the three types of investigated photoanodes, with a PCE of ~ 2%. The best PCE has been recorded for the 2.5 μm transparent layer. These data well compare with the previous section of this thesis on hydrophilic DES in DSSCs,[88] thus confirming the suitability of hydrophobic DES in DSSCs.[85-87] The unconventional HES brings a number of advantages, such as the use of routine alkyl-substituted record DSSC sensitizers, but without depressing the overall efficiency of the cell. The efficiency of the reference VOC cells was ~ 5%, in agreement with literature values for similar di-branched sensitizers.[89-90, 97] In this case, the higher PCE has been recorded for the thicker opaque layer. In summary, PCE of HES- and VOC-based cells are almost in the same range of values, which is encouraging for future studies where more performing dyes and photoanodes, such as those yielding record efficiencies, might be used.

Table 2.9. *DSSC parameters with different TiO_2 layers.*

Cell	Electrolyte	TiO_2 layer	V_{oc} (mV)	J_{sc} (mA cm^{-2})	FF (%)	PCE (%)
1	VOC	2.5-μm transparent	533	11.2	66	4.0
2	DES		585	6.6	65	2.5
3	VOC	5-μm transparent	562	14.0	63	5.0
4	DES		504	6.7	54	1.8
5	VOC	5-μm opaque	582	15.5	62	5.5
6	DES		530	7.2	53	2.0

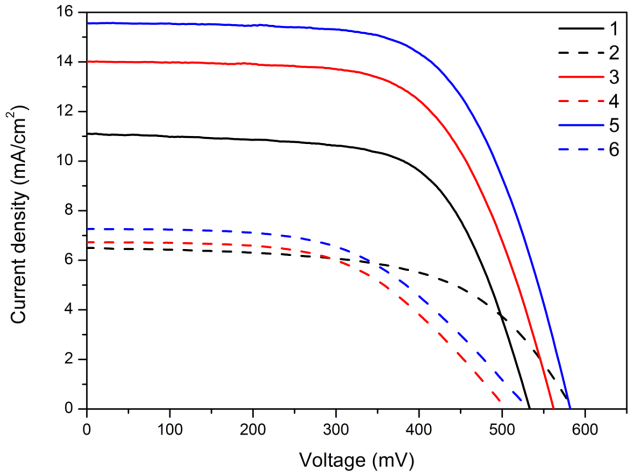

Figure 2.20. *J/V characteristics of DSSCs with organic or DES based electrolyte.*

A more detailed look at the PV characteristics revealed that the lower conversion efficiency mainly arose from the lower photocurrent, which was almost twice larger in the case of the VOC-based electrolyte. This result was expected since the presence of a viscous medium such as the HES weakens charge and mass transport in the electrolyte, thus leading to reduced currents. In contrast, fill factors were similar in both types of cells. More importantly, photovoltage of the HES-based 2.5-µm transparent device resulted higher than that of the corresponding VOC-based DSSC. The latter result is noteworthy in view of optimal PV characteristics in connecting cells to modules and panels.

The second stage of performance optimization consisted in testing the effect of a co-adsorbent in order to depress dye aggregation and self-quenching of the excited states. For this and the subsequent investigation phases, only the best performing architecture of **Table 2.9** has been considered (2.5-µm transparent photoanode layer). The standard CDCA (chenodeoxycholic acid) has been used as a co-adsorbent in 1:1 and 1:10 dye:CDCA ratios and compared with the sensitized cell in the absence of the co-adsorbent. The results, listed in **Table 2.10** and depicted in **Figure 2.21**, show that the effect of the presence of CDCA is negligible, likely due to the fact that the butterfly-like phenothiazine dye is less

subjected to aggregation phenomena compared to planar molecules. The 1:1 ratio was selected for the next investigation phase as a good compromise between efficiency and amount of co-adsorbent.

Table 2.10. *DSSC parameters in the presence of different CDCA relative concentrations*

Cell	Dye:CDCA	V_{oc} (mV)	J_{sc} (mA cm^{-2})	FF (%)	PCE (%)
1	1:0	533	7.0	55	2.0
2	1:1	539	7.7	54	2.2
3	1:10	562	7.4	54	2.2

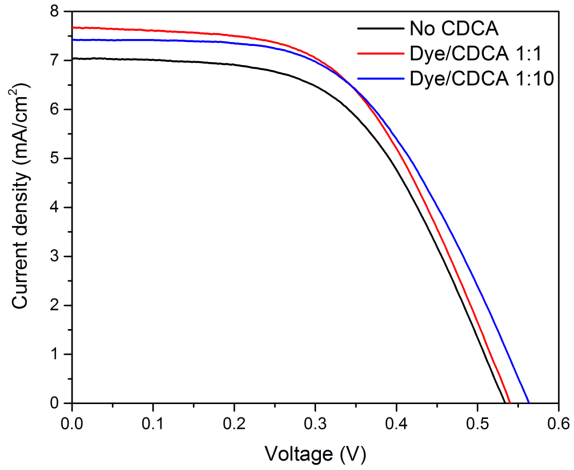

Figure 2.21. *J/V characteristics of cells of* ***Table 2.10****.*

Finally, the PCE of the HES-based cell was further increased by using a less intense incident light, specifically 0.5 sun, comparable to diffuse light conditions (**Table 2.11** and **Figure 2.22**). The final reached PCE after the optimization steps was 2.5%, in good agreement with previous DESs[88] or aqueous DSSCs.[57]

Table 2.11. *Photovoltaic characteristics of best-performing DES-based DSSC.*

Incident light	V_{oc} (mV)	J_{sc} (mA cm^{-2})	FF (%)	PCE (%)
1 sun	537	6.6	58	2.1
0.5 sun	521	4.0	60	2.5

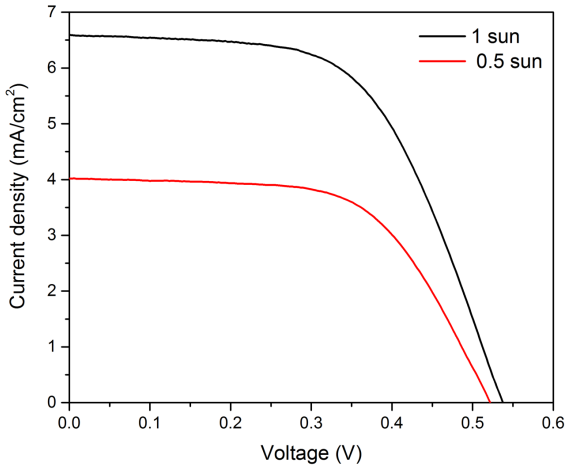

***Figure* 2.22.** *J/V characteristics of the best performing cell at 1 and 0.5 sun.*

The incident photon to current efficiency (IPCE), that is the external quantum efficiency of the PV cell, has been measured for the best HES cell and the corresponding VOC cell (**Figure 2.23**). The IPCE spectra cover the whole visible range, in agreement with the absorption spectrum of the sensitizer adsorbed onto a TiO_2 photoanode,[98] with a peak of nearly 50% from ca. 490 to 560 nm for HES-based cell and of about 70% for the VOC-based one. The differences in the IPCE values match the different experimental photocurrents. The shape of the IPCE spectrum also closely resembles that of the device containing the hydrophilic DES,[88] however, with an enhancement in the photoconversion due to a possible better charge transport in the electrolyte as demonstrated by the experimental data.

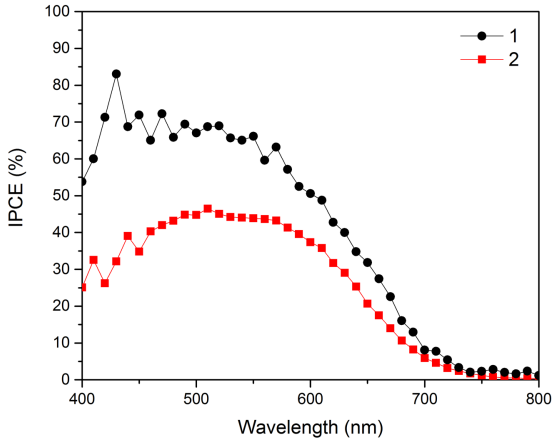

Figure 2.23. *IPCE plots of the HES-based best performing cell (red line) and of the corresponding VOC-based cell (black line).*

Since we expect that the role of the hydrophobic DES, in comparison with the VOC solvent, should be more critical at the different interfaces involving the electrolyte medium (in particular the dye-TiO_2/electrolyte interface), we decided to use electrochemical impedance spectroscopy (EIS) to focus on interfaces and charge recombination phenomena.[73-75] In an EIS experiment, a small sinusoidal voltage stimulus of a fixed frequency is applied to an electrochemical cell and its current response measured. The behaviour of an electrochemical system can be investigated by sweeping the frequency over several orders of magnitude (generally from a few mHz to several MHz). The analysis of the impedance spectra was performed in terms of Nyquist plots (**Figure 2.24**), where the imaginary part of the impedance is plotted as a function of the real part of the range of frequencies. Under soft illumination (0.25 sun), at open circuit voltage conditions, the properties of the sensitized TiO_2/electrolyte interface can be derived from the Nyquist plot in terms of recombination resistance (R_{rec}) and chemical capacitance (C_μ), which have been obtained by fitting the data with the equivalent circuit reported in the inset of the corresponding Figure. The apparent electron lifetime τ_n can also be calculated from $\tau_n = R_{rec} \times C_\mu$.[73, 99] The results of the EIS investigation are summarized in **Table 2.12**.

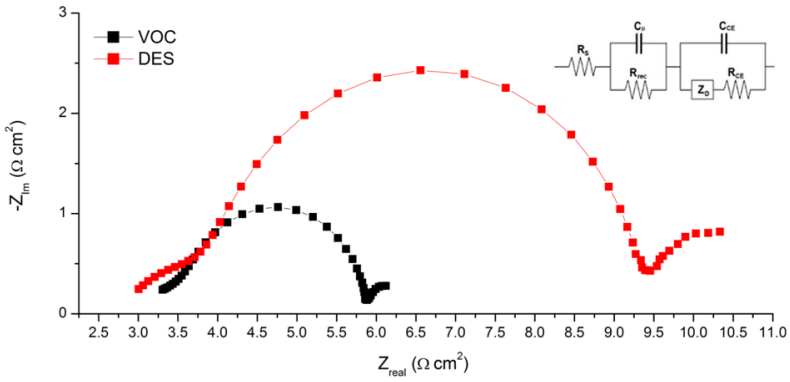

***Figure* 2.24.** *EIS data plots of DSSCs 1 and 2 from* ***Table* 2.9** *with VOC- and HES-based electrolyte, respectively.*

***Table* 2.12.** *Parameters calculated from EIS data plots of DSSCs with VOC- and DES-based electrolyte.*

Electrolyte	R_{rec} (Ω cm²)	C_{μ} (F cm^{-2})	τ_n (ms)
VOC	0.4	1.1×10^{-4}	0.05
DES	1.0	6.1×10^{-5}	0.06

Remarkably, the relevant EIS parameters collected in **Table 2.12** show that the interface phenomena operating in the VOC- and HES-based devices are substantially different. The most critical parameter is the charge recombination resistance between the sensitized oxide and the electrolyte, which controls the extent of the detrimental charge recombination, that is the back-transfer of electrons from TiO_2 to the oxidized form of the electrolyte redox species. In particular, a smaller R_{rec} indicates a faster charge recombination and therefore a larger dark current and a lower device voltage.[49] Since the recombination resistance controls how the generated charge may be lost, this parameter is key for the maximum performance attainable for the cell.

Most notably for the scope of this section, the R_{rec} value of the HES-based DSSC is more than twice higher than that of the conventional device based on the VOC medium, thus showing that charge recombination rates are much smaller in the former cell. This finding suggests that the presence of the hydrophobic DES

solvent in place of the conventional organic medium positively affects the critical dye-TiO_2/electrolyte interface, thereby minimizing unwanted pathways and possibly improving performances. Accordingly, the cell photovoltage of the HES-based cell is significantly higher (Table 2), improving from 0.53 V in the VOC electrolyte to almost 0.6 V. Accordingly, the electron lifetime of the HES-based cell resulted higher than that of the VOC-device though in this case differences are smaller due to the higher chemical capacitance of the latter.

2.4 Experimental section

All common reagents were obtained from commercial suppliers (Sigma-Aldrich or Alfa Aesar) at the highest purity grade and used without further purification. The photosensitizer 3,3′-[5,5′-[10-[2-[2-(2-methoxyethoxy)ethoxy]ethyl]-10*H*-phenothiazine-3,7-diyl]bis(thiophene-5,2-diyl)]bis(2-cyanoacrylic acid) (**PTZ-TEG**) and **PTZ-GLU** have been prepared according to the literature.[64] The photosensitizer 3,3′-(5,5′-(10-Octyl-10H-phenothiazine-3,7-diyl)bis(thiophene-5,2-diyl))bis(2-cyanoacrylic acid) (**PTZ-Th**) has been prepared according to the literature.[90] The co-adsorbents chenodeoxycholic acid (CDCA) (Sigma-Aldrich) and glucuronic acid (GA) (Sigma-Aldrich) have been obtained from a commercial supplier and used without further purification. Solaronix Mosalyte TDE-250 (a high performance non-volatile electrolyte, based on a 1-ethyl-3-methylimidazolium iodide; 1,3-dimethylimidazolium iodide; 1-ethyl-3-methylimidazolium tetracyanoborate mixture), FTO-coated glass plates (2.2 mm thick; sheet resistance ~7 ohm per square; Solaronix), Dyesol 18NR-T TiO_2 blend of active 20 nm anatase particles and Solaronix R/SP TiO_2 blend of > 100 nm anatase scatter particles were purchased from commercial suppliers. UV–O_3 treatment was performed using Novascan PSD Pro Series–Digital UV Ozone System. The thickness of the layers were measured by means of a VEECO Dektak 8 Stylus Profiler.

Z960 composition: 1.0 M 1,3-dimethylimidazolium iodide, 0.03 M iodine, 0.1 M guanidinium thiocyanate, 0.5 M tert-butylpyridine, 0.05 M LiI in a mixture of acetonitrile and valeronitrile (85/15, v/v).

DES preparation

Choline chloride-glycerol DES

The eutectic mixtures of choline chloride (Alfa Aesar)-glycerol (Alfa Aesar) (1:2 mol mol^{-1}) was prepared by heating under stirring up to 60 °C for 10 min the corresponding individual components until a clear solution was obtained.

DL-menthol-acetic acid HES

The employed DL-menthol-based eutectic mixture was prepared by adding acetic acid (the hydrogen bond donor) to DL-menthol in a 1:1 molar ratio. The corresponding mixture of the two compounds was then heated up to 50 °C until a clear solution was obtained (15 min), and then cooled down slowly to room temperature. Then, it was diluted with 10% v/v EtOH.

DES-DSSC preparation

DSSCs have been prepared adapting a procedure reported in the literature.[100] In order to exclude metal contamination, all of the containers were in glass or Teflon and were treated with EtOH and 10% HCl prior to use. Plastic spatulas and tweezers have been used throughout the procedure. FTO glass plates were cleaned in a detergent solution for 15 min using an ultrasonic bath, rinsed with pure water and EtOH. After treatment in a UV-O_3 system for 18 min, the FTO plates were treated with a freshly prepared 40 mM aqueous solution of $TiCl_4$ for 30 min at 70 °C and then rinsed with water and EtOH.

In the case of the cells with blocking layer, the treatment with $TiCl_4$ is replaced by a spray pyrolysis deposition of a solution of 20 mM titanium diisopropoxide bis(acetylacetonate) (Sigma-Aldrich) in anhydrous isopropanol at 450 °C for 30 min and then allowed to cool down to room temperature.

A transparent layer of 0.20 cm^2 was screen-printed using a 20-nm transparent TiO_2 paste (Dyesol 18NR-T). The coated transparent film was dried at 125 °C for 5 min and when needed another layer was screen-printed by using a light scattering TiO_2 paste with particles >100 nm (Solaronix R/SP). The coated films were thermally treated at 125 °C for 5 min, 325 °C for 10 min, 450 °C for 15 min, and 500 °C for 15 min. The heating ramp rate was 5-10 °C/ min. The sintered layer was treated again with 40 mM aqueous $TiCl_4$ (70 °C for 30 min), rinsed with EtOH and heated at 500 °C for 30 min. After cooling down to 80 °C, the TiO_2 coated plate was immersed into a 0.2 mM solution of the dye in the presence of the co-adsorbent (typically 1:10 glucuronic acid) for 20 h at room temperature in the dark.

Platinum-based counter electrodes were prepared according to the following procedure: a 1-mm hole was made in a FTO plate, using diamond drill bits. The electrodes were then cleaned with a detergent solution for 15 min using an ultrasonic bath, 10% HCl, and finally acetone for 15 min using an ultrasonic bath. Then, a 10 µL of a 5×10^{-3} M solution of H_2PtCl_6 in EtOH was added and the electrodes were thermally treated at 500 °C for 30 min.

PEDOT-based counter electrodes were prepared adapting a literature procedure.[72] Electropolymerization of EDOT (Sigma-Aldrich) was performed with an Autolab Potentiostat/galvanostat PGStat302N in the galvanostatic mode; a two-electrode cell with a 2 cm × 3.75 cm FTO glass as counter electrode and a predrilled washed 2 cm × 3.75 cm FTO glass as working electrode was used and a constant current of 0.602 A was applied for 400 s (film thickness about 560 nm, measured by profilometry).

The dye sensitized TiO_2 electrode and the counter electrode were assembled into a sealed sandwich-type cell by heating with a hot-melt ionomer-class resin (Surlyn 30-µm thickness) as a spacer between the electrodes.

The electrolyte solution was prepared by mixing at room temperature iodine, KI or PMII, and if necessary additives (*i.e.* GuSCN, 4-picoline, 4-*tert*-Butylpyridine, or pyridine) in the proper eutectic solvent (40% aqueous diluted DES or EtOH diluted HES) and kept in dark in the air. The electrolyte solution is used within one week from preparation. A drop of the electrolyte solution was added to the hole and introduced inside the cell by vacuum backfilling. Finally, the hole was sealed with a sheet of Surlyn and a cover glass. A reflective foil at the back side of the counter electrode was taped to reflect unabsorbed light back to the photoanode.

DES-DSSC measurements

Photovoltaic measurements of DSSCs were carried out using a 500 W xenon light source (ABET Technologies Sun 2000 Solar Simulator). The power of the simulated light was calibrated to AM 1.5 (100 mW cm^{-2}) using a reference Si

photodiode. Values were recorded immediately after cells assembling. I–V curves were obtained by applying an external bias to the cell and measuring the generated photocurrent with a Keithley model 2400 digital source meter. Incident photon-to-current conversion efficiencies (IPCEs) were recorded as a function of excitation wavelength (between 300–800 nm), using a monochromator (HORIBA Jobin Yvon) and a 400 W xenon lamp as incident light, in AC mode. The monochromatic light was mechanically chopped (chopping frequency of 1 Hz) and the AC-photocurrent response was measured using a lockin-amplifier. A white light bias (0.3 sun) was applied to the sample during IPCE measurements.

Dye loading

The amount of adsorbed dye has been measured for each sample by desorbing the dye, after the photovoltaic investigation on the dye-coated films, using a 0.1 M solution of NaOH in EtOH–H_2O (1:1) and by measuring its UV-Vis spectrum in a known volume of the solution. Comparison with the spectra of freshly prepared solutions of the dye in the same solvent, at known concentrations, are used to determine the amounts of desorbed dye.

Electrochemical impedance spectroscopy

Electrochemical Impedance Spectroscopy (EIS) spectra were obtained using an Eg&G PARSTAT 2263 galvanostat-potentiostat. Measurements were performed in the 100 kH 0.1 Hz frequency range using an AC stimulus of 70 mV under dark conditions and with different applied voltages including open circuit conditions.

2.5 Bibliography

1. Alonso, D. A.; Baeza, A.; Chinchilla, R.; Guillena, G.; Pastor, I. M.; Ramon, D. J., "Deep Eutectic Solvents: The Organic Reaction Medium of the Century". *Eur. J. Org. Chem.* **2016**, 612-632, doi: 10.1002/ejoc.201501197

2. Constable, D. J. C.; Jimenez-Gonzalez, C.; Henderson, R. K., "Perspective on Solvent Use in the Pharmaceutical Industry". *Organic Process Research & Development* **2007,** *11*, 133-137, doi: 10.1021/op060170h

3. Shuklov, I. A.; Dubrovina, N. V.; Börner, A., "Fluorinated Alcohols as Solvents, Cosolvents and Additives in Homogeneous Catalysis". *Synthesis* **2007,** *2007*, 2925-2943, doi: 10.1055/s-2007-983902

4. Aparicio, S.; Alcalde, R., "The green solvent ethyl lactate: an experimental and theoretical characterization". *Green Chem.* **2009,** *11*, 65-78, doi: 10.1039/B811909K

5. Gu, Y.; Jérôme, F., "Glycerol as a sustainable solvent for green chemistry". *Green Chem.* **2010,** *12*, 1127-1138, doi: 10.1039/C001628D

6. Pace, V.; Hoyos, P.; Castoldi, L.; Domínguez de María, P.; Alcántara, A. R., "2-Methyltetrahydrofuran (2-MeTHF): A Biomass-Derived Solvent with Broad Application in Organic Chemistry". *ChemSusChem* **2012,** *5*, 1369-1379, doi: 10.1002/cssc.201100780

7. Earle, M. J.; Katdare, S. P.; Seddon, K. R., "Paradigm Confirmed: The First Use of Ionic Liquids to Dramatically Influence the Outcome of Chemical Reactions". *Organic Letters* **2004,** *6*, 707-710, doi: 10.1021/ol036310e

8. Romero, A.; Santos, A.; Tojo, J.; Rodríguez, A., "Toxicity and biodegradability of imidazolium ionic liquids". *J. Hazard. Mater.* **2008,** *151*, 268-273, doi: https://doi.org/10.1016/j.jhazmat.2007.10.079

9. Plechkova, N. V.; Seddon, K. R., "Applications of ionic liquids in the chemical industry". *Chem. Soc. Rev.* **2008,** *37*, 123-150, doi: 10.1039/B006677J

10. Smith, E. L.; Abbott, A. P.; Ryder, K. S., "Deep Eutectic Solvents (DESs) and Their Applications". *Chem. Rev.* **2014,** *114*, 11060-11082, doi: 10.1021/cr300162p

11. Abbott, A. P.; El Ttaib, K.; Frisch, G.; McKenzie, K. J.; Ryder, K. S., "Electrodeposition of copper composites from deep eutectic solvents based on choline chloride". *Phys. Chem. Chem. Phys.* **2009,** *11*, 4269-4277, doi: 10.1039/B817881J

12. Zhang, Q.; De Oliveira Vigier, K.; Royer, S.; Jerome, F., "Deep eutectic solvents: syntheses, properties and applications". *Chem. Soc. Rev.* **2012,** *41*, 7108-7146, doi: 10.1039/C2CS35178A

13. Abbott, A. P.; Harris, R. C.; Ryder, K. S.; D'Agostino, C.; Gladden, L. F.; Mantle, M. D., "Glycerol eutectics as sustainable solvent systems". *Green Chem.* **2011,** *13*, 82-90, doi: 10.1039/C0GC00395F

14. Yu, Y.; Lu, X.; Zhou, Q.; Dong, K.; Yao, H.; Zhang, S., "Biodegradable Naphthenic Acid Ionic Liquids: Synthesis, Characterization, and Quantitative Structure–Biodegradation Relationship". *Chem. Eur. J.* **2008,** *14*, 11174-11182, doi: 10.1002/chem.200800620

15. Weaver, K. D.; Kim, H. J.; Sun, J.; MacFarlane, D. R.; Elliott, G. D., "Cyto-toxicity and biocompatibility of a family of choline phosphate ionic liquids designed for pharmaceutical applications". *Green Chem.* **2010,** *12*, 507-513, doi: 10.1039/B918726J

16. Ilgen, F.; Ott, D.; Kralisch, D.; Reil, C.; Palmberger, A.; König, B., "Conversion of carbohydrates into 5-hydroxymethylfurfural in highly concentrated low melting mixtures". *Green Chem.* **2009,** *11*, 1948-1954, doi: 10.1039/B917548M

17. Abbott, A. P.; Capper, G.; Davies, D. L.; Rasheed, R. K.; Tambyrajah, V., "Novel solvent properties of choline chloride/urea mixtures". *Chem. Commun.* **2003**, 70-71, doi: 10.1039/B210714G

18. Abbott, A. P.; Boothby, D.; Capper, G.; Davies, D. L.; Rasheed, R. K., "Deep Eutectic Solvents Formed between Choline Chloride and Carboxylic Acids: Versatile Alternatives to Ionic Liquids". *J. Am. Chem. Soc.* **2004,** *126*, 9142-9147, doi: 10.1021/ja048266j

19. Pena-Pereira, F.; Namieśnik, J., "Ionic Liquids and Deep Eutectic Mixtures: Sustainable Solvents for Extraction Processes". *ChemSusChem* **2014,** *7*, 1784-1800, doi: 10.1002/cssc.201301192

20. Tang, B.; Zhang, H.; Row, K. H., "Application of deep eutectic solvents in the extraction and separation of target compounds from various samples". *J. Sep. Sci.* **2015,** *38*, 1053-1064, doi: 10.1002/jssc.201401347

21. Piemontese, L.; Perna, M. F.; Logrieco, A.; Capriati, V.; Solfrizzo, M., "Deep Eutectic Solvents as Novel and Effective Extraction Media for Quantitative Determination of Ochratoxin A in Wheat and Derived Products". *Molecules* **2017,** *22*, doi: 10.3390/molecules22010121

22. Carriazo, D.; Serrano, M. C.; Gutiérrez, M. C.; Ferrer, M. L.; del Monte, F., "Deep-eutectic solvents playing multiple roles in the synthesis of polymers and related materials". *Chem. Soc. Rev.* **2012,** *41*, 4996-5014, doi: 10.1039/C2CS15353J

23. del Monte, F.; Carriazo, D.; Serrano, M. C.; Gutiérrez, M. C.; Ferrer, M. L., "Deep Eutectic Solvents in Polymerizations: A Greener Alternative to Conventional Syntheses". *ChemSusChem* **2014,** *7*, 999-1009, doi: 10.1002/cssc.201300864

24. García-Álvarez, J., "Deep Eutectic Mixtures: Promising Sustainable Solvents for Metal-Catalysed and Metal-Mediated Organic Reactions". *Eur. J. Inorg. Chem.* **2015,** *2015*, 5147-5157, doi: 10.1002/ejic.201500892

25. Mancuso, R.; Maner, A.; Cicco, L.; Perna, F. M.; Capriati, V.; Gabriele, B., "Synthesis of thiophenes in a deep eutectic solvent: heterocyclodehydration and iodocyclization of 1-mercapto-3-yn-2-ols in a choline chloride/glycerol medium". *Tetrahedron* **2016,** *72*, 4239-4244, doi: https://doi.org/10.1016/j.tet.2016.05.062

26. Cicco, L.; Rodriguez-Alvarez, M. J.; Perna, F. M.; Garcia-Alvarez, J.; Capriati, V., "One-pot sustainable synthesis of tertiary alcohols by combining ruthenium-catalysed isomerisation of allylic alcohols and chemoselective addition of polar organometallic reagents in deep eutectic solvents". *Green Chem.* **2017,** *19*, 3069-3077, doi: 10.1039/C7GC00458C

27. Marset, X.; Khoshnood, A.; Sotorríos, L.; Gómez-Bengoa, E.; Alonso Diego, A.; Ramón Diego, J., "Deep Eutectic Solvent Compatible Metallic Catalysts: Cationic Pyridiniophosphine Ligands in Palladium Catalyzed Cross-Coupling Reactions". *ChemCatChem* **2016,** *9*, 1269-1275, doi: 10.1002/cctc.201601544

28. Marset, X.; Guillena, G.; Ramón Diego, J., "Deep Eutectic Solvents as Reaction Media for the Palladium-Catalysed C−S Bond Formation: Scope and Mechanistic Studies". *Chem. Eur. J.* **2017,** *23*, 10522-10526, doi: 10.1002/chem.201702892

29. Marset, X.; De Gea, S.; Guillena, G.; Ramón, D. J., "NCN–Pincer–Pd Complex as Catalyst for the Hiyama Reaction in Biomass-Derived Solvents". *ACS Sustainable Chem. Eng.* **2018,** *6*, 5743-5748, doi: 10.1021/acssuschemeng.8b00598

30. Muller, C. R.; Meiners, I.; Dominguez de Maria, P., "Highly enantioselective tandem enzyme-organocatalyst crossed aldol reactions with acetaldehyde in deep-eutectic-solvents". *RSC Adv.* **2014,** *4*, 46097-46101, doi: 10.1039/C4RA09307K

31. Sheldon, R. A., "Biocatalysis and Biomass Conversion in Alternative Reaction Media". *Chem. Eur. J.* **2016,** *22*, 12984-12999, doi: 10.1002/chem.201601940

32. Vitale, P.; Abbinante, V. M.; Perna, F. M.; Salomone, A.; Cardellicchio, C.; Capriati, V., "Unveiling the Hidden Performance of Whole Cells in the Asymmetric Bioreduction of Aryl-containing Ketones in Aqueous Deep Eutectic Solvents". *Adv. Synth. Catal.* **2017,** *359*, 1049-1057, doi: 10.1002/adsc.201601064

33. Vitale, P.; Perna, M. F.; Agrimi, G.; Pisano, I.; Mirizzi, F.; Capobianco, V. R.; Capriati, V., "Whole-Cell Biocatalyst for Chemoenzymatic Total Synthesis of Rivastigmine". *Catalysts* **2018,** *8*, doi: 10.3390/catal8020055

34. Cicco, L.; Rios-Lombardia, N.; Rodriguez-Alvarez, M. J.; Moris, F.; Perna, F. M.; Capriati, V.; Garcia-Alvarez, J.; Gonzalez-Sabin, J., "Programming cascade reactions interfacing biocatalysis with transition-metal catalysis in Deep Eutectic Solvents as biorenewable reaction media". *Green Chem.* **2018**, doi: 10.1039/C8GC00861B

35. Martínez, R.; Berbegal, L.; Guillena, G.; Ramón, D. J., "Bio-renewable enantioselective aldol reaction in natural deep eutectic solvents". *Green Chem.* **2016,** *18*, 1724-1730, doi: 10.1039/C5GC02526E

36. Massolo, E.; Palmieri, S.; Benaglia, M.; Capriati, V.; Perna, F. M., "Stereoselective organocatalysed reactions in deep eutectic solvents: highly tunable and biorenewable reaction media for sustainable organic synthesis". *Green Chem.* **2016,** *18*, 792-797, doi: 10.1039/C5GC01855B

37. Brenna, D.; Massolo, E.; Puglisi, A.; Rossi, S.; Celentano, G.; Benaglia, M.; Capriati, V., "Towards the development of continuous, organocatalytic, and stereoselective reactions in deep eutectic solvents". *Beilstein J. Org. Chem.* **2016,** *12*, 2620-2626, doi: 10.3762/bjoc.12.258

38. Milano, F.; Giotta, L.; Guascito, M. R.; Agostiano, A.; Sblendorio, S.; Valli, L.; Perna, F. M.; Cicco, L.; Trotta, M.; Capriati, V., "Functional Enzymes in Nonaqueous Environment: The Case of Photosynthetic Reaction Centers in Deep Eutectic Solvents". *ACS Sustainable Chem. Eng.* **2017,** *5*, 7768-7776, doi: 10.1021/acssuschemeng.7b01270

39. Millia, L.; Dall'Asta, V.; Ferrara, C.; Berbenni, V.; Quartarone, E.; Perna, F. M.; Capriati, V.; Mustarelli, P., "Bio-inspired choline chloride-based deep eutectic solvents as electrolytes for lithium-ion batteries". *Solid State Ionics* **2018,** *323*, 44-48, doi: https://doi.org/10.1016/j.ssi.2018.05.016

40. García-Álvarez, J.; Hevia, E.; Capriati, V., "Reactivity of Polar Organometallic Compounds in Unconventional Reaction Media: Challenges and Opportunities". *Eur. J. Org. Chem.* **2015,** *2015*, 6779-6799, doi: 10.1002/ejoc.201500757

41. Mallardo, V.; Rizzi, R.; Sassone, F. C.; Mansueto, R.; Perna, F. M.; Salomone, A.; Capriati, V., "Regioselective desymmetrization of diaryltetrahydrofurans via directed ortho-lithiation: an unexpected help from green chemistry". *Chem. Commun.* **2014,** *50*, 8655-8658, doi: 10.1039/C4CC03149K

42. Vidal, C.; García-Álvarez, J.; Hernán-Gómez, A.; Kennedy, A. R.; Hevia, E., "Introducing Deep Eutectic Solvents to Polar Organometallic Chemistry: Chemoselective Addition of Organolithium and Grignard Reagents to Ketones in Air". *Angew. Chem. Int. Ed.* **2014,** *53*, 5969-5973, doi: 10.1002/anie.201400889

43. Sassone, F. C.; Perna, F. M.; Salomone, A.; Florio, S.; Capriati, V., "Unexpected lateral-lithiation-induced alkylative ring opening of tetrahydrofurans in deep eutectic solvents: synthesis of functionalised primary alcohols". *Chem. Commun.* **2015,** *51*, 9459-9462, doi: 10.1039/C5CC02884A

44. Vidal, C.; García-Álvarez, J.; Hernán-Gómez, A.; Kennedy, A. R.; Hevia, E., "Exploiting Deep Eutectic Solvents and Organolithium Reagent Partnerships: Chemoselective Ultrafast Addition to Imines and Quinolines Under Aerobic Ambient Temperature Conditions". *Angew. Chem. Int. Ed.* **2016,** *55*, 16145-16148, doi: 10.1002/anie.201609929

45. Cicco, L.; Sblendorio, S.; Mansueto, R.; Perna, F. M.; Salomone, A.; Florio, S.; Capriati, V., "Water opens the door to organolithiums and Grignard reagents: exploring and comparing the reactivity of highly polar organometallic compounds in unconventional reaction media towards the synthesis of tetrahydrofurans". *Chem. Sci.* **2016,** *7*, 1192-1199, doi: 10.1039/C5SC03436A

46. Jhong, H.-R.; Wong, D. S.-H.; Wan, C.-C.; Wang, Y.-Y.; Wei, T.-C., "A novel deep eutectic solvent-based ionic liquid used as electrolyte for dye-sensitized solar cells". *Electrochem. Commun.* **2009,** *11*, 209-211, doi: http://dx.doi.org/10.1016/j.elecom.2008.11.001

47. Bagnall, D. M.; Boreland, M., "Photovoltaic technologies". *Energy Policy* **2008,** *36*, 4390-4396, doi: 10.1016/j.enpol.2008.09.070

48. O'Regan, B.; Grätzel, M., "A low-cost, high-efficiency solar cell based on dye-sensitized colloidal TiO2 films". *Nature* **1991,** *353*, 737-740, doi:

49. Kalyanasundaram, K., *Dye-sensitized Solar Cells*. EFPL Press: 2010.

50. Hagfeldt, A.; Boschloo, G.; Sun, L.; Kloo, L.; Pettersson, H., "Dye-Sensitized Solar Cells". *Chem. Rev.* **2010,** *110*, 6595-6663, doi: 10.1021/cr900356p

51. Zakeeruddin, S. M.; Grätzel, M., "Solvent-Free Ionic Liquid Electrolytes for Mesoscopic Dye-Sensitized Solar Cells". *Adv. Funct. Mater.* **2009,** *19*, 2187-2202, doi: 10.1002/adfm.200900390

52. Dong, R.-X.; Shen, S.-Y.; Chen, H.-W.; Wang, C.-C.; Shih, P.-T.; Liu, C.-T.; Vittal, R.; Lin, J.-J.; Ho, K.-C., "A novel polymer gel electrolyte for highly

efficient dye-sensitized solar cells". *J. Mater. Chem. A* **2013,** *1*, 8471-8478, doi: 10.1039/C3TA11331K

53. Manfredi, N.; Bianchi, A.; Causin, V.; Ruffo, R.; Simonutti, R.; Abbotto, A., "Electrolytes for Quasi Solid-State Dye-Sensitized Solar Cells Based on Block Copolymers". *J Polym Sci Pol Chem* **2014,** *52*, 719-727, doi: 10.1002/pola.27055

54. Wang, P.; Zakeeruddin, S. M.; Moser, J. E.; Nazeeruddin, M. K.; Sekiguchi, T.; Grätzel, M., "A stable quasi-solid-state dye-sensitized solar cell with an amphiphilic ruthenium sensitizer and polymer gel electrolyte". *Nature Materials* **2003,** *2*, 402-407, doi: 10.1038/nmat904

55. Wang, M.; Grätzel, C.; Zakeeruddin, S. M.; Grätzel, M., "Recent developments in redox electrolytes for dye-sensitized solar cells". *Energy Environ. Sci.* **2012,** *5*, 9394-9405, doi: 10.1039/C2EE23081J

56. Docampo, P.; Guldin, S.; Leijtens, T.; Noel, N. K.; Steiner, U.; Snaith, H. J., "Lessons Learned: From Dye-Sensitized Solar Cells to All-Solid-State Hybrid Devices". *Adv. Mater.* **2014,** *26*, 4013-4030, doi: 10.1002/adma.201400486

57. Bella, F.; Gerbaldi, C.; Barolo, C.; Grätzel, M., "Aqueous dye-sensitized solar cells". *Chem. Soc. Rev.* **2015,** *44*, 3431-3473, doi: 10.1039/C4CS00456F

58. Liu, Y.; Hagfeldt, A.; Xiao, X. R.; Lindquist, S. E., "Investigation of influence of redox species on the interfacial energetics of a dye-sensitized nanoporous TiO2 solar cell". *Sol. Energy Mater. Sol. Cells* **1998,** *55*, 267-281, doi: 10.1016/s0927-0248(98)00111-1

59. Leandri, V.; Ellis, H.; Gabrielsson, E.; Sun, L.; Boschloo, G.; Hagfeldt, A., "An organic hydrophilic dye for water-based dye-sensitized solar cells". *Phys. Chem. Chem. Phys.* **2014,** *16*, 19964-19971, doi: 10.1039/C4CP02774D

60. Bella, F.; Galliano, S.; Falco, M.; Viscardi, G.; Barolo, C.; Grätzel, M.; Gerbaldi, C., "Unveiling iodine-based electrolytes chemistry in aqueous dye-sensitized solar cells". *Chem. Sci.* **2016**, doi: 10.1039/C6SC01145D

61. Zhang, Q.; De Oliveira Vigier, K.; Royer, S.; Jérôme, F., "Deep eutectic solvents: syntheses, properties and applications". *Chem. Soc. Rev.* **2012,** *41*, 7108-7146, doi: 10.1039/C2CS35178A

62. Chakrabarti, M. H.; Mjalli, F. S.; AlNashef, I. M.; Hashim, M. A.; Hussain, M. A.; Bahadori, L.; Low, C. T. J., "Prospects of applying ionic liquids and deep eutectic solvents for renewable energy storage by means of redox flow batteries". *Renewable Sustainable Energy Rev.* **2014,** *30*, 254-270, doi: http://dx.doi.org/10.1016/j.rser.2013.10.004

63. Nazeeruddin, M. K.; De Angelis, F.; Fantacci, S.; Selloni, A.; Viscardi, G.; Liska, P.; Ito, S.; Takeru, B.; Grätzel, M., "Combined Experimental and DFT-TDDFT Computational Study of Photoelectrochemical Cell Ruthenium Sensitizers". *J. Am. Chem. Soc.* **2005,** *127*, 16835-16847, doi: 10.1021/ja052467l

64. Manfredi, N.; Cecconi, B.; Calabrese, V.; Minotti, A.; Peri, F.; Ruffo, R.; Monai, M.; Romero-Ocana, I.; Montini, T.; Fornasiero, P.; Abbotto, A., "Dye-sensitized photocatalytic hydrogen production: distinct activity in a glucose derivative of a phenothiazine dye". *Chem. Commun.* **2016,** *52*, 6977-6980, doi: 10.1039/C6CC00390G

65. Jiang, X.; Marinado, T.; Gabrielsson, E.; Hagberg, D. P.; Sun, L.; Hagfeldt, A., "Structural Modification of Organic Dyes for Efficient Coadsorbent-Free Dye-Sensitized Solar Cells". *J. Phys. Chem. C* **2010,** *114*, 2799-2805, doi: 10.1021/jp908552t

66. Boschloo, G.; Häggman, L.; Hagfeldt, A., "Quantification of the Effect of 4-tert-Butylpyridine Addition to I-/I3- Redox Electrolytes in Dye-Sensitized Nanostructured TiO2 Solar Cells". *J. Phys. Chem. B* **2006,** *110*, 13144-13150, doi: 10.1021/jp0619641

67. Dell'Orto, E.; Raimondo, L.; Sassella, A.; Abbotto, A., "Dye-sensitized solar cells: spectroscopic evaluation of dye loading on TiO2". *J. Mater. Chem.* **2012,** *22*, 11364-11369, doi: 10.1039/c2jm30481c

68. Nazeeruddin, M. K.; Kay, A.; Rodicio, I.; Humphry-Baker, R.; Mueller, E.; Liska, P.; Vlachopoulos, N.; Graetzel, M., "Conversion of light to electricity by cis-X2bis(2,2'-bipyridyl-4,4'-dicarboxylate)ruthenium(II) charge-transfer sensitizers (X = Cl-, Br-, I-, CN-, and SCN-) on nanocrystalline titanium dioxide electrodes". *J. Am. Chem. Soc.* **1993,** *115*, 6382-6390, doi: 10.1021/ja00067a063

69. Law, C.; Moudam, O.; Villarroya-Lidon, S.; O'Regan, B., "Managing wetting behavior and collection efficiency in photoelectrochemical devices based on water electrolytes; improvement in efficiency of water/iodide dye

sensitised cells to 4%". *J. Mater. Chem.* **2012,** *22*, 23387-23394, doi: 10.1039/C2JM35245A

70. Ito, S.; Chen, P.; Comte, P.; Nazeeruddin, M. K.; Liska, P.; Péchy, P.; Grätzel, M., "Fabrication of screen-printing pastes from TiO2 powders for dye-sensitised solar cells". *Progr. Photovolt: Res. Appl.* **2007,** *15*, 603-612, doi: 10.1002/pip.768

71. Zhang, Q.; Myers, D.; Lan, J.; Jenekhe, S. A.; Cao, G., "Applications of light scattering in dye-sensitized solar cells". *Phys. Chem. Chem. Phys.* **2012,** *14*, 14982-14998, doi: 10.1039/C2CP43089D

72. Ellis, H.; Vlachopoulos, N.; Häggman, L.; Perruchot, C.; Jouini, M.; Boschloo, G.; Hagfeldt, A., "PEDOT counter electrodes for dye-sensitized solar cells prepared by aqueous micellar electrodeposition". *Electrochim. Acta* **2013,** *107*, 45-51, doi: http://dx.doi.org/10.1016/j.electacta.2013.06.005

73. Fabregat-Santiago, F.; Garcia-Belmonte, G.; Mora-Sero, I.; Bisquert, J., "Characterization of nanostructured hybrid and organic solar cells by impedance spectroscopy". *Phys. Chem. Chem. Phys.* **2011,** *13*, 9083-9118, doi: 10.1039/C0CP02249G

74. Halme, J.; Vahermaa, P.; Miettunen, K.; Lund, P., "Device Physics of Dye Solar Cells". *Adv. Mater.* **2010,** *22*, E210-E234, doi: 10.1002/adma.201000726

75. Bisquert, J.; Fabregat-Santiago, F.; Mora-Seró, I.; Garcia-Belmonte, G.; Giménez, S., "Electron Lifetime in Dye-Sensitized Solar Cells: Theory and Interpretation of Measurements". *J. Phys. Chem. C* **2009,** *113*, 17278-17290, doi: 10.1021/jp9037649

76. Armaroli, N.; Balzani, V., Solar Heat and Electricity. In *Energy for a Sustainable World*, Wiley-VCH Verlag GmbH & Co. KGaA: 2010; pp 167-201.

77. Armaroli, N.; Balzani, V., "Solar Electricity and Solar Fuels: Status and Perspectives in the Context of the Energy Transition". *Chem. Eur. J.* **2016,** *22*, 32-57, doi: 10.1002/chem.201503580

78. Green, M. A.; Ho-Baillie, A., "Perovskite Solar Cells: The Birth of a New Era in Photovoltaics". *ACS Energy Letters* **2017,** *2*, 822-830, doi: 10.1021/acsenergylett.7b00137

79. Kakiage, K.; Aoyama, Y.; Yano, T.; Oya, K.; Fujisawa, J.-i.; Hanaya, M., "Highly-efficient dye-sensitized solar cells with collaborative sensitization by silyl-anchor and carboxy-anchor dyes". *Chem. Commun.* **2015,** *51*, 15894-15897, doi: 10.1039/C5CC06759F

80. Wu, J.; Lan, Z.; Lin, J.; Huang, M.; Huang, Y.; Fan, L.; Luo, G., "Electrolytes in Dye-Sensitized Solar Cells". *Chem. Rev.* **2015,** *115*, 2136-2173, doi: 10.1021/cr400675m

81. Liu, P.; Hao, J.-W.; Mo, L.-P.; Zhang, Z.-H., "Recent advances in the application of deep eutectic solvents as sustainable media as well as catalysts in organic reactions". *RSC Adv.* **2015,** *5*, 48675-48704, doi: 10.1039/C5RA05746A

82. van Osch, D. J. G. P.; Zubeir, L. F.; van den Bruinhorst, A.; Rocha, M. A. A.; Kroon, M. C., "Hydrophobic deep eutectic solvents as water-immiscible extractants". *Green Chem.* **2015,** *17*, 4518-4521, doi: 10.1039/C5GC01451D

83. Dietz, C. H. J. T.; van Osch, D. J. G. P.; Kroon, M. C.; Sadowski, G.; van Sint Annaland, M.; Gallucci, F.; Zubeir, L. F.; Held, C., "PC-SAFT modeling of CO2 solubilities in hydrophobic deep eutectic solvents". *Fluid Phase Equilibria* **2017,** *448*, 94-98, doi: https://doi.org/10.1016/j.fluid.2017.03.028

84. van Osch, D. J. G. P.; Parmentier, D.; Dietz, C. H. J. T.; van den Bruinhorst, A.; Tuinier, R.; Kroon, M. C., "Removal of alkali and transition metal ions from water with hydrophobic deep eutectic solvents". *Chem. Commun.* **2016,** *52*, 11987-11990, doi: 10.1039/C6CC06105B

85. Ribeiro, B. D.; Florindo, C.; Iff, L. C.; Coelho, M. A. Z.; Marrucho, I. M., "Menthol-based Eutectic Mixtures: Hydrophobic Low Viscosity Solvents". *ACS Sustainable Chem. Eng.* **2015,** *3*, 2469-2477, doi: 10.1021/acssuschemeng.5b00532

86. Florindo, C.; Branco, L. C.; Marrucho, I. M., "Development of hydrophobic deep eutectic solvents for extraction of pesticides from aqueous environments". *Fluid Phase Equilibria* **2017,** *448*, 135-142, doi: https://doi.org/10.1016/j.fluid.2017.04.002

87. Cao, J.; Yang, M.; Cao, F.; Wang, J.; Su, E., "Well-Designed Hydrophobic Deep Eutectic Solvents As Green and Efficient Media for the Extraction of Artemisinin from Artemisia annua Leaves". *ACS Sustainable Chem. Eng.* **2017,** *5*, 3270-3278, doi: 10.1021/acssuschemeng.6b03092

88. Boldrini, C. L.; Manfredi, N.; Perna, F. M.; Trifiletti, V.; Capriati, V.; Abbotto, A., "Dye-Sensitized Solar Cells that use an Aqueous Choline Chloride-Based Deep Eutectic Solvent as Effective Electrolyte Solution". *Energy Technology* **2017,** *5*, 345-353, doi: 10.1002/ente.201600420

89. Manfredi, N.; Cecconi, B.; Abbotto, A., "Multi-Branched Multi-Anchoring Metal-Free Dyes for Dye-Sensitized Solar Cells". *Eur. J. Org. Chem.* **2014,** *2014*, 7069-7086, doi: 10.1002/ejoc.201402422

90. Cecconi, B.; Manfredi, N.; Ruffo, R.; Montini, T.; Romero-Ocaña, I.; Fornasiero, P.; Abbotto, A., "Tuning Thiophene-Based Phenothiazines for Stable Photocatalytic Hydrogen Production". *ChemSusChem* **2015,** *8*, 4216-4228, doi: 10.1002/cssc.201501040

91. Hammond, O. S.; Bowron, D. T.; Edler, K. J., "The Effect of Water upon Deep Eutectic Solvent Nanostructure: An Unusual Transition from Ionic Mixture to Aqueous Solution". *Angew. Chem. Int. Ed.* **2017,** *56*, 9782-9785, doi: 10.1002/anie.201702486

92. Fischer, M. K. R.; Wenger, S.; Wang, M.; Mishra, A.; Zakeeruddin, S. M.; Grätzel, M.; Bäuerle, P., "D-π-A Sensitizers for Dye-Sensitized Solar Cells: Linear vs Branched Oligothiophenes". *Chem. Mater.* **2010,** *22*, 1836-1845, doi: 10.1021/cm903542v

93. Robson, K. C. D.; Koivisto, B. D.; Yella, A.; Sporinova, B.; Nazeeruddin, M. K.; Baumgartner, T.; Grätzel, M.; Berlinguette, C. P., "Design and Development of Functionalized Cyclometalated Ruthenium Chromophores for Light-Harvesting Applications". *Inorg. Chem.* **2011,** *50*, 5494-5508, doi: 10.1021/ic200011m

94. Tsao , H. N.; Yi , C.; Moehl, T.; Yum, J.-H.; Zakeeruddin, S. M.; Nazeeruddin, M. K.; Grätzel, M., "Cyclopentadithiophene Bridged Donor–Acceptor Dyes Achieve High Power Conversion Efficiencies in Dye-Sensitized Solar Cells Based on the tris-Cobalt Bipyridine Redox Couple". *ChemSusChem* **2011,** *4*, 591-594, doi: 10.1002/cssc.201100120

95. Leandri, V.; Ruffo, R.; Trifiletti, V.; Abbotto, A., "Asymmetric Tribranched Dyes: An Intramolecular Cosensitization Approach for Dye-Sensitized Solar Cells". *Eur. J. Org. Chem.* **2013,** *2013*, 6793-6801, doi: 10.1002/ejoc.201300962

96. Baldoli, C.; Bertuolo, S.; Licandro, E.; Viglianti, L.; Mussini, P.; Marotta, G.; Salvatori, P.; De Angelis, F.; Manca, P.; Manfredi, N.; Abbotto, A., "Benzodithiophene based organic dyes for DSSC: Effect of alkyl chain substitution on dye efficiency". *Dyes Pigm.* **2015,** *121*, 351-362, doi: https://doi.org/10.1016/j.dyepig.2015.04.028

97. Hung Wei-, I.; Liao, Y. Y.; Hsu, C. Y.; Chou, H. H.; Lee, T. H.; Kao, W. S.; Lin Jiann, T., "High-Performance Dye-Sensitized Solar Cells Based on Phenothiazine Dyes Containing Double Anchors and Thiophene Spacers". *Chem. Asian J.* **2013,** *9*, 357-366, doi: 10.1002/asia.201301228

98. Manfredi, N.; Boldrini, C. L.; Abbotto, A., "Organic Sensitizers for Photoanode Water Splitting in Dye-Sensitized Photoelectrochemical Cells". *ChemElectroChem* **2018,** *5*, 2395-2402, doi: 10.1002/celc.201800592

99. Manfredi, N.; Trifiletti, V.; Melchiorre, F.; Giannotta, G.; Biagini, P.; Abbotto, A., "Performance enhancement of a dye-sensitized solar cell by peripheral aromatic and heteroaromatic functionalization in di-branched organic sensitizers". *New J. Chem.* **2018,** *42*, 9281-9290, doi: 10.1039/C7NJ05188C

100. Ito, S.; Murakami, T. N.; Comte, P.; Liska, P.; Grätzel, C.; Nazeeruddin, M. K.; Grätzel, M., "Fabrication of thin film dye sensitized solar cells with solar to electric power conversion efficiency over 10%". *Thin Solid Films* **2008,** *516*, 4613-4619, doi: 10.1016/j.tsf.2007.05.090

3 Chapter 3: Water splitting in dye-sensitized photoelectrochemical cells (DS-PEC)

Aim of this section

Metal-free organic sensitizers with di-branched configuration, bearing different heteroaromatic donor moieties, have been employed in a systematic study upon the effect of the sensitizers at the photoanode in the photoelectrochemical hydrogen production. Namely, phenothiazine, phenoxazine and carbazole based dyes, have been tested in presence of a sacrificial electron donor (SED) to evaluate hydrogen production, charge transfer phenomena and the external quantum efficiency (EQE) of the system. Moreover, the three sensitizers have been tested in presence of a common water oxidation catalyst (WOC) to preliminary evaluate the stability in photoelectrochemical water splitting and hydrogen and oxygen evolution. According to experimental data, the phenothiazine based derivative **PTZ-Th** has been recognized as the best performing sensitizer, considering its superior light harvesting capability and more efficient electron injection into the semiconductor, in photoelectrochemical waters splitting.

3.1 Introduction

The unprecedented technological development of the last century has been accompanied by critical issues related to the retrieval and consumption of natural resources for the production of energy, in particular the massive use of fossil fuels like natural gas, oil and coal.[1] This intensive use has been associated to relevant emergencies, including pollution and climate crisis. It is therefore urgent to reduce the use of fossils for fuel production and develop and make accessible new sustainable fuels for transportation and other uses.[2-3] Nature provides us sunlight and basic elements to synthesize biomasses that, during millennia, have been transformed in fossil fuels. This suggests the use of solar energy and abundant and renewable sources to provide the fuels for the new millennium.

The main problem in the conversion of solar energy into electricity or fuels is that the involved processes are threshold-limited, and this implies consequences on conversion efficiency. Furthermore, the solar energy is discontinuous and subject to intensity fluctuations due to diurnal cycles and atmospheric conditions. Therefore, storage of solar energy is needed to make this route viable for society needs. Present strategies for storing the excess of electricity have been the use of batteries[4] and the production of solar fuels via photovoltaics in combination with electrolyzers, a solution which implies too demanding costs.[5] A good alternative strategy to store solar energy is the direct conversion into chemical energy mimicking natural photosynthesis.[6]

In the field of artificial photosynthesis, many efforts have been done in the last years to provide a reliable system to produce solar fuels from water and sunlight. Photocatalytic and photoelectrochemical methods have been extensively exploited to solve this issue.[7-11] Even if the photocatalytic approach has been more extensively investigated for its greater device straightforwardness, it is not intrinsically capable to produce hydrogen and

oxygen separately. Therefore, photoelectrochemical cells (PEC) are considered to be the best option for generating solar fuels from sunlight and water.

Dye-sensitized photoelectrosynthesis or photoelectrochemical cells (DS-PEC) appear to be the best compromise between efficiency and technical issues. This device integrates molecular sensitizers, able to efficiently harvest the visible portion of the solar spectrum, and a high band-gap semiconductor in a structure like the one used in dye-sensitized solar cells (DSSC).[12-20]

A DS-PEC is constituted by a (photo)anode and a (photo)cathode where water oxidation and reduction, respectively, take place. Compared to a PEC, where the water splitting processes at the electrodes are performed by the same component, e.g. a semiconductor,[21] in a DS-PEC the different steps are separated and operated by different components, which gives the opportunity of separate optimization. In a DS-PEC, light harvesting and charge injection are played by a dye-sensitizer. Injected charges (electrons in a photoanode or holes in a photocathode) are then transferred from the dye excited state to a n- or p-type semiconductor, respectively. Consequently, a radical cation or anion of the dye is produced. The neutral dye is regenerated by the extraction of electrons from a water oxidation catalyst (WOC), in the case of a photoanode, and holes from a water reduction catalyst (WRC), in the case of a photocathode, affording, after process reiterations, water oxidation and reduction at the water-catalyst interface. In the photoelectrochemical production of solar fuels, the bottleneck appears to be the water oxidation process, because of its four-electron nature. A related problem is the low stability of molecules at the very positive potentials needed to drive the reaction.[22]

It is evident that DS-PEC have a greater potential compared to PEC since the fundamental steps of light harvesting and charge generation are fulfilled by the dye, that can be specifically designed to optimize these abilities. Therefore, the design of the dye is a critical step. The optimal dye-sensitizer should be easy to synthesize and purify, not toxic, based on earth abundant elements, and have a

reproducible and low cost batch-to-batch preparation. In addition, the structure of the dye should allow optimal tuning of optical (wide and strong light harvesting) and electronic (charge donation and extraction) properties and proper interface and solubility characteristics.

In the last decade, few molecular sensitizers have been explored to improve the effectiveness of DS-PEC, compared to the wide engagement on the front of the oxidation and, to a less extent, reduction catalysts. The research on photosensitizers has been mostly focused on conventional organometallic dyes,[23-35] while the exploitation of metal free organic sensitizers has been so far very limited.[36-44] This fact is even more surprising if we consider the massive literature in organic dyes for other solar related applications such as DSSC,[45-47] and dye sensitized photocatalytic hydrogen generation.[8] The most extensively used organometallic dyes are Ru(II) polypyridyl complexes either as photosensitizers or as catalysts due to their interesting properties such as stability in water and suitable electronic and optical properties.[26, 31, 48] However, the use of Ru(II) and other metal complexes implies a number of critical issues such as higher costs, limited natural abundance, limited absorption spectra flexibility, and, in some cases, toxicity. The extensive use of metal-free sensitizers would imply a number of relevant advantages such as low cost synthesis, ready industrial scale-up, and virtually unlimited tuning of optical and electronic properties. The design of efficient DS-PEC organic sensitizers is then urgent and could be an important breakthrough in the field of water splitting, like what has happened with DSSC.

We have recently reported a series of di-branched donor-(π-acceptor)$_2$ phenothiazine-based sensitizers (PTZ) functionalized with an alkyl terminal and containing different thiophene-based spacers.[49] These sensitizers have already been successfully employed in photocatalytic hydrogen production exhibiting enhanced efficiency and stability under solar irradiation in the long term. Furthermore, a study by our group upon the effect of molecular design on

photocatalytic activity has pointed out the superior efficiency of carbazole (CBZ) based derivatives compared to the PTZ analogues. The molecular design of these dyes appears highly appropriate to the use as sensitizers also in the anodic sensitization of a DS-PEC.

In this section, the effect of molecular design of the dye, depicted in **Figure 3.1**, on the electronic properties, stabilities, and photoinduced electron transfer properties in a water splitting photoelectrochemical cell has been investigated in presence of a sacrificial electron donor and a ruthenium based WOC. The series of sensitizers has been completed with the inclusion of a phenoxazine (POZ) derivative, which shares with PTZ the same geometrical and functionalization pattern but where the bridge sulphur atom has been replaced by an oxygen atom. In order to investigate in details the light harvesting and charge generation, transport, and collection mechanisms, the water oxidation step has been bypassed by replacing the WOC with a sacrificial electron donor (SED), which is irreversibly oxidized in place of water with a faster and more straightforward monoelectronic process.[50] The study of a DS-PEC in presence of a SED is then important for sensitizer molecular design, since the recorded results reflect the properties of the dye absorbed onto the semiconductor and its interaction with the electrolyte, discarding all the problems that can arise from the interaction with the WOC and the much slower dye regeneration due to water oxidation. By keeping in mind the central role of the organic sensitizers, we have selected commonly used SED and WOC, for a ready evaluation of effectiveness of the work. We selected hydroquinone (H_2Q) as a SED, because of its interesting properties and different oxidation potential and mechanism.[39] Finally, we have chosen the common benchmark [Ru(bda)(pic)$_2$] (bda = 2,2′-bipyridine-6,6′-dicarboxylate, pic = 4-picoline) as a WOC to be used in solution.[29-30, 51]

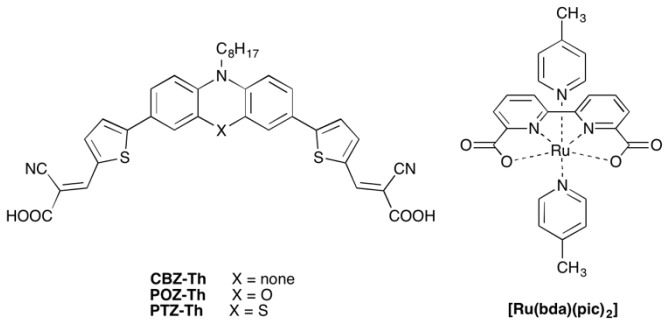

Figure 3.1. *Dyes and catalyst investigated in this section.*

3.2 Choice and properties of the dyes

Three different dyes with substantial structural differences have been tested during this study on organic sensitizers for DS-PEC. We decided to investigate the influence of different donor group over the photoelectrochemical water splitting. The main difference lies in the choice of carbazole (CBZ) electron donor group over two different azine-based donor moieties, namely phenothiazine (PTZ) and phenoxazine (POZ): the first was a planar building block,[52] the others were butterfly-like structures containing oxygen (POZ) or sulphur (PTZ).[53-54]

The sensitizers were synthesized according to a procedure previously reported in literature,[55] and their optical properties, as well as electrochemical properties, were investigated and the data summarized in **Table 3.1**. The UV-Vis investigation, both in solution and adsorbed onto a transparent 3.5-µm-thick TiO_2 film, was performed and the results depicted in **Figure 3.2**.

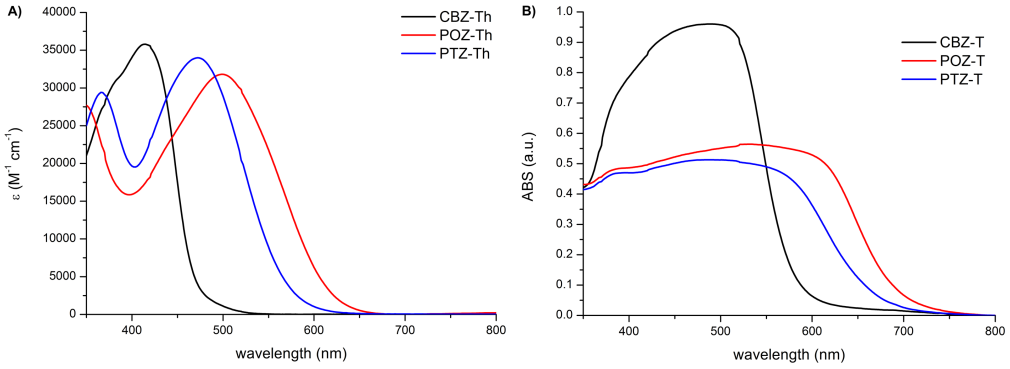

Figure 3.2. *UV-Vis spectra of the investigated dyes in 10^{-5} M solution in DMSO (**A**) and adsorbed onto a 3.5-µm transparent TiO_2 photoanode (**B**).*

Since we were interested in the photoelectrochemical properties of the sensitized photoanodes, it was important to evaluate the absorption spectra of such sensitizers adsorbed on the semiconductor. As it was possible to notice, after absorption on TiO_2, there was a broadening of the absorption band up to about 720 nm in the case of **POZ-Th**, whereas the absorption edge in the case of the solution was located at about 580 nm. The same behaviour was observed also for the other dyes. The amount of dye adsorbed was evaluated after desorption in a 0.1 M NaOH solution in water/ethanol 1:1 *v/v* and reported in **Table 3.2**. The **CBZ-Th** absorbed was almost twice as much as **PTZ-Th** and **POZ-Th**; this can be due to the different conformation of the molecules. As already said, in fact, **PTZ-Th** and **POZ-Th** has a butterfly-like structure whereas the **CBZ-Th** is planar: in this way, the latter is able to pack itself on the TiO_2 surface better than **PTZ-Th** and **POZ-Th**, which usually form a monolayer of dye. This data well matches the UV-Vis spectrum on TiO_2: **CBZ-Th** absorbance is double that of the other two dyes.

Cyclic voltammetry (CV) curves (**Figure 3.3**), collected in 0.1 M $TBABF_4$ in CH_3CN, showed a quasi-reversible behaviour for the oxidation process in all the investigated dyes, both in solution[55] and on transparent 3.5-µm-thick TiO_2 film. The LUMO levels were derived from electrochemical HOMO values in solution and optical bandgaps, measured by means of Tauc plots.[56] HOMO and LUMO values are reported in **Table 3.1** and in **Table 3.2** and depicted in **Figure 3.4** together with the oxidation potential of SED[57] and WOC, calculated on $E_{½}$.[51]

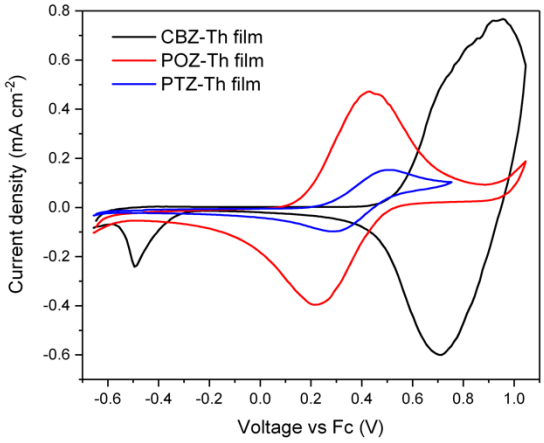

Figure 3.3. *CV of dyes* ***CBZ-Th***, ***POZ-Th*** *and* ***PTZ-Th*** *on TiO_2 films in 0.1 M $TBABF_4$ in CH_3CN, at a scan rate of 100 mV s^{-1}.*

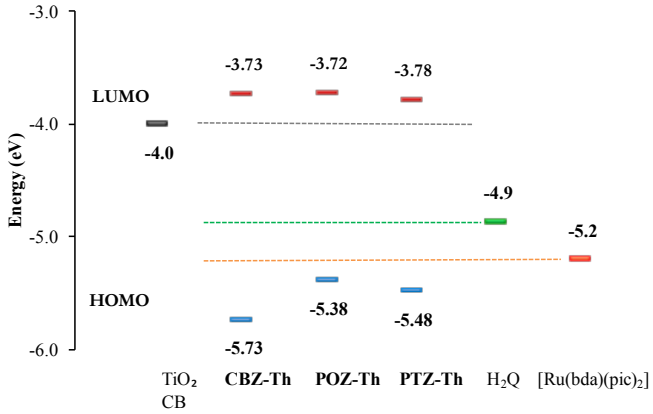

Figure 3.4. *Energy levels scheme of the investigated dyes, of the SED (H_2Q) and of the Ru-WOC*

Even if the HOMO energy levels measured in solution were fairly similar for **CBZ-Th** and **POZ-Th** dyes (~ -5.60 eV), the different bandgaps significantly affected their LUMO energies, and thus the electron injection efficiency to the TiO_2 semiconductor. In particular, the LUMO energy of the **POZ-Th** dye was very close to the conduction band (CB) of TiO_2 (-4.0 eV).[58]

In the case of the sensitized films, HOMO energy levels measured showed a larger shift in energies compared to the values measured in solution. Otherwise, considering the different values of the energy bandgaps obtained evaluating the UV-Vis absorption edge, the calculated LUMO energy were fairly similar for

CBZ-Th and **POZ-Th** dyes (~ -3.70 eV), and slightly higher for the **PTZ-Th** dye (~ -3.80 eV).

Table 3.1. *Main optical and electrochemical characterization of the CBZ, POZ, and PTZ dyes in solution[a].*

Sample	λ_{max}[b] (nm)	λ_{onset}[b] (nm)	ε[b] ($M^{-1}\,cm^{-1}$)	V_{ox}[b] (V vs Fc) ± 10 mV	HOMO[b,c] (eV) ± 0.05 eV	E_{gap}^{opt} [b] (eV)	LUMO [b,c] (eV) ± 0.05 eV
CBZ-Th	414	475	35800 ± 100	0.41	-5.64	2.26	-3.38
POZ-Th	534	625	31800 ± 1500	0.41	-5.64	1.87	-3.77
PTZ-Th	470	578	34 000 ± 1 000	0.15	-5.38	2.05	-3.33

[a] Ref. 55. [b] Dye solution 10^{-5} M in DMSO. [c] Vacuum potential = Fc/Fc^+ + 5.23 V.

Table 3.2. *Main optical and electrochemical characterization of the sensitizers adsorbed onto 3.5-µm transparent TiO_2 photoanode film.*

Sample	λ_{max}[a] (nm)	λ_{onset}[a] (nm)	Dye loading (µmol cm^{-2})	V_{ox}[a] (V vs Fc) ± 10 mV	HOMO[a,b] (eV) ± 0.05 eV	E_{gap}^{opt} [a] (eV)	LUMO [a,b] (eV) ± 0.05 eV
CBZ-Th	491	620	0.115	0.53	-5.73	2.00	-3.73
POZ-Th	534	746	0.0617	0.15	-5.38	1.66	-3.72
PTZ-Th	492	728	0.0685	0.25	-5.48	1.70	-3.78

[a] 3.5-µm transparent TiO_2 photoanode. [b] Vacuum potential = Fc/Fc^+ + 5.23 V.

3.3 Photoelectrochemical measurements

The photoelectrochemical characterization was performed in a three-electrode configuration purpose-designed photoelectrochemical cell (**Figure 3.5**). The sensitized TiO_2 photoanodes (prepared by screen-printing a commercial TiO_2

paste on FTO glass) were used as working electrode (WE), whereas a platinum wire as counter electrode (CE) and an Ag/AgCl 3 M KCl electrode as a pseudo-reference (RE). Aqueous phosphate buffer solution (PBS), prepared using commercially available PBS tablets (Sigma Aldrich) and 0.5 M KNO_3, was chosen as electrolyte and the current has been recorded under chopped irradiation (0.75 sun AM 1.5 G filtered $\lambda > 400$ nm (0.70 sun)).

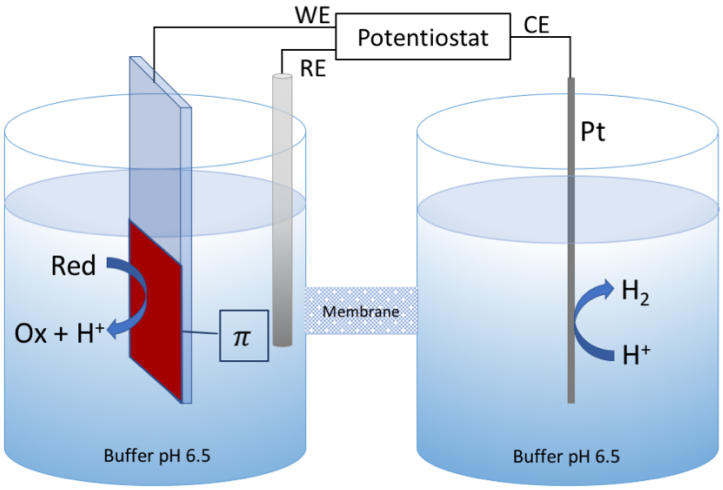

Figure 3.5. *Scheme of our three-electrode configuration purpose-designed PhotoElectrochemical Cell.*

The choice of this unusual solution, instead of the more common 0.1 M PBS solution,[39] was justified by a better performance recorded during photocurrent-time measurements. In fact, **Figure 3.6** reports a chronoamperometry (CA) measurement performed on the same dye (**CBZ-Th**) with both the standard PBS composition and the one with KNO_3 added that was chosen for this study; it is evident that the latter solution offers better and more stable performances over time.

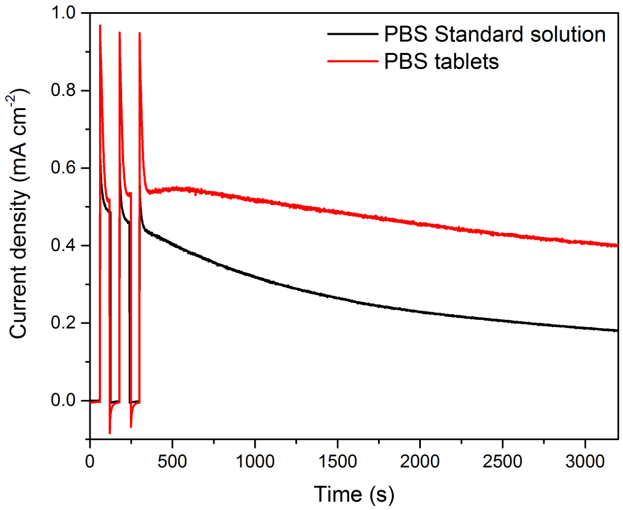

Figure 3.6. *Chronoamperometry of TiO_2 films sensitized with* ***CBZ-Th*** *dye in pH 6.5 PBS 0.1 M (black line) and pH 6.5 PBS from commercial tablets, KNO_3 0.5 M (red line), with H_2Q as an irreversible SED under irradiation (700 W m^{-2} AM 1.5 G filtered $\lambda > 400$ nm) with an external bias of ~ 0.59 V vs RHE.*

The experiments have been performed in presence of electrolyte itself and in presence of hydroquinone (H_2Q) as an irreversible SED (*vide infra*).

Upon photoexcitation, an electron of the absorbed dye (TiO_2/dye) is promoted to the LUMO level (TiO_2/dye*, Eq. 1) and then injected into the TiO_2 conduction band (CB) from the sensitizer through an electron transfer (et) mechanism, generating a radial-cation specie ($TiO_2(e^-)$/dye$^{+\bullet}$, Eq. 2). The dye$^{+\bullet}$ is restored to its ground state by reaction with hydroquinone (H_2Q) in solution, that is thus oxidized to a semiquinone radical-anion ($Q^{-\bullet}$, Eq. 3).[59] This process generates two protons and, at the end, two radical-anions can react and lead to the overall rapid disproportionation of two molecules of semiquinone radical-anion to quinone (Q) and H_2Q.[60] This photooxidative process is shown in **Scheme 1**.

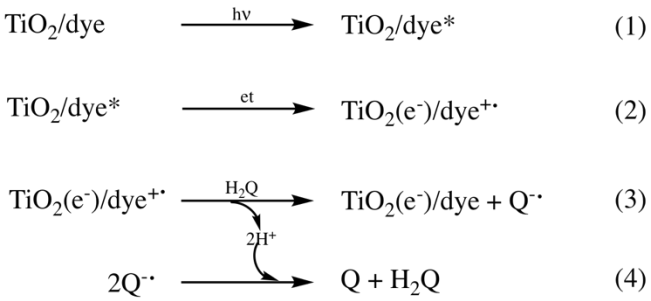

Scheme 1. *Photocatalytic process in presence of H_2Q as SED*

To evaluate the best external bias to be used in the photoelectrochemical measurements, linear sweep voltammetries (LSV) in dark and under irradiation, sweeping from -0.19 to 1.09 V vs RHE, were performed on the differently sensitized photoanodes. In order to have a proof of the effect of the SED, the same measurement has been performed both with and without the SED in the electrolyte solutions. The results of the LSV experiments are depicted in **Figure 3.7** and **Figure 3.8**.

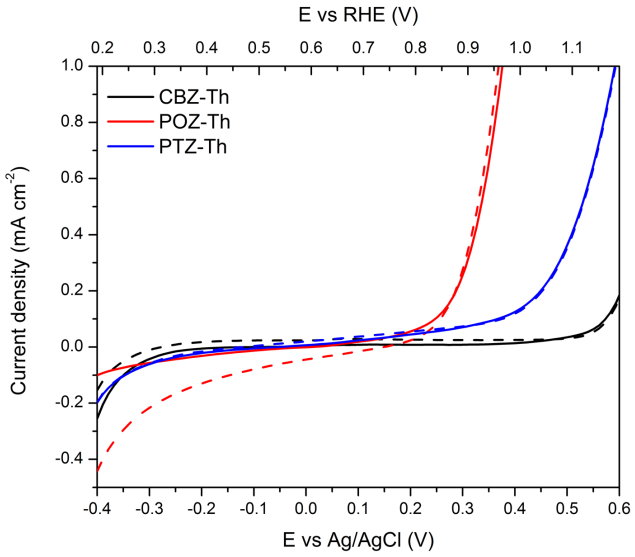

Figure 3.7. *Linear sweep voltammograms of TiO_2 films sensitized with the investigated dyes in pH 6.5 PBS, KNO_3 0.5 M, without SED under irradiation (700 W m^{-2} AM 1.5 G filtered $\lambda > 400$ nm, dashed line) and in dark (solid line) at a scan rate of 20 mV s^{-1}.*

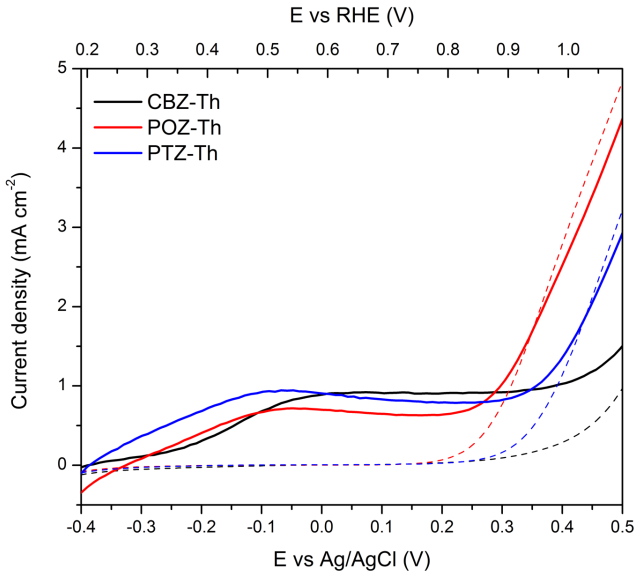

Figure 3.8. *Linear sweep voltammograms of TiO_2 films sensitized with the investigated dyes in pH 6.5 PBS, KNO_3 0.5 M, with H_2Q as irreversible SED under irradiation (700 W m^{-2} AM 1.5 G filtered $\lambda >$ 400 nm, solid line) and in dark (dashed line) at a scan rate of 20 mV s^{-1}.*

The almost complete absence of any difference between the signal recorded in dark and the one recorded in light conditions in the cell containing the PBS without SED (**Figure 3.7**) was an unambiguous clue that the SED was absolutely necessary in order to regenerate the dye and, so, allow the system to work.

The profile of the LSV voltammograms of the sensitized photoanodes recorded in PBS in presence of H_2Q as a SED (**Figure 3.8**) was in good agreement with the cyclic voltammograms recorded in presence of organic-based electrolyte (**Figure 3.3**). As working potential, we decided to use the potential that maximized the light/dark ratio, and to be able to use the same external bias, we decided to perform measurements at 0.59 V vs RHE (0 V vs Ag/AgCl).

Photocurrent-time measurements in presence of the H_2Q in PBS solution at pH 6.5 were shown in **Figure 3.9**, and were carried out at about 0.6 V vs RHE as external bias in presence of a Pt wire as CE. The recorded photocurrents values were collected in **Table 3.3**. As it was possible to notice, the highest initial photocurrent was reached by the **PTZ-Th** dye with a value of 1.66 mA cm^{-2}, a

lower value was yielded by the **CBZ-Th** with 0.98 mA cm^{-2} whereas the **POZ-Th** started with a value of 0.94 mA cm^{-2}.

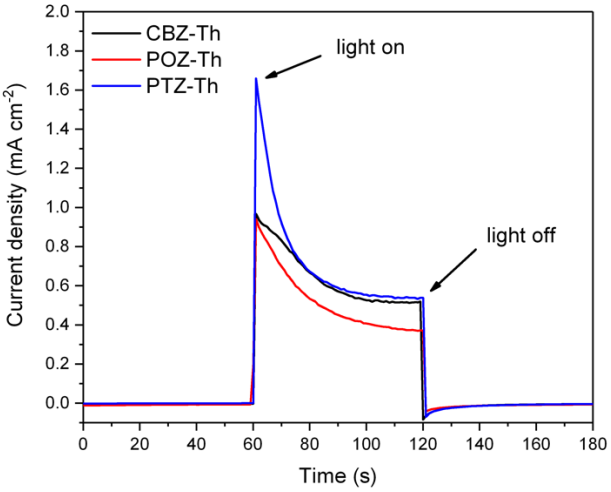

Figure 3.9. *Chronoamperometry of TiO_2 films sensitized with the investigated dyes in pH 6.5 PBS, KNO_3 0.5 M, with H_2Q as irreversible SED under irradiation (700 W m^{-2} AM 1.5 G filtered $\lambda > 400$ nm) with an external bias of ~ 0.6 V vs RHE.*

A longer CA measurement allowed to study the stability of the system and also to measure the gas evolution, in this case hydrogen in the cathodic compartment. All the three dyes tested in DS-PEC had a photocurrent loss during time, but the proportion was different. **CBZ-Th** started with the same current of **PTZ-Th** but finished with the same current of **POZ-Th**, so it was evident that the behaviour of the dyes was different.

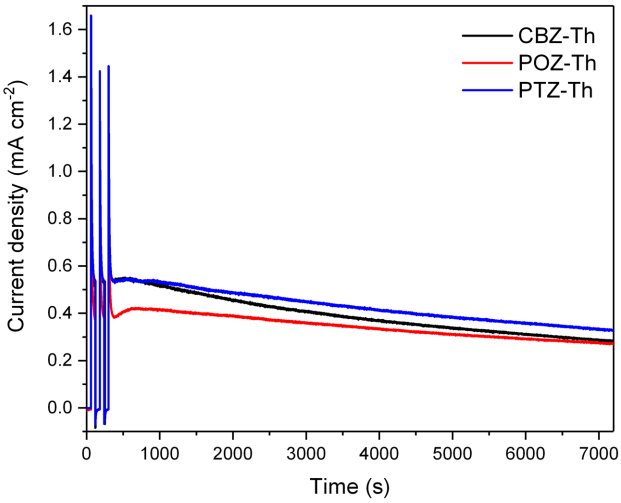

Figure 3.10. *Chronoamperometry of TiO_2 films sensitized with the investigated dyes in pH 6.5 PBS, KNO_3 0.5 M, with H_2Q as an irreversible SED under irradiation (700 W m^{-2} AM 1.5 G filtered $\lambda > 400$ nm) with an external bias of ~ 0.59 V vs RHE over a 2-hour illumination period.*

The capability of photoanodes to transform photons in electrons was also evaluated through the incident photon to current efficiency (IPCE), or external quantum efficiency (EQE), measurement with added H_2Q (**Figure 3.11**).

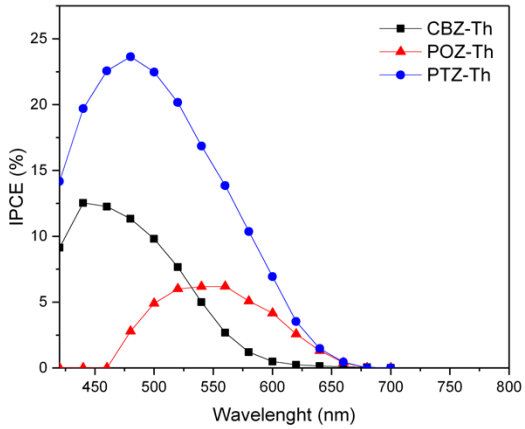

Figure 3.11. *Incident photon to current efficiency (IPCE) data of sensitized TiO_2 films in pH 6.5 PBS, KNO_3 0.5 M, with H_2Q as an irreversible SED under monochromatic irradiation with an applied bias of ~ 0.6 V vs RHE.*

For all the investigated dyes, there was a good match between the recorded IPCE spectral range and the absorption spectra on TiO_2. The intensity of the signal,

instead, qualitatively reflected the current density measured, so that the **PTZ-Th** showed the highest value with an impressive 24% maximum at 480 nm while the **POZ-Th** had the lowest IPCE.

Since we obtained interesting results in the DS-PEC using a SED, we also wanted to test our dyes using a WOC in order to perform the water oxidation reaction. Usually, two different methods were employed to study dye-sensitized photoanodes in presence of a catalyst: co-deposition of dye and catalyst onto the semiconductor or deposition of a covalently-linked dye-catalyst dyad. Since in this work we focused our attention on the dye sensitizer and not on the water-splitting performance in presence of a catalyst, for sake of simplicity we decided to employ a catalyst dissolved in the buffer solution instead of the two most common approaches. In this case, it was well known that the efficiency would have been far lower than with co-adsorbed catalyst onto TiO_2. Nevertheless, we believed that in this work, focused on photosensitizers comparison, the simpler approach of non-absorbed catalyst in solution was enough, yet allowing for lower quantities of gas generated. We chose a catalyst commonly used for dye-sensitized water splitting, even if with different sensitizing systems, the $Ru(bda)(pic)_2$.[30, 51]

The same photoelectrochemical measurements shown above were performed using the Ru-based WOC depicted in **Figure 3.1** ($Ru(bda)(pic)_2$), dissolved in pH 6.5 PBS, 0.5 M KNO_3, at 0.2 mM concentration. The photoanode and the Pt-cathode compartments of the cell were separated by a Nafion® Proton Exchange Membrane (PEM).

The LSV voltammograms showed a lower current density than that with the H_2Q as a SED and this was clearly due to the more complex and energy-demanding 4-electron process for water oxidation (**Figure 3.12**). It was however possible to see a clear difference between dark and light signal for all the three dyes investigated. The highest light/dark ratio in this case was reached at a bias

of 0.79 V vs RHE (0.2 V vs Ag/AgCl), so the chronoamperometric measurements were carried out at this potential.

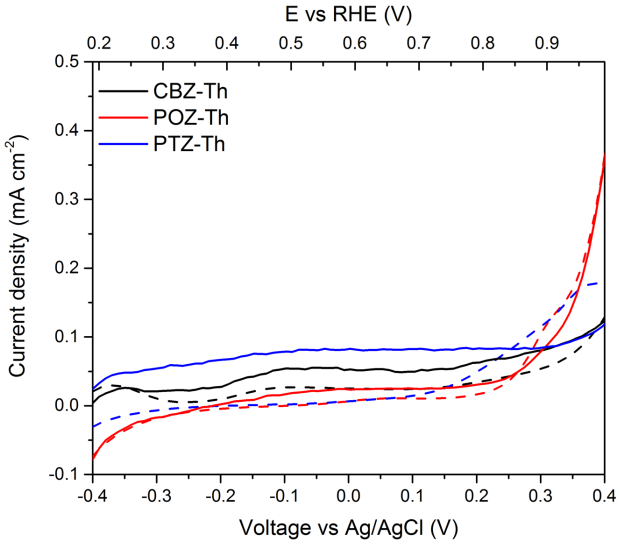

Figure 3.12. *Linear sweep voltammograms of TiO_2 films sensitized with the investigated dyes in pH 6.5 phosphate buffer solution, KNO_3 0.5 M, in presence of Ru(bpa)(pic)$_2$ as a WOC under irradiation (700 W m^{-2} AM 1.5 G filtered λ > 400 nm, solid line) and in dark (dashed line) at a scan rate of 20 mV s^{-1}.*

Photocurrent-time measurements in presence of the Ru-catalyst in PBS solution at pH 6.5 were shown in **Figure 3.13**, and were carried out at about 0.79 V vs RHE as external bias in presence of a Pt wire as CE. The recorded photocurrents values were collected in **Table 3.3**. In this case, the initial photocurrent was similar for all the dyes, **PTZ-Th** started with a value of 0.22 mA cm^{-2}, **CBZ-Th** dye starting with a value of 0.23 mA cm^{-2} and **POZ-Th** of 0.04 mA cm^{-2}.

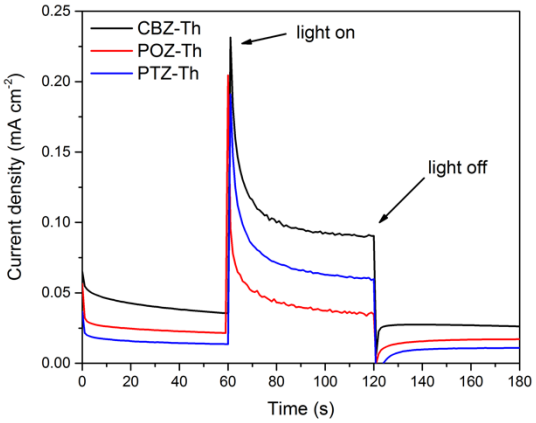

Figure 3.13. *Chronoamperometry of TiO_2 films sensitized with the investigated dyes in pH 6.5 phosphate buffer solution, KNO_3 0.5 M, in presence of $Ru(bpa)(pic)_2$ as a WOC under irradiation (700 W m^{-2} AM 1.5 G filtered λ > 400 nm) with an external bias of ~ 0.79 V vs RHE.*

Chronoamperometric measurements were also performed over a two-hour illumination period to investigate the stability of the dyes on TiO_2 and also the production of oxygen and hydrogen (**Figure 3.14**). On the contrary of the plots recorded with DS-PEC containing SED, in presence of WOC the photocurrent density generated by the photoanodes increased over time. Regarding the trend of the dyes, they followed the same measured in presence of SED, with the best performance given by **PTZ-Th**, followed by **CBZ-Th** and **POZ-Th**.

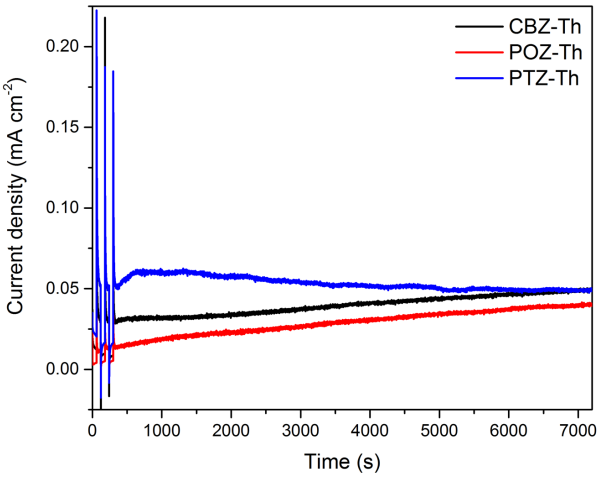

Figure 3.14. *Chronoamperometry of TiO_2 films sensitized with the investigated dyes in pH 6.5 PBS, KNO_3 0.5 M, in presence of $[Ru(bda)(pic)_2]$ as a WOC under irradiation (700 W m^{-2} AM 1.5 G filtered λ > 400 nm) with an external bias of ~ 0.79 V vs RHE over a 2-hour illumination period.*

The gas production was measured with a gas-chromatograph. While it was possible to easily detect the amount of hydrogen evolved, for oxygen it was possible to see the signal but not to easily quantify it. For this reason, a first test has been run to verify that both dyes and WOC could properly work and give origin to the water splitting process, measuring the photocurrent properties and only the evolution of hydrogen in the cathodic compartment. It is in fact much simpler to measure hydrogen than oxygen because the signal present in the chromatogram can be ascribed only to the gas evolved during the reaction, since no hydrogen is present in air. On the other hand, oxygen detection is much more difficult, because it can be present in the anodic compartment both for a not perfect purging and leaks from the cell gaskets. **Table 3.3** collects data from the preliminary screening, where we focused on hydrogen evolution; after optimization of the system, also oxygen could be evaluated, so another set of photoanodes has been measured and the results are shown in **Table 3.4**.

Table 3.3. *Photocurrent densities obtained from chronoamperometric measurements, charge passed over 2-hour illumination, faradaic efficiency and hydrogen evolved in **CBZ-Th**, **POZ-Th**, and **PTZ-Th** based DS-PEC, both with a SED and a WOC.*

Sample	SED or WOC[a]	$\Delta j_{d\text{-}l}$[b] (μA cm^{-2})	Δj_{2h}[c] (%)	Q (C)	FE_{H2} (%)	H_2 evolved (μmol)
CBZ-Th	SED	510	-49	1.20	15.8	0.99
	WOC	63.0	+18	0.328	18.6	0.32
POZ-Th	SED	370	-36	1.22	11.9	0.75
	WOC	19.5	+60	0.169	28.3	0.25
PTZ-Th	SED	540	-39	1.53	18.7	1.48
	WOC	50.4	+7.8	0.195	22.5	0.23

[a] *Dye-sensitized photoanodes in a PEC filled with pH 6.5 PBS, KNO_3 0.5 M, and 20 mM H_2Q or 0.2 mM $Ru(bda)(pic)_2$;* [b] *Current density difference between dark and light over a 180 s chronoamperometry;* [c] *Current density loss/gain over a 2 h chronoamperometry under illumination (0.7 sun, λ>400 nm).*

As shown in **Table 3.3**, there was a clear difference in the behaviour of the dyes over a two-hour illumination period. When dyes were tested in a cell with the

SED, the current density decreased over time till almost a 50% loss, while when the WOC was present in the buffer solution the current density increased. It is also possible to notice that the faradaic efficiency for hydrogen production was in all cases higher with the WOC than with the SED; this could be due to the different charge circulated in the system. In fact, when the amount of electric charge was high, it was possible that the platinum was not able to properly work as a reduction catalyst, since the platinum wire surface was limited and might become overloaded with electrons, so it is more likely that recombination phenomena occurred and less hydrogen was evolved. On the contrary, when the charge was low, platinum could more efficiently employ the charge to reduce protons to hydrogen.

Table 3.4. *Photocurrent densities obtained from chronoamperometric measurements, charge passed over 2-hour illumination, faradaic efficiency and oxygen evolved in* ***CBZ-Th****,* ***POZ-Th****, and* ***PTZ-Th*** *based DS-PEC, both with a SED and a WOC.*

Sample	SED or WOC[a]	$\Delta j_{d\text{-}l}$[b] (μA cm^{-2})	Δj_{2h}[c] (%)	Q (C)	FE_{O2} (%)	O_2 evolved (μmol)
CBZ-Th	SED	510	-49	1.20	/	/
	WOC	22.8	+63	0.140	69	0.25
POZ-Th	SED	370	-36	1.22	/	/
	WOC	7.0	+178	0.101	69	0.18
PTZ-Th	SED	540	-39	1.53	/	/
	WOC	35.3	-5.7	0.190	66	0.32

[a] *Dye-sensitized photoanodes in a PEC filled with pH 6.5 PBS, KNO_3 0.5 M, and 20 mM H_2Q or 0.2 mM Ru(bda)(pic)$_2$;* [b] *Current density difference between dark and light over a 180 s chronoamperometry;* [c] *Current density loss/gain over a 2 h chronoamperometry under illumination (0.7 sun, λ>400 nm).*

Photocurrent generation in presence of the SED was higher than 500 μA cm^{-2}, a value which is comparable with the best reported performances for organic sensitizers.[39] The best photon-charge conversion was recorded for **CBZ-Th** and **PTZ-Th**. This is in agreement with their higher molar absorptivities in solution, though it should be noted that their absorption band as photoanode films is

blue-shifted compared to the POZ derivative. Indeed, the higher generated current values of **CBZ-Th** and **PTZ-Th** well matched their improved IPCE behaviour. Since on the whole the optical properties of **CBZ-Th** and **PTZ-Th** both in solution or as films are not better than those of **POZ-Th**, we conclude that the superior external quantum efficiency of the two more performing dyes, which comprises the light harvesting ability and the internal quantum efficiency, mainly arises from a higher value of the latter parameter. IPCE also partially accounts for the higher photoelectrochemical performance of **PTZ-Th** compared to **CBZ-Th**. It should also be noted that the amount of generated charge is higher for **PTZ-Th** despite its lower loading on the semiconductor. We therefore argue that the lower loading (likely arising from the butterfly geometry), associated to a suppression of detrimental dye–dye intermolecular excited state self-quenching, might play a central role in the enhanced performances. The data in presence of the WOC shows the same trend seen with the SED and confirms that the most efficient system is the **PTZ-Th** dye. Finally, we note that the use of the dyes in combination with a WOC revealed a stable photocurrent generation over a considerable time for all the three sensitizers, designating them as promising alternatives to the more common Ru-based complexes.

The amount of both evolved hydrogen and oxygen follows the same trend as for charge generation and collection. In particular, the amount of evolved gas at the CE is in the rank **PTZ-Th > CBZ-Th > POZ-Th**, in agreement with the aforementioned discussion. These values quantitatively well compare with gas generation properties previously reported in the recent literature for organic sensitizers.[61] Such evaluation is even more favourable if considering that the other representative reported measurements are carried out at much higher (up to 3 sun) intensities, to be compared with our device set-up at 0.70 sun.[51]

3.4 Experimental section

The following materials were purchased from commercial suppliers: FTO-coated glass plates (2.2 mm thick; sheet resistance ~7 ohm per square; Solaronix); Dyesol 18NR-T transparent TiO_2 blend of active 20 nm anatase particles. All reagents were obtained from commercial suppliers at the highest purity grade and used without further purification. The dyes and the catalyst have been synthesized according to literature.[30, 55]

Absorption spectra were recorded with a V-570 Jasco spectrophotometer. UV-O_3 treatment was performed using Novascan PSD Pro Series – Digital UV Ozone System. The thickness of the layers was measured by means of a VEECO Dektak 8 Stylus Profiler. Cyclic Voltammetry (CV) was carried out at scan rate of 100 mV s^{-1}, using a AUTOLAB PGSTAT302N potentiostat in a three-electrode electrochemical cell under Ar. The working, counter, and the pseudo-reference electrodes were a glassy carbon pin for the dyes in solution or a sensitized 3.5 μm thick TiO_2 film, a Pt wire and an Ag/AgCl electrode (3 M KCl), respectively. The working electrodes discs were well polished with alumina 0.1 μm suspension. The preparation and sensitization of the 3.5-μm-thick TiO_2 film is described below. The Pt wire was sonicated for 15 min in deionized water, washed with 2-propanol, and cycled for 50 times in 0.5 M H_2SO_4 before use. The Ag/AgCl pseudo-reference electrode was calibrated, by adding ferrocene (10^{-3} M) to the test solution after each measurement. All potentials have been reported in the reversible hydrogen electrode (RHE) scale by shifting the potentials by $E_{RHE} = E_{Ag/AgCl} + 0.059\ pH + E°_{Ag/AgCl\ (KCl\ 3\ M)} = E_{Ag/AgCl} + 0.059 \times 6.5 + 0.21\ V = E_{Ag/AgCl} + 0.59\ V$, according to the literature.[62]

The photoanodes have been prepared as described below adapting a procedure reported in the literature.[63] In order to exclude metal contamination all of the containers were in glass or Teflon and were treated with EtOH and 10% HCl prior to use. Plastic spatulas and tweezers have been used throughout the

procedure. FTO glass plates were cleaned in a detergent solution for 15 min using an ultrasonic bath, rinsed with pure water and EtOH. After treatment in a UV-O_3 system for 18 min, a transparent active layer of 4.25 cm^2 was screen-printed using Dyesol 18NR-T active transparent TiO_2 paste. The coated films were thermally treated at 125 °C for 6 min, 325 °C for 10 min, 450 °C for 15 min, and 500 °C for 15 min. The heating ramp rate was 5 - 10 °C/min.

FTO plates coated with 3.5 μm transparent TiO_2 film, prepared as described above, were treated in a UV-O_3 system for 20 min at room temperature, then immersed into a 2 x 10^{-4} M solution in EtOH of the dye for 2 h at room temperature in the dark. The stained substrates were rinsed with EtOH and dried with a stream of dry nitrogen. The UV-Vis spectra, CV and LSV were recorded in comparison with a bare 3.5 μm transparent TiO_2 film.

Photoelectrochemical measurements of DS-PEC were carried out with black metal mask on top of the photoanode of 0.50 cm^2 surface area under a 500 W Xenon light source (ABET Technologies Sun 2000 class ABA Solar Simulator). The power of the simulated light was calibrated to 75 mW cm^{-2} (70 mW cm^{-2}, λ>400 nm) using a reference Si cell photodiode equipped with an IR-cutoff filter (KG-5, Schott) to reduce the mismatch in the region of 350-750 nm between the simulated light and the AM 1.5 spectrum. The LSV (scan rate 20 mV s^{-1}) and CA measurements on the DS-PEC were performed using a AUTOLAB PGSTAT302N potentiostat in a three-electrode purposely designed photoelectrochemical cell filled with pH 6.5 PBS (Sigma Aldrich, product number P4417), KNO_3 0.5 M under Ar in presence of a Nafion®-115 (Alfa Aesar) proton exchange membrane, and the data collected with GPES electrochemical interface (EcoChemie).

IPCE measurements were carried out using monochromatic light through a monochromator (Jasco) illuminating on the active area of the working electrode (0.50 cm^2). The light intensity was monitored using a reference Si cell photodiode (THORLABS, S120VC) and corrected to calculate the IPCE values. The current

intensity was measured using an AUTOLAB PGSTAT302N potentiostat in a three-electrode purposely designed photoelectrochemical cell and the data collected with GPES electrochemical interface (EcoChemie).

The gas production was measured by means of an Agilent 6850 gas-chromatograph, using Ar as gas carrier (flow rate 25 mL min^{-1}) and equipped with thermal conductivity detector and a molecular sieve 5 Å column (2 m x 2 mmID, temperature 70 °C). Argon mixtures with 100 ppm and 10 000 ppm of H_2 and O_2 were used for calibration. Evolved O_2 was calculated taking into account small leaks of air into the PEC device: the amount of O_2 coming from air was subtracted from the total measured one (i.e. the quantity proportional to the measured N_2, surely coming from leaks).

3.5 Bibliography

1. 2016."International Energy Agency".

2. Armaroli, N.; Balzani, V., "Towards an electricity-powered world". *Energy Environ. Sci.* **2011,** *4*, 3193-3222, doi: 10.1039/C1EE01249E

3. Armaroli, N.; Balzani, V., "Solar Electricity and Solar Fuels: Status and Perspectives in the Context of the Energy Transition". *Chem. Eur. J.* **2016,** *22*, 32-57, doi: 10.1002/chem.201503580

4. Letcher, T., *Storing Energy* 1st edition ed.; Elsevier: 2016.

5. Armaroli, N.; Balzani, V., "The Hydrogen Issue". *ChemSusChem* **2010,** *4*, 21-36, doi: 10.1002/cssc.201000182

6. Barber, J., "Photosynthetic energy conversion: natural and artificial". *Chem. Soc. Rev.* **2009,** *38*, 185-196, doi: 10.1039/B802262N

7. Zhang, X.; Peng, T.; Song, S., "Recent advances in dye-sensitized semiconductor systems for photocatalytic hydrogen production". *J. Mater. Chem. A* **2016,** *4*, 2365-2402, doi: 10.1039/C5TA08939E

8. Cecconi, B.; Manfredi, N.; Montini, T.; Fornasiero, P.; Abbotto, A., "Dye-Sensitized Solar Hydrogen Production: The Emerging Role of Metal-Free Organic Sensitizers". *Eur. J. Org. Chem.* **2016,** *2016*, 5194-5215, doi: 10.1002/ejoc.201600653

9. Queyriaux, N.; Kaeffer, N.; Morozan, A.; Chavarot-Kerlidou, M.; Artero, V., "Molecular cathode and photocathode materials for hydrogen evolution in photoelectrochemical devices". *J. Photochem. Photobiol. C: Photochem. Rev.* **2015,** *25*, 90-105, doi: http://dx.doi.org/10.1016/j.jphotochemrev.2015.08.001

10. Barber, J.; Tran, P. D., "From natural to artificial photosynthesis". *Journal of The Royal Society Interface* **2013,** *10*, doi: 10.1098/rsif.2012.0984

11. Swierk, J. R.; Mallouk, T. E., "Design and development of photoanodes for water-splitting dye-sensitized photoelectrochemical cells". *Chem. Soc. Rev.* **2013,** *42*, 2357-2387, doi: Doi 10.1039/C2cs35246j

12. Alstrum-Acevedo, J. H.; Brennaman, M. K.; Meyer, T. J., "Chemical Approaches to Artificial Photosynthesis. 2". *Inorg. Chem.* **2005,** *44*, 6802-6827, doi: 10.1021/ic050904r

13. Concepcion, J. J.; House, R. L.; Papanikolas, J. M.; Meyer, T. J., "Chemical approaches to artificial photosynthesis". *Proc. Natl. Acad. Sci. U.S.A.* **2012,** *109*, 15560, doi:

14. Walter, M. G.; Warren, E. L.; McKone, J. R.; Boettcher, S. W.; Mi, Q.; Santori, E. A.; Lewis, N. S., "Solar Water Splitting Cells". *Chem. Rev.* **2010,** *110*, 6446-6473, doi: 10.1021/cr1002326

15. Balzani, V.; Credi, A.; Venturi, M., "Photochemical Conversion of Solar Energy". *ChemSusChem* **2008,** *1*, 26-58, doi: 10.1002/cssc.200700087

16. Grätzel, M., "Photoelectrochemical cells". *Nature* **2001,** *414*, 338, doi: 10.1038/35104607

17. Brennan, B. J.; Lam, Y. C.; Kim, P. M.; Zhang, X.; Brudvig, G. W., "Photoelectrochemical Cells Utilizing Tunable Corroles". *ACS Appl. Mater. Interfaces* **2015,** *7*, 16124-16130, doi: 10.1021/acsami.5b05050

18. Li, J.; Miao, J.; Long, G.; Zhang, J.; Li, Y.; Ganguly, R.; Zhao, Y.; Liu, Y.; Liu, B.; Zhang, Q., "N-Heteroheptacenequinone and N-heterononacenequinone: synthesis, physical properties, crystal structures and photoelectrochemical behaviors". *J Mater Chem C* **2015,** *3*, 9877-9884, doi: 10.1039/C5TC02010G

19. Wang, Z.; Miao, J.; Long, G.; Gu, P.; Li, J.; Aratani, N.; Yamada, H.; Liu, B.; Zhang, Q., "Full Characterization and Photoelectrochemical Behavior of Pyrene-fused Octaazadecacene and Tetraazaoctacene". *Chem. Asian J.* **2015,** *11*, 482-485, doi: 10.1002/asia.201501276

20. Gu, P.-Y.; Wang, Z.; Xiao, F.-X.; Lin, Z.; Song, R.; Xu, Q.-F.; Lu, J.-M.; Liu, B.; Zhang, Q., "An ambipolar azaacene as a stable photocathode for metal-free light-driven water reduction". *Materials Chemistry Frontiers* **2017,** *1*, 495-498, doi: 10.1039/C6QM00113K

21. Fujishima, A.; Honda, K., "Electrochemical Photolysis of Water at a Semiconductor Electrode". *Nature* **1972,** *238*, 37-38, doi:

22. Youngblood, W. J.; Lee, S.-H. A.; Maeda, K.; Mallouk, T. E., "Visible Light Water Splitting Using Dye-Sensitized Oxide Semiconductors". *Acc. Chem. Res.* **2009,** *42*, 1966-1973, doi: Doi 10.1021/Ar9002398

23. Zhang, L.; Gao, Y.; Ding, X.; Yu, Z.; Sun, L., "High-Performance Photoelectrochemical Cells Based on a Binuclear Ruthenium Catalyst for Visible-Light-Driven Water Oxidation". *ChemSusChem* **2014,** *7*, 2801-2804, doi: 10.1002/cssc.201402561

24. Yamamoto, M.; Wang, L.; Li, F.; Fukushima, T.; Tanaka, K.; Sun, L.; Imahori, H., "Visible light-driven water oxidation using a covalently-linked molecular catalyst-sensitizer dyad assembled on a TiO2 electrode". *Chem. Sci.* **2016,** *7*, 1430-1439, doi: 10.1039/C5SC03669K

25. Li, L.; Duan, L. L.; Xu, Y. H.; Gorlov, M.; Hagfeldt, A.; Sun, L. C., "A photoelectrochemical device for visible light driven water splitting by a molecular ruthenium catalyst assembled on dye-sensitized nanostructured TiO2". *Chem. Commun.* **2010,** *46*, 7307-7309, doi: 10.1039/c0cc01828g

26. Gao, Y.; Zhang, L.; Ding, X.; Sun, L., "Artificial photosynthesis - functional devices for light driven water splitting with photoactive anodes based on molecular catalysts". *Phys. Chem. Chem. Phys.* **2014,** *16*, 12008-12013, doi: 10.1039/C3CP55204G

27. Gao, Y.; Duan, L.; Yu, Z.; Ding, X.; Sun, L., "Artificial photosynthesis: photosensitizer/catalyst supramolecular assemblies for light driven water oxidation". *Faraday Discuss.* **2014,** *176*, 225-232, doi: 10.1039/C4FD00127C

28. Gao, Y.; Ding, X.; Liu, J.; Wang, L.; Lu, Z.; Li, L.; Sun, L., "Visible Light Driven Water Splitting in a Molecular Device with Unprecedentedly High Photocurrent Density". *J. Am. Chem. Soc.* **2013,** *135*, 4219-4222, doi: 10.1021/ja400402d

29. Duan, L.; Bozoglian, F.; Mandal, S.; Stewart, B.; Privalov, T.; Llobet, A.; Sun, L., "A molecular ruthenium catalyst with water-oxidation activity comparable to that of photosystem II". *Nat Chem* **2012,** *4*, 418-423, doi:

http://www.nature.com/nchem/journal/v4/n5/abs/nchem.1301.html#supplementary-information

30. Duan, L.; Fischer, A.; Xu, Y.; Sun, L., "Isolated Seven-Coordinate Ru(IV) Dimer Complex with [HOHOH]− Bridging Ligand as an Intermediate for Catalytic Water Oxidation". *J. Am. Chem. Soc.* **2009,** *131*, 10397-10399, doi: 10.1021/ja9034686

31. Ding, X.; Gao, Y.; Zhang, L.; Yu, Z.; Liu, J.; Sun, L., "Visible Light-Driven Water Splitting in Photoelectrochemical Cells with Supramolecular Catalysts on Photoanodes". *Acs Catal* **2014,** *4*, 2347-2350, doi: 10.1021/cs500518k

32. Tian, H., "Molecular Catalyst Immobilized Photocathodes for Water/Proton and Carbon Dioxide Reduction". *ChemSusChem* **2015,** *8*, 3746-3759, doi: 10.1002/cssc.201500983

33. Ji, Z.; He, M.; Huang, Z.; Ozkan, U.; Wu, Y., "Photostable p-Type Dye-Sensitized Photoelectrochemical Cells for Water Reduction". *J. Am. Chem. Soc.* **2013,** *135*, 11696-11699, doi: 10.1021/ja404525e

34. Fan, K.; Li, F.; Wang, L.; Daniel, Q.; Gabrielsson, E.; Sun, L., "Pt-free tandem molecular photoelectrochemical cells for water splitting driven by visible light". *Phys. Chem. Chem. Phys.* **2014,** *16*, 25234-25240, doi: 10.1039/C4CP04489D

35. Alibabaei, L.; Luo, H.; House, R. L.; Hoertz, P. G.; Lopez, R.; Meyer, T. J., "Applications of metal oxide materials in dye sensitized photoelectrosynthesis cells for making solar fuels: let the molecules do the work". *J. Mater. Chem. A* **2013,** *1*, 4133-4145, doi: 10.1039/C2TA00935H

36. Moore, G. F.; Blakemore, J. D.; Milot, R. L.; Hull, J. F.; Song, H.-e.; Cai, L.; Schmuttenmaer, C. A.; Crabtree, R. H.; Brudvig, G. W., "A visible light water-splitting cell with a photoanode formed by codeposition of a high-potential porphyrin and an iridium water-oxidation catalyst". *Energy Environ. Sci.* **2011,** *4*, 2389-2392, doi: 10.1039/C1EE01037A

37. Swierk, J. R.; Méndez-Hernández, D. D.; McCool, N. S.; Liddell, P.; Terazono, Y.; Pahk, I.; Tomlin, J. J.; Oster, N. V.; Moore, T. A.; Moore, A. L.; Gust, D.; Mallouk, T. E., "Metal-free organic sensitizers for use in water-splitting dye-

sensitized photoelectrochemical cells". *Proc. Natl. Acad. Sci. U.S.A.* **2015,** *112*, 1681-1686, doi: 10.1073/pnas.1414901112

38. Lindquist, R. J.; Phelan, B. T.; Reynal, A.; Margulies, E. A.; Shoer, L. E.; Durrant, J. R.; Wasielewski, M. R., "Strongly oxidizing perylene-3,4-dicarboximides for use in water oxidation photoelectrochemical cells". *J. Mater. Chem. A* **2016**, doi: 10.1039/C5TA05790F

39. Wee, K.-R.; Sherman, B. D.; Brennaman, M. K.; Sheridan, M. V.; Nayak, A.; Alibabaei, L.; Meyer, T. J., "An aqueous, organic dye derivatized SnO2/TiO2 core/shell photoanode". *J. Mater. Chem. A* **2016**, doi: 10.1039/C5TA06678F

40. Kirner, J. T.; Finke, R. G., "Water-oxidation photoanodes using organic light-harvesting materials: a review". *J. Mater. Chem. A* **2017,** *5*, 19560-19592, doi: 10.1039/C7TA05709A

41. Kaeffer, N.; Massin, J.; Lebrun, C.; Renault, O.; Chavarot-Kerlidou, M.; Artero, V., "Covalent Design for Dye-Sensitized H2-Evolving Photocathodes Based on a Cobalt Diimine–Dioxime Catalyst". *J. Am. Chem. Soc.* **2016,** *138*, 12308-12311, doi: 10.1021/jacs.6b05865

42. Li, L.; Duan, L.; Wen, F.; Li, C.; Wang, M.; Hagfeldt, A.; Sun, L., "Visible light driven hydrogen production from a photo-active cathode based on a molecular catalyst and organic dye-sensitized p-type nanostructured NiO". *Chem. Commun.* **2012,** *48*, 988-990, doi: 10.1039/C2CC16101J

43. Click, K. A.; Beauchamp, D. R.; Huang, Z.; Chen, W.; Wu, Y., "Membrane-Inspired Acidically Stable Dye-Sensitized Photocathode for Solar Fuel Production". *J. Am. Chem. Soc.* **2016,** *138*, 1174-1179, doi: 10.1021/jacs.5b07723

44. Gardner, J. M.; Beyler, M.; Karnahl, M.; Tschierlei, S.; Ott, S.; Hammarström, L., "Light-Driven Electron Transfer between a Photosensitizer and a Proton-Reducing Catalyst Co-adsorbed to NiO". *J. Am. Chem. Soc.* **2012,** *134*, 19322-19325, doi: 10.1021/ja3082268

45. Mahmood, A., "Triphenylamine based dyes for dye sensitized solar cells: A review". *Solar Energy* **2016,** *123*, 127-144, doi: https://doi.org/10.1016/j.solener.2015.11.015

46. Manfredi, N.; Cecconi, B.; Abbotto, A., "Multi-Branched Multi-Anchoring Metal-Free Dyes for Dye-Sensitized Solar Cells". *Eur. J. Org. Chem.* **2014,** *2014*, 7069-7086, doi: 10.1002/ejoc.201402422

47. Higashino, T.; Imahori, H., "Porphyrins as excellent dyes for dye-sensitized solar cells: recent developments and insights". *Dalton Transactions* **2015,** *44*, 448-463, doi: 10.1039/C4DT02756F

48. Ashford, D. L.; Brennaman, M. K.; Brown, R. J.; Keinan, S.; Concepcion, J. J.; Papanikolas, J. M.; Templeton, J. L.; Meyer, T. J., "Varying the Electronic Structure of Surface-Bound Ruthenium(II) Polypyridyl Complexes". *Inorg. Chem.* **2015,** *54*, 460-469, doi: 10.1021/ic501682k

49. Cecconi, B.; Manfredi, N.; Ruffo, R.; Montini, T.; Romero-Ocaña, I.; Fornasiero, P.; Abbotto, A., "Tuning Thiophene-Based Phenothiazines for Stable Photocatalytic Hydrogen Production". *ChemSusChem* **2015,** *8*, 4216-4228, doi: 10.1002/cssc.201501040

50. Rao, N. N.; Dube, S., "Photoelectrochemical generation of hydrogen using organic pollutants in water as sacrificial electron donors". *Int. J. Hydrogen Energy* **1996,** *21*, 95-98, doi: http://dx.doi.org/10.1016/0360-3199(95)00045-3

51. Li, H.; Li, F.; Wang, Y.; Bai, L.; Yu, F.; Sun, L., "Visible-Light-Driven Water Oxidation on a Photoanode by Supramolecular Assembly of Photosensitizer and Catalyst". *Chempluschem* **2016,** *81*, 1056-1059, doi: 10.1002/cplu.201500539

52. Boger, D. L., *Comprehensive heterocyclic chemistry*. Pergamon Press, Ltd.: Oxford, 1984.

53. McDowell, J. J. H., "The crystal and molecular structure of pheno-thiazine". *Acta Crystallographica Section B* **1976,** *32*, 5, doi: 10.1107/S0567740876002215

54. Park, S. S.; Won, Y. S.; Choi, Y. C.; Kim, J. H., "Molecular Design of Organic Dyes with Double Electron Acceptor for Dye-Sensitized Solar Cell". *Energy & Fuels* **2009,** *23*, 3732-3736, doi: 10.1021/ef900207y

55. Manfredi, N.; Monai, M.; Montini, T.; Salamone, M.; Ruffo, R.; Fornasiero, P.; Abbotto, A., "Enhanced photocatalytic hydrogen generation

using carbazole-based sensitizers". *Sustainable Energy Fuels* **2017,** *1*, 694-698, doi: 10.1039/C7SE00075H

56. Tauc, J., "Optical properties and electronic structure of amorphous Ge and Si". *Mater. Res. Bull.* **1968,** *3*, 37-46, doi: https://doi.org/10.1016/0025-5408(68)90023-8

57. Chambers, J. Q., "Electrochemistry of quinones". *The Quinonoid Compounds (1988)* **2010**, doi: doi:10.1002/9780470772119.ch12 10.1002/9780470772119.ch12

58. Kalyanasundaram, K., *Dye-sensitized Solar Cells*. EFPL Press: 2010.

59. Rodenberg, A.; Orazietti, M.; Mosberger, M.; Bachmann, C.; Probst, B.; Alberto, R.; Hamm, P., "Quinones as Reversible Electron Relays in Artificial Photosynthesis". *Chemphyschem* **2016,** *17*, 1321-1328, doi: 10.1002/cphc.201501085

60. Becker, H.-D., "Photochemical Reactions with Phenols. IV. The Benzophenone-Sensitized Disproportionation of Hydroquinone Monoaryl Ethers". *J. Org. Chem.* **1967,** *32*, 2136-2140, doi: 10.1021/jo01282a601

61. Suryani, O.; Higashino, Y.; Mulyana, J. Y.; Kaneko, M.; Hoshi, T.; Shigaki, K.; Kubo, Y., "A near-infrared organic photosensitizer for use in dye-sensitized photoelectrochemical water splitting". *Chem. Commun.* **2017,** *53*, 6784-6787, doi: 10.1039/C7CC02730C

62. Hisatomi, T.; Kubota, J.; Domen, K., "Recent advances in semiconductors for photocatalytic and photoelectrochemical water splitting". *Chem. Soc. Rev.* **2014,** *43*, 7520-7535, doi: 10.1039/C3CS60378D

63. Ito, S.; Murakami, T. N.; Comte, P.; Liska, P.; Grätzel, C.; Nazeeruddin, M. K.; Grätzel, M., "Fabrication of thin film dye sensitized solar cells with solar to electric power conversion efficiency over 10%". *Thin Solid Films* **2008,** *516*, 4613-4619, doi: 10.1016/j.tsf.2007.05.090

4 Chapter 4: Conclusions

In this PhD project, we have devoted our attention to investigate new materials for solar energy conversion. More specifically, we studied organic dyes in either DSSCs and DS-PECs for the production of electricity and solar fuels.

Interesting results were obtained in herein described first ever systematic study of organic dyes applied for dye-sensitized water oxidation process, and furthermore the design of the photoelectrochemical cell has been optimized.

An interesting spin-off of this project was also realized using the same, or very similar, materials for photovoltaics applications. Namely, a pioneering investigation on a very new and important class of eco-friendly DES-based electrolytes has been carried out with very promising performances for future development of DSSC containing such innovative and green solvents, possibly leading to efficiency higher than those reported here.

In particular, in Section 2.2, the first example of a DSSC using an aqueous choline chloride-based DES as an effective electrolyte solvent has been described, leading to new possibilities for the sustainable use of DSSCs for renewable energy production. Different cell configurations (different hydrophilic dyes, different electrolyte composition and concentration, TiO_2 layer architecture, chemical nature of the counter electrodes, dyes, co-adsorbents and electrolyte additives) have been tested in order to optimize at the best the above-described DES-DSSC technology. In this way, the cell parameters were successfully optimized and overall efficiency was improved from values close to 0% to a value up to nearly 2%, which is quite comparable in absolute terms to mid-to-high ranked water-based DSSCs. In a world with dwindling oil resources, future work should thus mainly focus on further exploring the potential of using DESs as new, "green" media for solar devices in order to entirely replace hazardous

and toxic VOCs, which are still massively employed. Indeed, many DES components come from natural sources and do exhibit extremely low toxicity, and high biodegradability and renewability levels. Future developments could come from the high compositional flexibility of DESs and the possibility of fine-tuning their physico-chemical properties[1] to match the structure and features of dye-sensitizers and of other cell components. Thus, there is plenty of room to develop both fundamental and applied research in this field.

An example of the versatility of eutectic mixtures and their properties is described in the next section of this work (Section 2.3), where an innovative environmentally friendly non-volatile hydrophobic eutectic solvent has been tested in DSSCs. The unconventional mixture based on DL-menthol – acetic acid has been applied in cells with different types of photoanode layers (transparent vs opaque), thicknesses, amounts of the disaggregating agent, and intensity of the incident light, to eventually optimize the efficiency of the cell to a PCE value of 2.5%, which well compares with previous literature values for VOC-free (DES and/or aqueous media) liquid DSSCs. Although the higher viscosity of the HES medium compared to that of the VOC electrolyte is most probably responsible for a lower cell photocurrent, the photovoltage of the thin film HES-DSSC resulted significantly higher. Of note, the EIS investigation reveals that this is due to the much higher (more than twice compared to VOC) recombination resistance at the dye-TiO_2/electrolyte interface, a key factor for the maximum performance attainable for the cell. This testifies the critical role played by the HES in optimizing interface phenomena. The good performances, the higher voltage and the lower recombination resistances all suggest that the unconventional HES mixtures can play an important role in improving the eco-compatible and sustainable character of liquid DSSCs, thereby facilitating the transition towards an industrial development plan.

Chapter 3 was dedicated to the study of water splitting through DS-PEC. In that chapter, a number of metal-free organic dyes with different electronic and

geometrical features was fully characterized optically and electrochemically, both in solution and adsorbed onto a mesoporous TiO_2 photoanode. A systematic study of their use in photoelectrochemical water splitting was carried out. To properly evaluate the capabilities of each dye in photoelectrochemical application, a first screening in presence of a SED was carried out. This first set of measurements showed interesting properties and allowed us to reach photocurrent generation with all the dyes comparable to the state of the art. Moreover, the evaluation of the optical and charge transfer properties, compared to the amount of sensitizer adsorbed onto the semiconductor, was enlightening over the importance of the molecular design. In fact, as previously reported in a similar study,[2] the presence of different heteroatoms on the donor moiety was able to strongly influence the electronic properties of the adsorbed sensitizers. The superior light harvesting of the **POZ-Th** dye was not able to generate an efficiency in photon conversion as high as **CBZ-Th** and **PTZ-Th**. Concerning the two best performing dyes, **CBZ-Th** and **PTZ-Th**, even if their performances in photoelectrochemical measurements were similar, the **PTZ-Th** showed a superior IPCE over a lower dye loading due to its peculiar donor geometry. In this application, where poisoning of the catalyst was not possible, the effect of the suppression of dye–dye intermolecular charge transfers due to the bended geometry of the phenothiazine donor core, played a primary role in the achieving of high performances. Moreover, the use of the dyes in combination with a WOC revealed a stable photocurrent generation over a considerable time for all the sensitizers, designating them as promising alternatives to the more common used Ru-based complexes. Finally, a proper molecular design and the use of simple building blocks was able to tune the photoelectrochemical behaviour of metal-free organic sensitizers improving efficiency and stability.

The results of this PhD thesis have been published in 4 peer-reviewed papers in high impact factor journal (see Ch. 5).

References

1. Hammond, O. S.; Bowron, D. T.; Edler, K. J., "Liquid structure of the choline chloride-urea deep eutectic solvent (reline) from neutron diffraction and atomistic modelling". *Green Chem.* **2016,** *18*, 2736-2744, doi: 10.1039/C5GC02914G

2. Manfredi, N.; Monai, M.; Montini, T.; Salamone, M.; Ruffo, R.; Fornasiero, P.; Abbotto, A., "Enhanced photocatalytic hydrogen generation using carbazole-based sensitizers". *Sustainable Energy Fuels* **2017,** *1*, 694-698, doi: 10.1039/C7SE00075H

5 List of publications

- Boldrini, C. L.; Manfredi, N.; Perna, F. M.; Trifiletti, V.; Capriati, V.; Abbotto, A., "Dye-Sensitized Solar Cells that use an Aqueous Choline Chloride-Based Deep Eutectic Solvent as Effective Electrolyte Solution". *Energy Technology* **2017**, *5* (2), 345-353, doi: 10.1002/ente.201600420.

- Gatti, T.; Manfredi, N.; Boldrini, C.; Lamberti, F.; Abbotto, A.; Menna, E., "A D-π-A organic dye – Reduced graphene oxide covalent dyad as a new concept photosensitizer for light harvesting applications". *Carbon* **2017**, *115*, 746-753, doi: 10.1016/j.carbon.2017.01.081.

- Manfredi, N.; Boldrini, C. L.; Abbotto, A., "Organic Sensitizers for Photoanode Water Splitting in Dye-Sensitized Photoelectrochemical Cells". *ChemElectroChem* **2018**, *5*, 2395-2402, doi: 10.1002/celc.201800592.

- Boldrini, C. L.; Manfredi, N.; Perna, F. M.; Capriati, V.; Abbotto, A., "Designing Eco-Sustainable Dye-Sensitized Solar Cells by the Use of a Menthol-based Hydrophobic Eutectic Solvent as an Effective Electrolyte Medium". *Chem. Eur. J.* **2018**, *in press*, doi: 10.1002/chem.201803668.

6 List of abbreviations

APCE: absorbed photon-to-current efficiency

BL: blocking layer

CA: chronoamperometry

CDCA: chenodeoxycholic acid

CE: counter electrode

ChCl: choline chloride

CV: cyclovoltammetry

DES: deep eutectic solvent

DS-PEC: dye sensitized photoelectrochemical cell

DSSC: dye-sensitized solar cell

EIS: Electrochemical Impedance Spectroscopy

EQE: external quantum efficiency

FE: Faradaic efficiency

GA: glucuronic acid

GC: gas-chromatograph

H_2Q: hydroquinone

HEC: hydrogen evolution catalyst

HES: hydrophobic eutectic solvent

IL: ionic liquid

IPCE: incident photon-to-current efficiency

LHE: light harvesting efficiency

LSV: linear sweep voltammetry

PBS: phosphate buffer solution

PCE: power energy conversion efficiencies

PEC: photoelectrochemical cell

PEM: proton exchange membrane

PMII: 1-methyl-3-propylimidazolium iodide

PV: photovoltaic

Q: quinone

RE: reference electrode

SC: semiconductor

SED: sacrificial electron donor

VOC: volatile organic solvent

WE: working electrode

WOC: water oxidation catalyst

WRC: water reduction catalyst